TUNNELS AND UNDERGROUND CITIES: ENGINEERING AND INNOVATION MEET ARCHAEOLOGY, ARCHITECTURE AND ART

Volume 6

Innovation in underground engineering, materials and equipment - Part 2

Editors:

Daniele Peila

Giulia Viggiani

Tarcisio Celestino

CRC Press
Taylor & Francis Group
A BALKEMA BOOK

TUNNELS AND UNDERGROUND CITIES: ENGINEERING AND INNOVATION MEET ARCHAEOLOGY, ARCHITECTURE AND ART

Taylor & Francis
Taylor & Francis Group
http://taylorandfrancis.com

PROCEEDINGS OF THE WTC2019 ITA-AITES WORLD TUNNEL CONGRESS, NAPLES, ITALY, 3-9 MAY, 2019

Tunnels and Underground Cities: Engineering and Innovation meet Archaeology, Architecture and Art

Volume 6: Innovation in underground engineering, materials and equipment - Part 2

Editors

Daniele Peila
Politecnico di Torino, Italy

Giulia Viggiani
University of Cambridge, UK
Università di Roma "Tor Vergata", Italy

Tarcisio Celestino
University of Sao Paulo, Brasil

CRC Press
Taylor & Francis Group
Boca Raton London New York

CRC Press is an imprint of the
Taylor & Francis Group, an **informa** business
A BALKEMA BOOK

Cover illustration:

View of Naples gulf

CRC Press/Balkema is an imprint of the Taylor & Francis Group, an informa business

Typeset by Integra Software Services Pvt. Ltd., Pondicherry, India

Published by: CRC Press/Balkema
Schipholweg 107C, 2316XC Leiden, The Netherlands
e-mail: Pub.NL@taylorandfrancis.com
www.crcpress.com – www.taylorandfrancis.com

ISBN: 978-0-367-46871-2 (Hbk)
ISBN: 978-1-003-03163-5 (eBook)

Tunnels and Underground Cities: Engineering and Innovation meet Archaeology, Architecture and Art, Volume 6: Innovation in underground engineering, materials and equipment - Part 2 – Peila, Viggiani & Celestino (Eds)
© 2020 Taylor & Francis Group, London, ISBN 978-0-367-46871-2

Table of contents

Tunnels and Underground Cities: Engineering and Innovation meet Archaeology, Architecture and Art, Volume 6: Innovation in underground engineering, materials and equipment - Part 2 – Peila, Viggiani & Celestino (Eds)

Preface

The World Tunnel Congress 2019 and the 45th General Assembly of the International Tunnelling and Underground Space Association (ITA), will be held in Naples, Italy next May.

The Italian Tunnelling Society is honored and proud to host this outstanding event of the international tunnelling community.

Hopefully hundreds of experts, engineers, architects, geologists, consultants, contractors, designers, clients, suppliers, manufacturers will come and meet together in Naples to share knowledge, experience and business, enjoying the atmosphere of culture, technology and good living of this historic city, full of marvelous natural, artistic and historical treasures together with new innovative and high standard underground infrastructures.

The city of Naples was the inspirational venue of this conference, starting from the title Tunnels and Underground cities: engineering and innovation meet Archaeology, Architecture and Art.

Naples is a cradle of underground works with an extended network of Greek and Roman tunnels and underground cavities dated to the fourth century BC, but also a vibrant and innovative city boasting a modern and efficient underground transit system, whose stations represent one of the most interesting Italian experiments on the permanent insertion of contemporary artwork in the urban context.

All this has inspired and deeply enriched the scientific contributions received from authors coming from over 50 different countries.

We have entrusted the WTC2019 proceedings to an editorial board of 3 professors skilled in the field of tunneling, engineering, geotechnics and geomechanics of soil and rocks, well known at international level. They have relied on a Scientific Committee made up of 11 Topic Coordinators and more than 100 national and international experts: they have reviewed more than 1.000 abstracts and 750 papers, to end up with the publication of about 670 papers, inserted in this WTC2019 proceedings.

According to the Scientific Board statement we believe these proceedings can be a valuable text in the development of the art and science of engineering and construction of underground works even with reference to the subject matters "Archaeology, Architecture and Art" proposed by the innovative title of the congress, which have "contaminated" and enriched many proceedings' papers.

Andrea Pigorini
SIG President

Renato Casale
Chairman of the Organizing Committee WTC2019

Tunnels and Underground Cities: Engineering and Innovation meet Archaeology, Architecture and Art, Volume 6: Innovation in underground engineering, materials and equipment - Part 2 – Peila, Viggiani & Celestino (Eds)
 ISBN 978-0-367-46871-2

Acknowledgements

REVIEWERS

The Editors wish to express their gratitude to the eleven Topic Coordinators: Lorenzo Brino, Giovanna Cassani, Alessandra De Cesaris, Pietro Jarre, Donato Ludovici, Vittorio Manassero, Matthias Neuenschwander, Moreno Pescara, Enrico Maria Pizzarotti, Tatiana Rotonda, Alessandra Sciotti and all the Scientific Committee members for their effort and valuable time.

SPONSORS

The WTC2019 Organizing Committee and the Editors wish to express their gratitude to the congress sponsors for their help and support.

Tunnels and Underground Cities: Engineering and Innovation meet Archaeology,
Architecture and Art, Volume 6: Innovation in underground engineering,
materials and equipment - Part 2 – Peila, Viggiani & Celestino (Eds)

WTC 2019 Congress Organization

HONORARY ADVISORY PANEL

Pietro Lunardi, President WTC2001 Milan
Sebastiano Pelizza, ITA Past President 1996-1998
Bruno Pigorini, President WTC1986 Florence

INTERNATIONAL STEERING COMMITTEE

Giuseppe Lunardi, Italy (Coordinator)
Tarcisio Celestino, Brazil (ITA President)
Soren Eskesen, Denmark (ITA Past President)
Alexandre Gomes, Chile (ITA Vice President)
Ruth Haug, Norway (ITA Vice President)
Eric Leca, France (ITA Vice President)
Jenny Yan, China (ITA Vice President)
Felix Amberg, Switzerland
Lars Barbendererder, Germany
Arnold Dix, Australia
Randall Essex, USA
Pekka Nieminen, Finland
Dr Ooi Teik Aun, Malaysia
Chung-Sik Yoo, Korea
Davorin Kolic, Croatia
Olivier Vion, France
Miguel Fernandez-Bollo, Spain (AETOS)
Yann Leblais, France (AFTES)
Johan Mignon, Belgium (ABTUS)
Xavier Roulet, Switzerland (STS)
Joao Bilé Serra, Portugal (CPT)
Martin Bosshard, Switzerland
Luzi R. Gruber, Switzerland

EXECUTIVE COMMITTEE

Renato Casale (Organizing Committee President)
Andrea Pigorini, (SIG President)
Olivier Vion (ITA Executive Director)
Francesco Bellone
Anna Bortolussi
Massimiliano Bringiotti
Ignazio Carbone
Antonello De Risi
Anna Forciniti
Giuseppe M. Gaspari

Giuseppe Lunardi
Daniele Martinelli
Giuseppe Molisso
Daniele Peila
Enrico Maria Pizzarotti
Marco Ranieri

ORGANIZING COMMITTEE

Enrico Luigi Arini
Joseph Attias
Margherita Bellone
Claude Berenguier
Filippo Bonasso
Massimo Concilia
Matteo d'Aloja
Enrico Dal Negro
Gianluca Dati
Giovanni Giacomin
Aniello A. Giamundo
Mario Giovanni Lampiano
Pompeo Levanto
Mario Lodigiani
Maurizio Marchionni
Davide Mardegan
Paolo Mazzalai
Gian Luca Menchini
Alessandro Micheli
Cesare Salvadori
Stelvio Santarelli
Andrea Sciotti
Alberto Selleri
Patrizio Torta
Daniele Vanni

SCIENTIFIC COMMITTEE

Daniele Peila, Italy (Chair)
Giulia Viggiani, Italy (Chair)
Tarcisio Celestino, Brazil (Chair)
Lorenzo Brino, Italy
Giovanna Cassani, Italy
Alessandra De Cesaris, Italy
Pietro Jarre, Italy
Donato Ludovici, Italy
Vittorio Manassero, Italy
Matthias Neuenschwander, Switzerland
Moreno Pescara, Italy
Enrico Maria Pizzarotti, Italy
Tatiana Rotonda, Italy
Alessandra Sciotti, Italy
Han Admiraal, The Netherlands
Luisa Alfieri, Italy
Georgios Anagnostou, Switzerland
Andre Assis, Brazil
Stefano Aversa, Italy
Jonathan Baber, USA
Monica Barbero, Italy
Carlo Bardani, Italy
Mikhail Belenkiy, Russia
Paolo Berry, Italy
Adam Bezuijen, Belgium
Nhu Bilgin, Turkey
Emilio Bilotta, Italy
Nikolai Bobylev, United Kingdom
Romano Borchiellini, Italy
Martin Bosshard, Switzerland
Francesca Bozzano, Italy
Wout Broere, The Netherlands
Domenico Calcaterra, Italy
Carlo Callari, Italy

Luigi Callisto, Italy
Elena Chiriotti, France
Massimo Coli, Italy
Franco Cucchi, Italy
Paolo Cucino, Italy
Stefano De Caro, Italy
Bart De Pauw, Belgium
Michel Deffayet, France
Nicola Della Valle, Spain
Riccardo Dell'Osso, Italy
Claudio Di Prisco, Italy
Arnold Dix, Australia
Amanda Elioff, USA
Carolina Ercolani, Italy
Adriano Fava, Italy
Sebastiano Foti, Italy
Piergiuseppe Froldi, Italy
Brian Fulcher, USA
Stefano Fuoco, Italy
Robert Galler, Austria
Piergiorgio Grasso, Italy
Alessandro Graziani, Italy
Lamberto Griffini, Italy
Eivind Grov, Norway
Zhu Hehua, China
Georgios Kalamaras, Italy
Jurij Karlovsek, Australia
Donald Lamont, United Kingdom
Albino Lembo Fazio, Italy
Roland Leucker, Germany
Stefano Lo Russo, Italy
Sindre Log, USA
Robert Mair, United Kingdom
Alessandro Mandolini, Italy
Francesco Marchese, Italy
Paul Marinos, Greece
Daniele Martinelli, Italy
Antonello Martino, Italy
Alberto Meda, Italy
Davide Merlini, Switzerland
Alessandro Micheli, Italy
Salvatore Miliziano, Italy
Mike Mooney, USA
Alberto Morino, Italy
Martin Muncke, Austria
Nasri Munfah, USA
Bjørn Nilsen, Norway
Fabio Oliva, Italy
Anna Osello, Italy
Alessandro Pagliaroli, Italy
Mario Patrucco, Italy
Francesco Peduto, Italy
Giorgio Piaggio, Chile
Giovanni Plizzari, Italy
Sebastiano Rampello, Italy
Jan Rohed, Norway
Jamal Rostami, USA
Henry Russell, USA
Giampiero Russo, Italy
Gabriele Scarascia Mugnozza, Italy
Claudio Scavia, Italy
Ken Schotte, Belgium
Gerard Seingre, Switzerland
Alberto Selleri, Italy
Anna Siemińska Lewandowska, Poland
Achille Sorlini, Italy
Ray Sterling, USA
Markus Thewes, Germany
Jean-François Thimus, Belgium
Paolo Tommasi, Italy
Daniele Vanni, Italy
Francesco Venza, Italy
Luca Verrucci, Italy
Mario Virano, Italy
Harald Wagner, Thailand
Bai Yun, China
Jian Zhao, Australia
Raffaele Zurlo, Italy

Innovation in underground engineering, materials and equipment - Part 2

Tunnels and Underground Cities: Engineering and Innovation meet Archaeology, Architecture and Art, Volume 6: Innovation in underground engineering, materials and equipment - Part 2 – Peila, Viggiani & Celestino (Eds)
 ISBN 978-0-367-46871-2

The design approach of cut & cover excavation in hyperbaric condition applied for Napoli/Cancello high speed railway

G. Lunardi, G. Cassani, A. Bellocchio & C. Nardone
Rocksoil S.p.A., Milan, Italy

M. Cafaro & G. Ghivarello
Salini Impregilo, Milan, Italy

R. Sorge & F. Carriero
Astaldi, Rome, Italy

ABSTRACT: In the frame of the high speed railway line Napoli-Bari, it is foreseen the realization of a cut and cover tunnel which partially develops below the ground water level. The top down construction will be performed using the compressed air in order to achieve a dry base during the soil excavation and the cast of the internal structures. All the benefits of this technology are discussed, including the aspects related to the environment. The practical application of the technique has revealed numerous detailed problems from a structural point of view: together with the additional load on structures, the limitation of the air losses has been a relevant topic. The measures implemented for the maintenance of the prescribed pressure are presented in the paper describing the solution developed to minimize the dissipation of compressed air through production joints. The air losses are estimated after a brief survey of the formulations available in literature.

1 INTRODUCTION

The project in question is part of the transport network upgrading along the transversal axis Naples - Benevento - Foggia - Bari. The works are aimed at giving adequate response to the changing mobility needs of travelers and goods and constitute a fundamental element for the development of southern Italy, for a better economic and social integration in the country and in Europe.

In this sense, the construction of the high capacity railway line Naples-Bari, together with the activation of the Rome-Naples high-speed railway system, will favor the integration of the railway infrastructure of the South-East with the Connecting Directories to northern Italy. This upgrading will have a paramount impact for the socio-economic development of the South, reconnecting two areas, Campania and Puglia.

The enhancement of the railway axis connecting the Tyrrhenian and the Adriatic coastlines will also allow the creation of a “tripole” (Rome, Naples and Bari) which will constitute one of the largest metropolitan systems in Europe. On the international front, as part of the new structure of the trans-European corridors (TEN-T) defined by the European Commission on 19 October 2011, the development of the Naples-Bari route, which specifically falls within the Corridor 5 Helsinki - Valletta, has been identified as a priority.

The rehabilitation and development of the Naples-Bari itinerary involves the doubling of the single-track railway sections and the change of the current alignment, in order to ensure the connections speeding up and the increase of the railway transport offer (Figure 1).

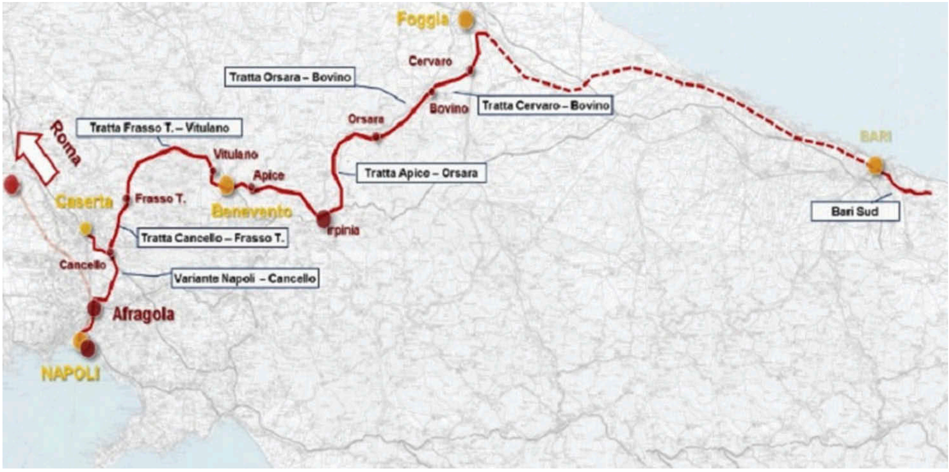

Figure 1. Transport network upgrading along the transversal axis Naples - Benevento - Foggia - Bari.

The entire work was divided into functional sections for realization purposes. The project in question is part of the first section (Naples-Cancello) particularly strategic in the overall arrangement of metropolitan, regional and long-distance connections.

In fact, the variant in the stretch between Naples and Cancello, allows bringing the tracks of the line to the new station of Naples Afragola, which in the future will become the station for passenger interchange between regional and AV services increasing overall accessibility to the railway transport in the Naples hub.

The line, in the section of interest develops for about 15.5 km through the municipalities of Casoria, Casalnuovo, Afragola, Caivano and Acerra (Figure 2). The chainage starts, in the south, from km 0+000.00 (coinciding with km 241+727 of the historical line) and ends, in the north, at km 15+585,066 (coinciding with km 229+530 of the historical line).

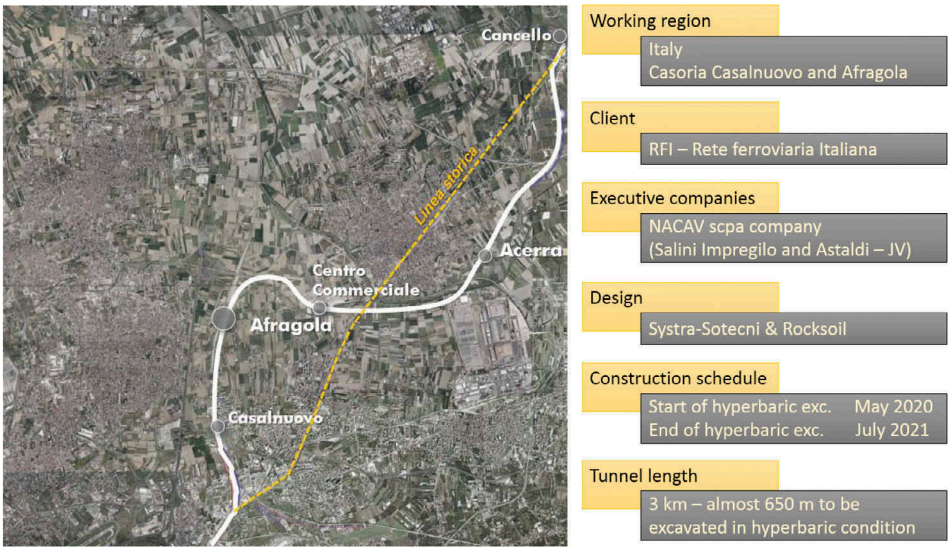

Figure 2. Section Overview.

Although, in general, the preferred solution is that of railway embankment, in some particular points the construction of viaducts or tunnels is envisaged in order to resolve specific interferences and to better integrate with the environment.

The tunnel cross section presents a geometrical variability as summarized below:

1. "Parapioggia" (Figure 3)
   In the first 180 m the tunnel has a rectangular section, in this stretch the tunnel presents a single tube section.
2. Top down tunnel with single-tube section (Figure 4)
   For about 300 m the tunnel continues with a top down section characterized by diaphragm walls horizontally restrained by roof and foundation r.c. slabs. In this stretch the section is a single tube section.
3. Top down tunnel with double-tube section (Figure 5)
   In the following stretch, the Circumvesuviana line joins the new Cassino line, therefore the tunnel presents a double-tube section and is constructed following the top down method
4. Top down tunnel with double-tube section and intermediate slab (Figure 6)
   In this stretch, due to the considerable excavation height an intermediate slab is foreseen to restrain horizontally the structure
5. Casalnuovo Station
   In correspondence of Casalnuovo station, the tunnel maintains the same structural concept. It is different from the adjacent stretches only in terms of width that is greater due to architectural purposes.
6. Top down tunnel with double-tube section
   In the last portion, the surface level decrease allowing to foresee only two horizontal slabs that correspond to the double-tube section

The tunnel interferes with the phreatic level in the first stretch, from pk 0+550 to pk 1+600. In order to perform all the excavation and construction activities in dry condition the tender design foresaw the execution of jet grouting plug. The soil treatment reduces the soil perme-

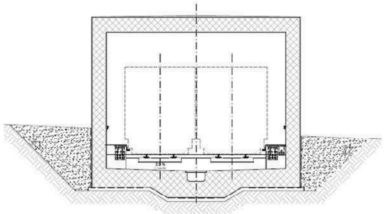

Figure 3. "Parapioggia".

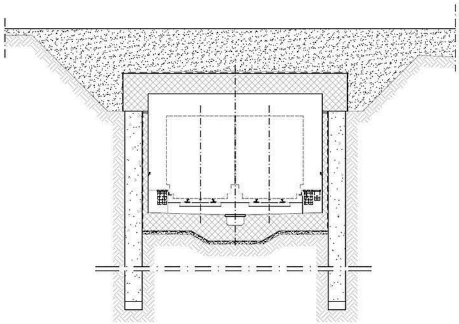

Figure 4. Top down tunnel with single-tube section.

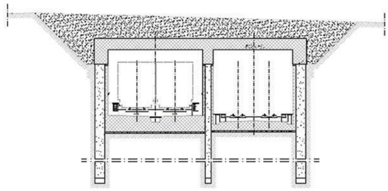

Figure 5. Top down tunnel with double-tube section.

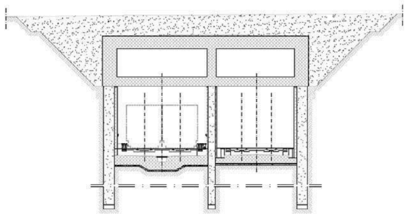

Figure 6. Top down tunnel with double-tube section and intermediate slab.

Table 1. Comparison of the alternative solutions.

	COMPRESSED AIR	JET GROUTING
Aquifer pollution	✔	✘
Duration of works	✔	✘
Flexibility	✔	✘
Production plant cost	✘	✔
Soil improvement cost	✔	✘
Soil to landfilling	✔	✘

ability, allowing creating a waterproof layer. Due to the water height to be counter-balanced the thickness of this treatment reached high values.

With regard to the bid issued by Italferr in 2016, it was requested to the Competitors to study an original technical solution which could solve the interference with the groundwater, par-ticularly with the possibility to get an easy compartmentalization between the following work-ing phases. For this purpose, NACAV scpa company, a JV between Salini Impregilo and Astaldi, decided to choose an original technical solution, already successfully used abroad, consisting in making use of pressurized air dig. Such choice allowed NACAV scpa company to get the job. Table 1 summarize the comparison of the alternative solutions.

That is the use of compressed air, whose application has a double advantage:

– a higher flexibility of the system in order to adapt to ground water level fluctuation;
– no impact on the environment due to the exclusion of any contamination of the groundwater, which serves as a reservoir for the water supply of the city.

2 COMPRESSED AIR EXCAVATION

2.1 *Famous historical applications*

The use of compressed air for excavation under water table has been used for long time especially for the mechanized excavation (TBM). In the field of artificial tunnels this technique has been developing in recent years, particularly in the countries of northern Europe, as, in certain contexts, it represents a valid alternative to traditional solutions, bringing improvements and advantages.

Historically, this type of technology finds its most widespread applications in the construction of underwater foundations and in particular through the use of pneumatic caissons. For example, the most important geotechnical applications include the foundations of the Eiffel Tower. In Italy, on the other hand, a well-known example is represented by the bridge of the Hach Industry in Rome for which the compressed air foundation was used for the first time in Italy, a caisson technique whose origin should be searched in France in 1841. Another mention must be made regarding the metro line 4 in Paris for which compressed air was applied for the Seine under-passing.

Among the underground tunnel in hyperbaric condition projects developed abroad are mentioned below (Schwarz & Hehenberger, 2004):

- Chlodwig-Platz, Cologne, Lot South - North-South suburban railway, Cologne Oil-free screw compressor;
- Stans/Terfens Tunnel - Inntal, construction lot H4-3 oil-free screw compressor;
- Vomp/Terfens tunnel - Inntal, construction lot H5 oil-free screw compressor;
- Allmend Tunnel Lucern - Central railway - double track - construction on lower level oil-free screw compressors;
- BF Olympiapark North, underground railway line 3 North - Ventilation;
- Fritzens/Braumkirchen - Inntal tunnels, construction lots H7-1, H7-2, H-3 oil-free screw compressors;
- AUDI Tunnel in Ingolstadt (Germany).

2.2 *General operating principles*

The excavation with compressed air of artificial tunnels built with the top-down method, as in the case of the GA01, generally requires a similar methodology dictated by technological needs, even if, depending on the site and the specific characteristics of the work, small variations are found in the examined cases.

In general, a r.c. wall in c.a. is constructed at the entrance of the tunnel and two watertight doors are installed for people and vehicles access. These accesses lead to a watertight seal chamber where the air is gradually pressurized to reach the design pressure value.

Through two more doors, the workers and the vehicles can access to the working construction site inside the tunnel, which is in a hyperbaric environment at the established pressure.

Through other two doors, both the vehicles and the workers can enter and exit (separately) in the compensation chamber, which must therefore be subjected to time periods of compression (entry) or decompression (exit).

The pressure value to be applied in the tunnel is equal to the corresponding value of hydrostatic pressure acting on the excavation bottom due to the water head at the time of the excavation under the top slab.

As the excavation proceeds, the pressure to be applied in the tunnel must be adjusted to the value of hydrostatic pressure to be balanced at the different advancement steps.

The internal pressure is thence an additional load acting on the structure in the temporary phase that should be considered in the structural analyses. It is to be remarked that in general the air pressure acts in the opposite direction of the most demanding loads: for both the retaining walls and the top slab the internal pressure partially counteract the earth and water pressure acting inward the tunnel. In other words, this methodology does not require a strengthening of the structure and furthermore, assuming the air pressure is maintained during the whole excavation process, it reduces the internal actions associated to the temporary phase.

While the compressed air system is active the global equilibrium toward the possible uplift should be checked: the internal pressure, determined to counteract the water pressure at the bottom of the excavation, can lead to a structure uplift in case of low backfilling. This condition should be taken into account performing a specific check, which should consider the internal pressure of the air, the weight of the structure, the backfilling load, the anchoring strength of the diaphragm walls in the ground.

The tunnel construction phases will thence be:

– Excavation to the diaphragm wall execution level;
– Realization of the diaphragm walls;
– Cast of the r.c. roof slab;
– Backfilling above the roof slab;
– Excavation below the roof slab, between the diaphragm walls, to the foundation level with the application of the prescribed air pressure;
– Cast of the internal structures and finishes installation;
– Deactivation of the internal air pressure.

3 THE APPLICATION TO THE CASE OF STUDY

3.1 *Technical and methodological aspects*

In the case of study, the maximum excavation level varies according to the T.O.R. of the alignment. Moreover, the excavation section changes due to the section type variability foreseen by the design and to the fact that the tunnel locally widens for the STI exits, for the wasteawater lifting plants and the relative inspection chambers and for the niches.

This configuration would require the adjustment of the air pressure of compressed air at each advance. For logistic purpose and to avoid excessive air losses at the tunnel face, the tunnel has been divided into compartments (n.14, Figure 7) limited on the sides and on the top by the tunnel structures and at the front by specific diaphragm walls.

The diaphragm walls that constitute the transversal partitions are executed together with the longitudinal ones and are placed at a variable distance each other, determined considering the expected losses.

At each of the 14 compartments will correspond a uniform design value of the air pressure (maximum value of the water head in the stretch individuated by the compartment) and fixed volume. To define correctly the design pressure to be maintained in each compartment, a specific piezometric monitoring has been performed during the development of the design, see Table 2. Since the records showed a certain variability due to weathering and to seasonal fluctuation, the maximum water level recorded has been considered. Furthermore, an addition possible raising of 1 m is precautionary assumed.

Considering the maximum hydraulic head in each compartment, he design pressure required for lowering the water table below the excavation surface ranges between 0.2 and 1 bar. The range already takes into account the variability of the excavation level in correspondence of a local structures such as the wastewater lifting plant.

The fact that the maximum pressure required by the system is equal to 1 bar confirms the effective advantage of the solution. The safety of workers in hyperbaric conditions represents an important aspect to be considered in the design phase since can have strong impact on the indirect costs of the project. Despite the regulatory environment is still developing on this topic and is not homogeneous comparing the references from different countries, the safety measures to be implemented always depend on the working pressure. In addition, all the standards available on the subject consider 1 bar as a limit for the first level of safety equipment since the human beings can easily adapt to such a pressure.

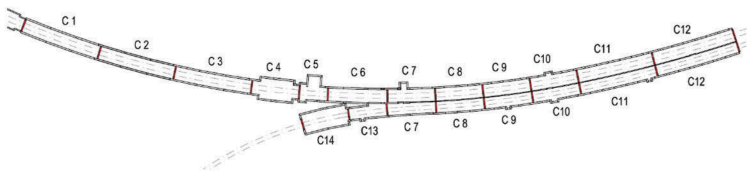

Figure 7. General plan with compartments.

Table 2. Piezometric readings from the geotechnical campaign.

		Head	H max	H min	08/03	22/03	23/03	16/04	14/05	01/06
	PK	mslm	mslm	mslm	m from head					
E1PZ	0+735,35	17.44	14.39	14.04			3.4	3.20	3.05	3.13
E3PZ	1+150.98	22.89	15.15	15.04		7.85		7.81	7.74	7.72
E4PZ	1+276.58	26.35	15.05	14.77	11.58			11.49	11.3	11.24
E5PZ	1+705.99	34.60	15.51	15.20		19.4		19.26	19.09	19.02

3.2 *Construction phases*

Once the slab is cast and backfilled according to the design final ground level, the compressed air plant shall be switched on and, when the design pressure value is achieved the tunnel excavation could start.

The excavation will be performed without any partialization of the face and proceeding by compartments: the excavation of a compartment will begin only after completion of the final structures of the previous one. The excavation muck will be transported out of the hyperbaric work area by means of a conveyor belt devised to ease the working process.

The choice of this system requires a certain space for its installation and, consequently, leads to postpone the application of the compressed air to the second compartment.

After the excavation of the first compartment and the cast of the internal structures the compressed air system is switched on. In order to guarantee the pressurization of the next compartment, some holes are provided in the partition wall before its demolition that is followed by the excavation. The compartment will be excavated up to its end, proceeding simultaneously in the two tubes if the tunnel present a double tube section.

At the end of the excavation process the waterproofing system will be installed and fixed to the structures in order to limit the air losses in the next phase. Once the cast of the internal structure is complete it's possible to proceed with the same construction process for the next compartment.

3.3 *Construction details*

In order to minimize the air losses during the excavation with compressed air, the construction joints have been studied in detail to improve the tightness both to water and to air. The calculations for the sizing of the plants depend on the equivalent overall permeability to air of the surfaces exposed to the air pressure. For the case of study, considering the average permeability of the soil to water measured by means of specific tests in situ, the following assumptions were made:

– During the excavation the structures and the soil present an equivalent overall permeability to air equal to 10^{-6} m/s;
– After the cast of the internal structures the equivalent overall permeability is assumed equal to at 10^{-8} m/s.

These values have been estimated considering all the precautions actuated to reduce the air losses and should be confirmed before the start of the excavation by means of a field test.

In order to optimize the design and to reduce the cost related to the compressed air plant the tightness of the structure should be studied in detail focusing on the weak points of the system with respect of the air leaks that are:

– The connection between the roof slab and the diaphragms;
– The longitudinal joints between diaphragms: this context shows the greatest number of discontinuities (every 2.5 m);
– Joints (casting joints and expansion joints) present on the slabs (linings, top and foundation slabs);
– Interface between the waterproofing sheets and the internal structures on the base slab and on the linings at the end of each compartment.

The precautions to be taken to improve the hydraulic seal of the structural joints and of the construction joints in the different parts of the structure must therefore be studied in order to obstruct also the air passage.

For the joint between the roof slab and the diaphragm wall, a waterstop is installed between the latter and the linings in order to stop a possible ascent of the ground water (Figure 8). Moreover, the waterproofing layer installed on the roof slab is mechanically fixed to the diaphragms below the contact section with the roof slab abutment providing protection against the rainwater inlet. This mechanical fixing also guarantees an excellent seal against compressed air, limiting considerably the air losses.

For the joint between the partition walls and the roof slab a waterstop is installed at the top of the capping beam as shown in Figure 9.

To limit the air losses that could occur at the joint between two adjacent diaphragm walls, in addition to the particular dovetail shape, a waterstop is inserted. This detail is foreseen for all the diaphragm wall, both the one of the tunnel and those of the partitions.

In correspondence of the construction or expansion joints, the detail studied to guarantee water tightness perform very well also as a barrier against air. In fact, while for the construction joints the continuity of the membrane is foreseen, in correspondence of the expansion joints a waterstop which allows to compensate the differential shrinkage of the structures is inserted guaranteeing continuity of the waterproofing system (Figure10).

At the end of each compartment, the waterproofing membrane is mechanically fixed to the linings and to the foundation slab to allow a perfect seal of the already executed portion: this allow considering for that part a lower permeability to air as cited before.

The TNT layer placed between the PVC and the lean concrete to protect the waterproofing membrane constitute an escape route for the air. In correspondence of the structural joints, the waterproofing package is fixed to the r.c. structure by anchored waterstops, but it is also necessary to secure it outward (on foundation slab and diaphragm walls).

Since the operations (excavation, laying of the waterproofing and casting of the internal structures) will be carried out compartment by compartment, it is envisaged to create this kind of joint at the end of each compartment (Figure 11).

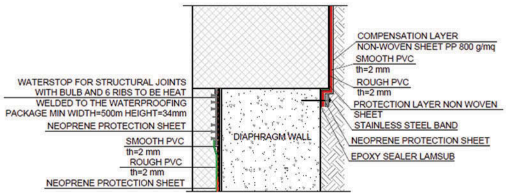

Figure 8. Joint between the roof slab and the diaphragm wall.

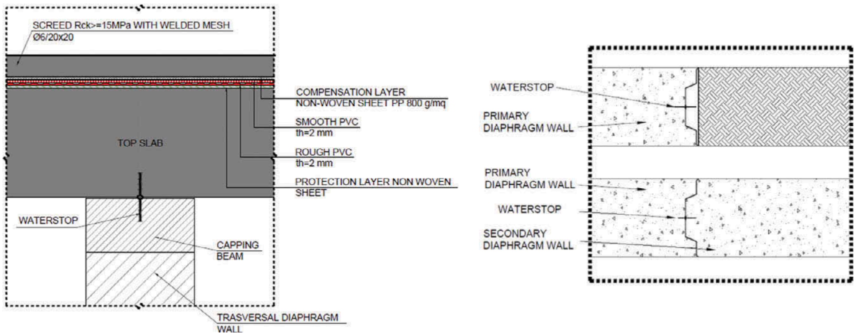

Figure 9. joint between the partition walls and the roof slab (left) joint between adjacent diaphragm walls (right).

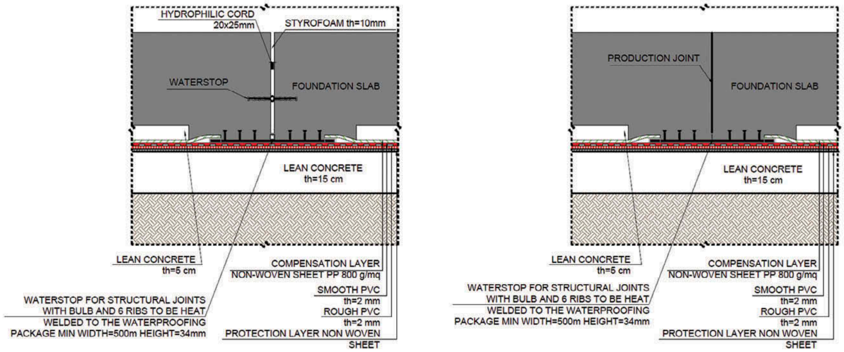

Figure 10. Longitudinal joint - foundation slab.

In detail, the waterproofing in correspondence of the lining is fixed to the diaphragm walls and the one in correspondence of the foundation slab is fixed to a specially made joist.

4 AIR LOSSES EVALUATION

The plant for the compressed air should be dimensioned considering all the factors that determine the required flow. In particular, once the volume of work is put under pressure, the main contributions are:

– Losses through structural joints
– Losses due to the opening and closing of access doors for vehicles and personnel
– The forced aspiration required to maintain healthy conditions in the workplace.

While the last contribution is a requirement dictated by the workers' safety manuals, the others must be estimated for a correct sizing of the plant (ITA-AITES WG5, 2015).

Of the two, the one linked to the opening and closing of the access doors has a minimal influence since it is foreseen a compression/decompression chamber for muck, means of transport and workers.

The contribution that have to be evaluated is therefore the one due to losses through ground and structural joints. For this purpose, the formulation of Schenck and Wagner, developed to evaluate air leaks during tunnel excavation, is applied (Semprich & Scheid, 2001).

$$Q = 2 \cdot k_a \cdot \frac{(P_1 - P_2)}{\gamma_w \cdot L} \cdot A \cdot \frac{P_1}{P_2}$$

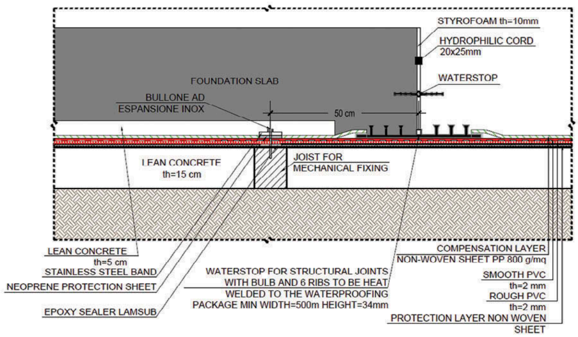

Figure 11. Mechanical fixing at the end of each compartment - Foundation slab.

- k_a is the permeability coefficient of the ground in the air that can be assumed equal to 70kw
- kw is the permeability coefficient of soil to water
- P_1 is the absolute pressure inside the tunnel that corresponds to the pressure necessary to lower the pitch below the excavation bottom plus the atmospheric pressure (Ptun + 1) atm
- P_2 is atmospheric pressure equal to 1 atm
- γ_w is the specific weight of water
- L is he length of the air path that corresponds to the tunnel overburden
- A is the area through which losses occur

It should be noted that it is not possible to determine the permeability coefficient of the soil to air by means of laboratory tests, since it is strongly dependent on the in-situ boundary conditions. For this reason, the aforementioned relation is used to estimate this coefficient starting from the water permeability of the medium. Obviously, the assessments made here shall be confirmed in the execution phase through specific in situ tests performed before the start of the excavation. On the basis of these results, it will be possible to adjust the design pressures in order to better control the lowering of the water table (Bull, 2003).

In order to guarantee a correct application of the internal pressure, the system also provides a series of instruments that allow a constant monitoring of losses: in every instant the incoming and outgoing air volume and the actual air pressure will be measured.

The Schenck and Wagner formulation is valid for laminar flow, which can be foreseen in material where $k_w < 1 \cdot 10^{-3}$ m/s (Jardine & McCallum, 2001). Given that in our case study, the permeability of the soil that varies between $1 \cdot 10^{-4}$ m/s and $1 \cdot 10^{-6}$ m/s the basic requirement is met.

The above formulation refers to the tunnel excavation with the traditional method, therefore there is no structure that prevents the escape of the air but the ground itself. For an artificial tunnel the volume of soil to be excavated is enclosed in a box consisting of diaphragm walls (laterally and frontally) and top slab. At the bottom of the excavation there is no structural element, but considering that the soil is saturated its permeability to air is very low.

In light of these considerations, the permeability value assumed for the calculation of the losses is equal to $1{\cdot}10^{-6}$ m/s before the final linings are casted and equal to $1{\cdot}10^{-8}$ m/s when the internal structures are finished.

Precautionary considering the maximum permeability until the installation of the mechanical fixing at the end of the compartment, the required air flow rate estimated considering one compartment not lined and a cumulative loss in the previous ones ranges between 45 and 95 m^3/min.

For the sizing of the plants it is considered appropriate to consider, in addition to the strictly necessary equipment, an additional compressor able to guarantee 50% of the estimated flow.

5 TECHNOLOGICAL ASPECTS

5.1 *Hyperbaric chamber*

Salini Impregilo and Astaldi designed a concrete structure for the access of personnel and equipment for the excavation of the pressurized tunnel.

For the case of study the transversal section of the hyperbaric chamber, 40 m long and 13 m wide, has been divided in three compartments: two for the accumulation of the excavated material (compartment A and B, see Figure 12) and one for the passage of vehicles and personnel (Compartment C, divided vertically in two volumes in order to separate the passage of vehicles and personnel). Considering that to entry in and exit from the excavation site it is necessary to follow specific procedures for the gradual compression and decompression, the construction site has been studied with the aim of minimizing the number of passages. In particular, in order to manage the muck transport it is envisaged the use of an extensible conveyor belt, hanged which will discharge the material coming from the front on a reversible belt feeding two shuttle belts. The shuttle belts will store the muck alternatively in one of the two compartments addressed to this specific function (Comp. A and B). When compressed they are used to collect the excavated material from the belt conveyor, and when depressurized, to load and transport away the ground, loading by a wheel loader. They are built with concrete walls and closed by self-sealing steel doors. One door, on the

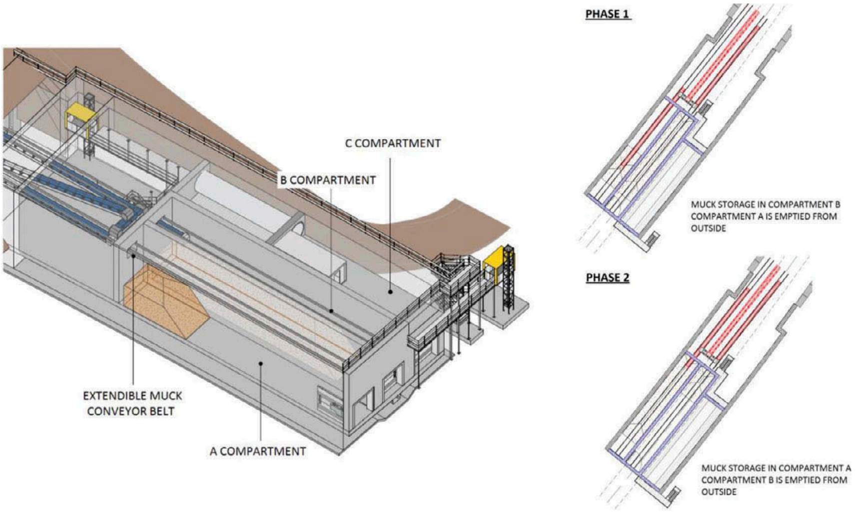

Figure 12. Hyperbaric Chamber.

atmospheric pressure side is large enough to accommodate the wheel loader; the other one, located on the pressurized side, presents the minimum dimensions to let in the conveyor belt and is controlled by hydraulic jacks.

The chamber dedicated to the equipment transfer is also equipped on both ends with self-sealing steel doors fitted with a remote-control device, to operate the door from the control cabin.

The personnel transfer chamber is a classical hyperbaric chamber steel made, including a main and an access chamber. The purpose of the access chamber is to make sure that at any time it is possible to shelter the crew retreating from the front, or to have a rescue team compressed for help the compressed crew.

A control cabin will be supplied and will be designed and equipped to manage all the information and controls for the excavation of the tunnel and the operations of the hyperbaric chambers, as well as the compressed air supplies. The hydraulic power pack to operate the jacks of the doors of the locks will be installed in the control cabin.

The hyperbaric equipment includes: all the 6 doors with relevant operating jacks and seals, the man-lock and relevant control panel, the hydraulic power pack, several steel plates, 600 x 600 mm size with relevant fixing frames, for concrete wall penetrators.

All pressurized equipment will be designed and constructed to meet the CE 12110 standard for air locks and compressed air shields. In particular, all parts which could not be hydraulically tested will be calculated with a safety coefficient 2 relative to the expected service pressure (in this case is 1 bar and safety coefficient 2).

The two ground locks and the equipment lock will be equipped with a closed circuit color video system which will be displayed by a screen installed into the control cabin.

A pressure recorder, installed in the control cabin, will be able to control: the pressure of the tunnel, the pressure of the man lock, the pressure in the ground locks and the pressure in the equipment lock. There are 3 pressure sensors installed in each of the different chambers and the recording interval is from 1 sec to 12 h.

5.2 *Compressors and pipelines for compressed air*

Compressors have been provided, placed outside, to supply and maintain the air at the desired pressure in the tunnel according to the design prescriptions. The compressed air system will have, in addition to the compressors:

- filtration system suitable for ensuring breathable air certified according to the regulations;
- cooling system to feed air in the tunnel at the correct temperature;
- extensible steel pipeline to carry the air to the front and a spare line placed in a position faraway from the operating area with the aim of having at least one operational pipeline even in case of damage to the other;
- control system, located in the tunnel near to the working front, able to maintain the air pressure established, compensating the decrease in pressure due to any leaks to the outside;
- system with a controlled air flow, allocated at the beginning of the tunnel, to allow the air to flow outwards in order to ensure an renewal of the air, according to the norm, that takes into account the number of people operating in the tunnel.

Inside the tunnel, in a closed environment, the operation with the electric motors of the equipment causes the air to heat up. To contain this air heating within the limits of comfort for people an air cooling and recirculation system will be provided. This system will consist of a cooling coil and an electric fan placed towards the tunnel entrance in order to recirculate the air from the working front. The cooled air that passes through the electric fan will be addressed directly to the working front by a flexible tube. This system therefore ensures that the personnel work in an environment with the correct temperature and humidity values.

In order to ensure the continuous operation of the "vital" systems inside the tunnel in case of shut-down of the power supply line, emergency generators located outside are designed to satisfy all the functions considered particularly sensitive for the operating personnel like breathing air, lighting, opening of doors, fire system, etc.

Every opening, even the small ones, that remain cause air leaks from the already excavated tunnel. To counter the consequent decrease of the desired pressure a sensor is installed near the working front which will automatically manage the operation of the compressors. This sensor can be adjusted so as to ensure the correct value of the air pressure for each working field.

6 CONSTRUCTION MACHINERY AND PLANTS

6.1 *Conveyors*

Inside the tunnel, in hyperbaric conditions, the fundamental criterion is to maintain conditions of wellbeing for the workers that are reflected in the air parameter control systems. A solution in this direction is the adoption of only electric motors in the tunnel for all the operating machines. Therefore the transport of excavated material along the tunnel is implemented with the use of a system of conveyor belts equipped with electric motors that are stretched to follow the excavation front. This system will be equipped with all the safety measures suitable for the particular environmental conditions in the tunnel as non-flammable components, temperature sensors, etc.

6.2 *Excavators*

The excavation of the materials and the consequent loading on the belt conveyor system is provided by Shaeff ITC machines. Indeed these machines combine the excavation function and the loading through a conveyor able to feed the conveyor belt system with continuity. Infact the conveyor belt system is designed with mobile elements able to follow the excavator and then receive anytime the excavated material.

6.3 *Electric construction vehicles*

All the operating machines and the equipment used inside the tunnel will be equipped with electric motors. This solution allows zero emissions into the tunnel environment and thus ensures a perfectly breathable air quality. Depending on the availability from the market and the required functions, some machines will be powered through the 380-volt power line while others will be equipped with rechargeable batteries; for this case an external installation will be provided for recharging the spare batteries.

6.4 *Molds*

The project foresees that, after having affixed the waterproof sheath under the base slab and the walls, a concrete base slab and a finishing concrete layer on the walls will be carried out. In particular, for the walls works a series of formwork sets are provided. The formworks will be equipped with anchors at the base and upper section and with wheels suitable for permitting translation. They will also be equipped with wall-mounted vibrators and concrete filling mouths positioned at various levels to facilitate the regular laying and a perfect surface finishing.

7 CONCLUSIONS

The choice adopted by Salini Impregilo and Astaldi for the excavation of the artificial tunnel Casalnuovo has proved innovative and represents an avantgarde in the national landscape.

The chosen solution allows controlling the water table, avoiding any risk connected to the transport of fine materials in case of a drowning and those induced by possible heaving due to jet grouting and above all the ground water pollution.

Following a careful design procedure, the safety of workers is guaranteed in any construction phase and assured by a redundancy of safety measures.

According to this technology Rocksoil has developed the structural design taking into account the additional actions acting on the bearing elements. In addition to it, all the construction joints have been studied in detail in order to limit as much as possible the air losses during construction.

Finally, the whole team, including both constructors and designers have worked side by side in order to define the construction process that could guarantee the success of the excavation and assure the workers safety.

REFERENCES

Semprich, S. & Scheid, Y. 2001. Unsaturated flow in a laboratory test for tunnelling under compressed air. *Proceedings of 15th Int. Conf. Soil Mech. And Geot. Eng.*, Vol. 2, 1413–1417. Instanbul: Balkema.

Schwarz, J. & Hehenberger, F. 2004. Compressed air for top down. *Proceedings Tunnels & Tunnelling International*, 36 (2).

Bull, J.W. 2003. *Numerical analysis and modelling in geomechanics*. London and New York: Spon Press of the Taylor & Francis Group.

Jardine, F.M. & McCallum, R.I. 1992. Engineering and Health in Compressed Air Work. *Proceedings of the International Conference*. Oxford.

ITA-AITES WG5, 2015. *Guidelines for good working practice in high pressure compressed air*.

Tunnels and Underground Cities: Engineering and Innovation meet Archaeology, Architecture and Art, Volume 6: Innovation in underground engineering, materials and equipment - Part 2 – Peila, Viggiani & Celestino (Eds)
 ISBN 978-0-367-46871-2

Innovative TBM transport logistics in the constructive lot H33 – Brenner Base Tunnel

A. Lussu
Brenner Base Tunnel, BBT-SE, Innsbruck, Austria

C. Kaiser & S. Grüllich
Arge Strabag-Salini/Impregilo, Innsbruck, Austria

A. Fontana
ÖBA-ARGE Pini & Partners, Innsbruck, Austria

ABSTRACT: The construction of the Tulfes Pfons lot, as part of the Brenner Base Tunnel (BBT), includes a 15 km long tunnel section excavated with an open gripper TBM. Due to the very difficult logistical conditions (steep access tunnel with a downward gradient of 11 %, a 90° turn to the main tubes with a small cross-section of 8 m diameter), an alternative TBM logistical supply solution was developed in collaboration with the contractor. Multi Service Vehicle (MSV) is a laser-controlled custom vehicle on rubber tires that can operate without rails. The MSV is able to handle both the steep access (11 %) and the 90° turn. In addition to the safety-related advantages, it was proven that the MSV system can keep pace with conventional TBM supply systems. After 12 km of excavated tunnel with a top performance of 61 m/day and monthly performances of up to 800 m/month in hard rock conditions with up to 1200 m overburden, it was clear that the use of the MSV has been a complete success. MSVs are becoming a cost efficient and technically approved alternative to conventional TBM supply equipment on rail.

1 INTRODUCTION

The Tulfes Pfons construction lot is the most northern construction lot and is considered one of the most complex lots of the Brenner Base Tunnel. It connects the Brenner base tunnel to the existing Lower Inn Valley tunnel which was built from 1989–1994. This construction lot with a total length of 42 km was awarded in June 2014 to the STRABAG/Salini/Impregilo joint venture, under the technical leadership of STRABAG. The construction works started in July 2014. The excavation works for the seven conventional tunnel drives using drill and blast method started in September 2014 with an official groundbreaking ceremony. In August 2018, 26 km from a total of 27 km conventionally driven tunnels have been excavated and 12 km from a total of 15 km with an open gripper TBM. The peak of tunnel excavation occurred between 2016 and 2017, when all eight drives were being excavated simultaneously:

2 PROJECT DESCRIPTION

The Tulfes-Pfons construction lot includes the following sections (see Figure 1):

- 15 km of exploratory tunnel A= 50 m²,
- 9.7 km of rescue tunnel (A= 35 m²) for the Lower Inn Valley tunnel with 28 cross-passages while rail operations were ongoing,

- 3.8 km and 1.9 km of connection tunnels (A= 115 m²) to link the Brenner Base Tunnel with the existing Lower Inn Valley tunnel,
- 3.2 km of the Innsbruck emergency stop (A=78 m²),
- 3.8 km of main tunnels for the Brenner Base Tunnel (A= 70 m²) and
- several access tunnels, cross-chambers and cross-passages .

The 15-km stretch of exploratory tunnel to be driven southwards is a challenge in itself. The exploratory tunnel is being used during the construction phase of the Brenner Base Tunnel to investigate the geological conditions in order to use this information for the tenders process of the main tunnels to be excavated above. In the operating phase, it will be used as a service and drainage tunnel.

In order to guarantee the best possible level of prospection, an open gripper TBM with a cutter head diameter of 8 m was stipulated in the tender. The local geological conditions can be constantly recorded and documented behind the shield all along the tunnel length. The visual documentation by the geologist is supported by probe drilling, lateral prospective drilling and ongoing seismic tests. These measures are helping to control the ongoing tunneling works as well as the prospection for the subsequent excavation of the parallel main tubes.

The excavation of the exploratory tunnel with a maximum overburden of 1,200 m using a gripper TBM presents a special challenge for the joint venture with regards to construction

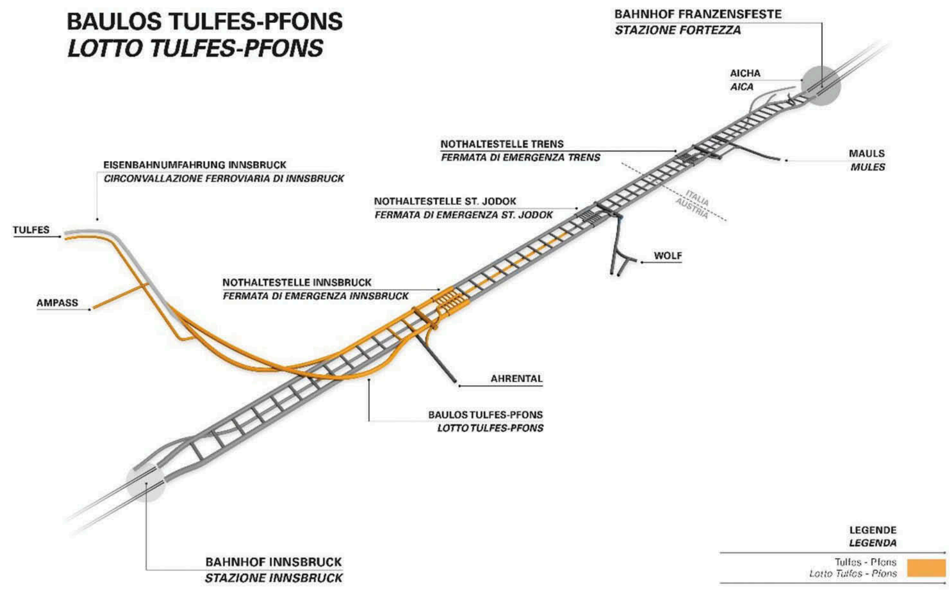

Figure 1. Tunnels to be excavated in construction lot H33 [BBT].

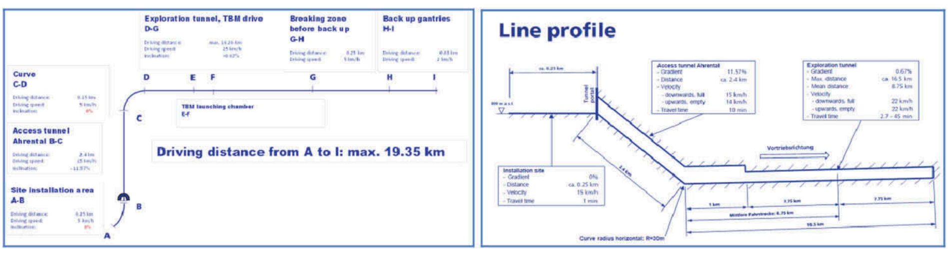

Figure 2. Plan view and longitudinal profile of the access tunnel and exploratory tunnel [ROWA].

engineering, safety engineering and logistical aspects. This article will deal primarily with logistics challenges and its safety related requirements.

3 PARTICULARITIES OF THE TBM LOGISTICS AT LOT TULFES PFONS

The challenges of all BBT construction lots is that the supply for the main tunnels has to be managed through long access tunnels running perpendicular to the main tunnel itself. For example the Ahrental access tunnel was driven from west to east from the northern Wipptal valley down to the level of the tunnel.

The access tunnel is 2.4 km long and has a maximum slope of 11.5 % (Figure 2) and cross section of approximately 92 m². At its end, the access tunnel terminates with a 90° turn into the exploratory tunnel which runs from north to south. About 1.2 km south of this junction, the assembly/launching chamber for the TBM was built.

4 CONTRACTOR’S SOLUTION - MULTI SERVICE VEHICLE

Detailed cycle analyses and studies that were carried out by the contractor showed that an optimal excavation cycle required 95 tons of consumables to be transported with a single vehicle from the portal to the TBM. This corresponds with a double stroke of 3.4 m of tunnel length. When the MSVs for this project were procured (Spring 2015), 55 tons was the maximum load capacity for MSVs with acceptable track accuracy for the curve demands of the tunnels. Therefore the length of the MSVs was limited due to trajectory deviation.

Therefore decisive developments jointly with ROWA, the MSV manufacturer, were necessary to improve the track accuracy and increase the load capacity of the vehicles accordingly. The 90° turn at the end of the access tunnel and the centered entrance to the TBM back-up gantries were the key challenges. The development of a “virtual rail” was the only way to improve the track accuracy and keep the trajectory deviation of the multiple axles to a minimum, while maintaining the 30 m curve radius. It was necessary to solve the following issues:

- Development of a software that would collect and evaluate the vehicle data from different steering sensors and distance sensors (on the front and sides of the vehicle). The steering of the MSV’s uses a complex, newly developed algorithm which considers the length of the platform cars, tow bar angles between the platform cars, steering angles of the axles and the axle spacing.
- The operational reliability of the sensors which were required to scan the surrounding of the MSVs. Some of the sensors available on the market proved not to be suitable for the extreme environmental conditions of a tunnel excavation (dust, humidity, surface vs. underground temperature differences, driving in a smoke-filled tunnel in case of fire, etc.)
- Suitability of the hardware components and/or the mechanical and structural parts (for example, the steering system, the shock absorbers, the braking system, axles, motors, chassis, wheels, electrical and hydraulic systems, steering and regulation systems, main on-board computer etc.).

It took six months for BBT SE and the JV of STRABAG/Salini/Impregilio, jointly with the pertinent authorities (fire and rescue brigades & the inspector for worker safety) to implement this innovative solution to handle the logistical challenges. A team that included members of the Joint Venture, the manufacturer ROWA and in-house experts from the JV headquarters in Vienna, Stuttgart and Milan compiled a specifications manual with basic requirement for design, equipment and operation of the self-steering MSVs.

The result was newly developed MSVs consisting of 5 mechanically linked platform cars, travelling rail-free and carrying 95 tons of material from the tunnel portal to the TBM backup. All 14 axles are steered automatically and independently so as to follow the new “virtual rail”. The first axle defines the track of the “rail” and the following axles follow it; any additional deviation is recognized by the various sensors and automatically compensated by the control software.

A further challenge for the working group was the slope of the lateral access tunnel. A fully loaded MSV was required to travel a 2.4 km stretch with a 11.5 % slope in traffic along with other vehicles in safe manner. Therefor a triple-redundant breaking system was developed and installed (see also chapter 6.5).

5 SAFETY

During numerous discussions the emergency services specified two requirements with regards to the use of the MSV's

- Requirement for the fire brigade to use the MSV's for rescue and firefighting services with all necessary equipment
- Evacuation of the workers from the exploratory tunnel in case of smoke (driving with maximum safety distance precautions due to poor visibility)

The requirements for the fire brigade train were taken from the tender documents and adapted in a special fire brigade MSV (see Reichel, 2019).

If visual conditions are insufficient for safe driving, the driver will steer the rescue vehicle via a monitor showing the stretch in front of the vehicle. Radar sensors show the distance to the tunnel walls and the driver must therefore steer the vehicle in a way to always remain in the largest possible distance to the tunnel walls. The radar sensor also scans the area in front of the vehicle for obstacles.

6 TECHNICAL DESCRITPION OF THE MSV

The technical data and the various configuration of the MSV's being used in the Construction Lot Tulfes Pfons are listed as follows.

Figure 3. Layout of the ROWA Multi Service Vehicle [ROWA].

6.1 *Configuration of the MSV's supplying the TBM*

The TBM is supplied by three MSV long trains, each of them carries consumables for two 1,7m strokes, i.e. a total length of 3,4m. The consumables include:

- Steel Ribs (UNP140/160/180, TH29), wire mesh (AQ60), elements of conveyor belt frames, anchor bolts, rails, pipes – pre loaded on pallets
- Invert segments: 2 elements, 5 m in width, 1.7 m in length, 1.4 m in height, weight: 14 t per segment
- Covers for the invert segments: 2 elements, 3.18 m in width, 1.7 m in length, 0.3 m in height, weight approx. 4 t
- 1 container with back fill grout of the invert segments 1.5 m^3, empty weight ~1.85 ton, full 4.15 t

Table 1. Technical data of the ROWA Train [ROWA].

Installed diesel power:	approx. 460	kW
Maximum speed on a 0.67% upward gradient; full train:	25	km/h
Maximum speed on a -11% downward gradient; full train:	15	km/h
Maximum speed on a 11% upward gradient; empty train:	15	km/h
Maximum speed on a 11% upward gradient; full train (exception):	5	km/h
Weight of the empty train:	approx. 35	t
Loaded weight on the way towards the TBM:	max. 95	t
Weight of the full train (towards the TBM):	max. 132	t
Load on the return trip:	max. 17	t
Weight of the train on the return trip:	max. 52	t
Maximum axle load	approx. 90	kN
Maximum wheel load	approx. 45	kN
Minimum curve radius	30	m
Length:	52.4	m
No. of steered and braked axles	14	
No. of driven/powered axles	7	

- 1 shotcrete tank: volume 8 m³, weight 25 t per full bucket, 5 t empty

Figure 4. MSV configurations [ROWA].

1 short train for special transports (for example to transport drums of conveyor belt and medium voltage cable)

- Vehicle load capacity: about 30 t
- Tare weight: about 18 t
- Length: 22.9 m

Figure 5. Special transports [ROWA].

6.2 *Special vehicles (Self rescue and Rescuelfirefighters)*

1 short train for self-rescue

- Autonomous rescue container for 25 people for 8 hrs stay on a platform car
- Always parked about 50–100 m behind the TBM

Figure 6. Special vehicle (Self Rescue MSV) [ROWA].

1 short train for/firefighter/rescue MSV)

- Each of the two cars holds an isolated rescue container with an integrated driver's cabin and self-contained air supply (regeneration technology)

- Six people plus the driver can fit in the rescue container of the motor vehicle. Nineteen people plus the driver can fit in the rescue container of the trailer vehicle. The air supply is meant to last 10 hours for max. 20 people.
- The vehicle is always ready for use at the Ahrental portal

Figure 7. Special vehicle (Fire fighter/rescue MSV) [ROWA].

6.3 *Driving modes for the MSV's*

6.3.1 *Normal driving mode*

This is the driving mode used during normal operations. In this mode, the driver simply regulates the vehicle's speed or uses the brake. The actual steering of the vehicle is done in all sections of the tunnel (site installation area, Ahrental access tunnel, assembly/launching chamber, and exploratory tunnel) by the intelligent steering system.

The driver has to choose the listed tunnel sections by using joystick in the operators cabin. For all tunnel sections a predefined track is specified.

6.3.2 *Manual mode*

The manual mode is an "emergency -mode" which is only needed if there are no guide plates installed at the tunnel walls. Since the steering cannot be adjusted automatically by the lateral sensors, the driver must steer the vehicle manually. In order to maintain sufficient track accuracy at low speed, a trim function has been built in.

6.3.3 *Manoeuvre mode*

The manoeuvre mode is required when a MSV must be driven out of a special situation, for example, if it comes too close to the tunnel wall or if it is stopped due to an obstacle detected by the safety controls. In this case, the driver must select the manoeuvre mode on the touch screen. Having done this, the driver can select and control individual axles or groups of axles to manoeuvre the train out of the situation. In this mode, the vehicle's top speed is only 1 km/h.

6.4 *Train control and steering system*

The following sensors are required to scan the surrounding of the MSV's:

- Laser scanners (in the front of both driver's cabins, with a range of about 26 m, tested on autonomous driven wheel loaders and other underground machinery)
- Radar sensors (in the front of both driver's cabins, with a range of about 40 m tested on road vehicles with ACC, functional even in poor visibility conditions and able to detect objects even at greater distances)
- Laser sensors (on the sides of the vehicle, in order to constantly monitor the distance to the tunnel wall), each platform car has 3 laser sensors with a range of about 3 m,
- Ultrasonic sensors (on the sides of the vehicle, in order to constantly monitor the distance to tunnel wall, when laser sensor functionality is limited by smoke or dust, range: about 5 m, tested on other underground machinery to detect objects at short distances)

On-site tests were carried out before production began to assess how the surface of the tunnel walls would be detected by the sensors. Reflecting strips and guide plates were installed on the tunnel walls to test how the identification of the track could be improved, which was acknowledged as a problematic issue. Reflecting guide plates placed on the tunnel wall at intervals of 3 m to 6 m provided the best results.

The tunnel wall or the reflecting plates on the wall are identified by the radar sensors and laser scanners installed below the driver's cabin. Based on that information the steering software creates a "virtual rail", which can run in the middle of the tunnel or at a certain distance to the tunnel wall. An electronic map of position and distance information leads the first axle, which is virtually steered as if along an actual rail. The virtual rail is also used to define the track position of all the following axles. Due to a complex, newly developed algorithm (input value for example the tow bar angle, steering angle and speed) all axles follow exactly the track of the previous axle. The tolerances and inaccuracies resulting from the sensor system, which are the reason for the track deviations, are equalized by the continuous measurement of the ultrasonic and laser sensors on the sides of the platform cars. Since the lengths of the platform cars and the distances between the following axles are known, the newly developed algorithm ensures that the distance of the following axle to the tunnel wall is the same as distance of the previous axle.

The steering sensors (front and sides) are redundant, so there are multiple sensors per platform car. Using the virtual rail it is possible to indicate a pre-defined track in the various tunnel sections to be followed by the self-steering MSV's in automatic mode. However, the driver of the vehicle always maintains control over the speed, steering and if necessary emergency braking.

6.5 *Braking system/Braking levels*

The MSV's has independent braking systems (sustained-action braking system, service/foot-brake and parking break), which engage and release in different ways

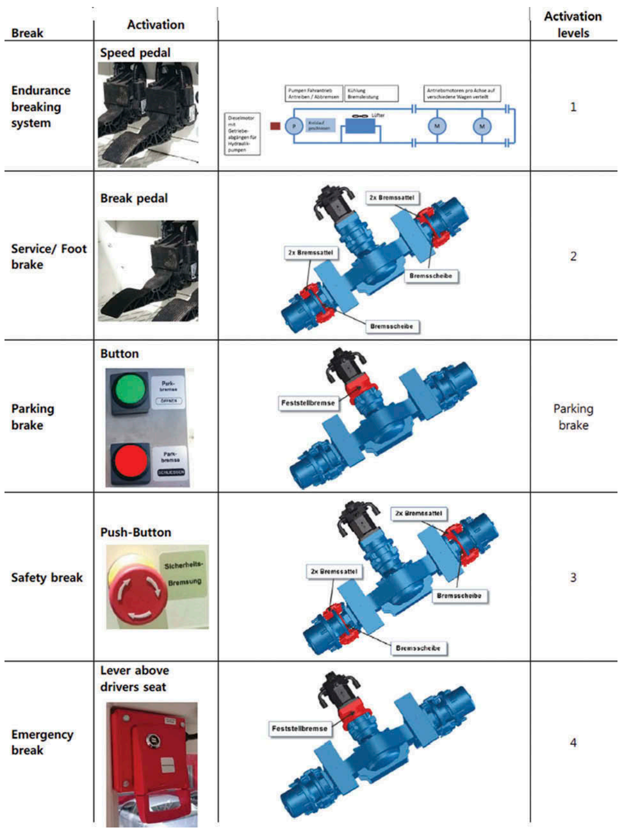

Figure 8. MSV Braking systems [ROWA].

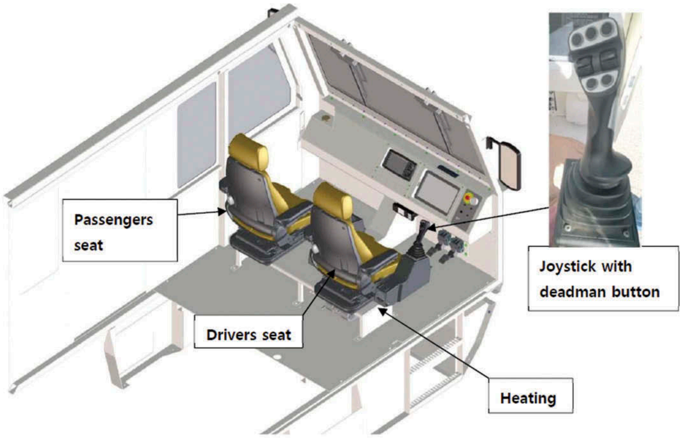

Figure 9. Layout of the driver's cabin [ROWA].

7 COMPARISON OF THE MSVS WITH A NORMAL BOUND TBM SUPPLY SYSTEM

After the successful completion of a 12 km TBM drive, it was concluded that MSVs could be more advantageous than conventional rail bound logistics systems for this construction lot. In the special conditions of the Brenner Base Tunnel, with its steep access tunnel and long tunnel drives, the following advantages of the MSVs as compared to rail-bound supply trains were determined:

- Continuous supply transport from the site installation area via the access tunnel and the exploratory tunnel to the TBM without re-loading in the tunnel.
- Avoiding the use of over 10 standard trucks which would be required in case of handing over the consumables to a rail bound train. This means less traffic in the access tunnel which is already congested with trucks to supply the drill and blast tunnel drives and inner lining works.
- There is no need to install rails behind the TBM, making access to the TBM much more flexible. The TBM can be reached with normal vehicles as well. For safety reasons, the

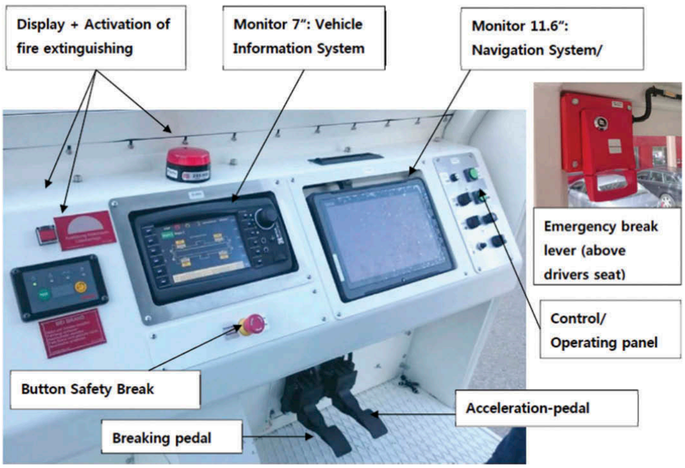

Figure 10. Layout of panel in Driver's cabin [ROWA].

number of vehicles is restricted and only 8-seater buses with specially trained drivers are used to transport workers and staff. In case of a smoke-free accident on the TBM, a rescue vehicle or ambulance can drive directly up to the TBM. Rescue times are significantly reduced and rescue services avoid having to change vehicles, especially since they have all their equipment with them.

8 SUMMARY

Till 31.08.2018 12 km (about 80 %) of the excavation of the exploratory tunnel in construction lot Tulfes Pfons have been completed, the use of the self-steering MSV's can already be determined as a success. The three MSV long trains have travelled approx. 115,000 km without major problems.

The availability of the MSV's is currently about 99 %, which means that standstill times due to breakdowns were significantly less compared to a rail-bound supply system. Furthermore all the standstill times required for to maintain and repair the rail track and switches are eliminated while using MSV's.

On-site tests have shown that the MSV's perform well as a rescue vehicle.

What's new in these MSVs:

- The first worldwide use of self-steering MSVs (almost autonomous driving in a tunnel project
- The first use of a virtual rail created by a tight sensor network with laser, ultrasonic and radar measurements to create an electronic map with positioning and distance information
- The development of a complex control software in order the minimize track deviations of the various axles which are steered independently but in total synchronic
- An extension of the MSV length (up to ten platform cars) and the consequent increase is load capacity at any time due to the currently installed software and algorithms.

The self-steering MSV's currently used in the Brenner Base Tunnel are the first step in developing driver-less tunnel supply vehicles, which will certainly be the future of supply logistics in tunnel construction sites. It takes courage from all project parties involved to share the risk to use new technologies.

REFERENCES

Bergmeister, K.; Reinhold, C. 2017. Learning and optimization from the exploratory tunnel – Brenner Base Tunnel. *Geomechanics & Tunneling* 10, No. 5, S. 467–476

Bergmeister, K. 2019. Tunnel construction methods of the Brenner Base Tunnel and their logistical challenges – A multi-criteria decision approach. *ITA-AITES World Tunnel Congress 2019*, Naples, Italy.

Reichel, E. 2019. Novel safety concept at the Austrian construction lots of the Brenner Base Tunnel. *ITA-AITES World Tunnel Congress 2019*, Naples, Italy.

Rowa 2018. Rowa Tunnelling Logistics AG, Wangen, Swiss

Schwarz, C. 2019. Seismic prediction of the rock quality at the Brenner Base Tunnel. *ITA-AITES World Tunnel Congress 2019*, Naples, Italy.

Insam, R.; Carrera, E.; Crapp, R.: Das Entwässerungssystem des Brenner Basistunnels. *Swiss Tunnel Congress*, Luzern, 2018.

Tunnels and Underground Cities: Engineering and Innovation meet Archaeology, Architecture and Art, Volume 6: Innovation in underground engineering, materials and equipment - Part 2 – Peila, Viggiani & Celestino (Eds)

Experiences from tunnel boring when hard-to-very hard rock with focus in performance predictions and cutter life assessments

F.J. Macias
JMConsulting – Rock Engineering, Oslo, Norway

ABSTRACT: The use of hard rock tunnel boring machines (TBMs) has become widely and generally used with success but in too many cases, due to inappropriate assessments, with undesirable consequences. A process of great complexity is involved during tunnel boring. When hard-to-very hard rock (i.e. low-to-extremely low boreability), the complexity is accentuated becoming, in many cases, critical for the achievement of the final schedule and reasonable tunnelling cost. Performance predictions and costs estimates have a major influence on the planning and risk management of TBM excavation projects. A proper understanding of tunnel boring and wear processes in hard rock enhances an appropriate applicability of the models for performance prediction and cutter life assessments. The paper compiles experiences and outcomes from research and consulting collaborations on several hard rock TBM projects and during the revise and extend of the current version of the NTNU prediction model for TBM performance and cutter life.

1 INTRODUCTION

The Tunnel Boring Machine (TBM) approach has become widely used and is currently an important method employed by the tunnelling industry for civil and mining infrastructures. Nowadays, the TBM method, due to the technology development, is applicable in an increasingly wider range of rock mass conditions: excavations can now be carried out in almost all rock conditions using this method, given certain economic constraints.

A process of great complexity is involved when tunnel boring due to the interaction between the rock mass and the machine. The prediction of performances (e.g. Penetration rate) and cutter life are not straightforward issues and involve major risk assessments. When hard-to-very hard rock (i.e. low-to-extremely low boreability) the complexity is accentuated becoming, in many cases, critical for the achievement of the final schedule and reasonable tunnelling cost

Understanding of tunnel boring and wear processes thus enhances performance prediction and cutter life assessments in hard rock tunnel boring project. Performance predictions and costs estimates are often decisive in the selection of excavation methods and have a major influence on the planning and risk management of TBM excavation projects.

The paper compiles experiences and outcomes from research and consulting collaborations on several hard rock TBM projects and during the revise and extend of the current version of the NTNU prediction model for TBM performance and cutter life.

2 HARD ROCK TUNNEL BORING

2.1 *Rock boreability in hard rock*

'Rock mass boreability' is a comprehensive parameter of rocks under excavation and expresses the result of the interaction between a given rock mass and a TBM. Boreability can be defined as the resistance (in terms of ease or difficulty) encountered by a TBM as it penetrates a rock mass composed of intact rock containing planes of weakness.

Penetration rate and cutter wear are influenced by intact rock and the rock mass properties. Intact rock properties are typically defined in terms of strength, abrasivity, porosity, schistosity and rock petrography.

Rock mass fracturing (e.g. planes of weakness or discontinuities, orientation…) is found to be the geological factor that exerts the greatest influence on net penetration rate, and which consequently also has a major impact on tunnelling costs in hard rock (Bruland, 2000). A high rock mass fracturing parameter means greater rock mass boreability during hard rock TBM excavation. In addition, the penetration rate may also be influenced by in situ rock stress, groundwater and other factors.

Hard rock refers to a minimum UCS values > 50 MPa (High rock strength) and typically UCS values > 100 MPa (Very high strength) according to the classification given by ISRM (1978).

2.2 *Performance prediction and cutter life models for hard-to-very hard rock*

The net penetration rate (m/h) is determined from both rock mass properties and machine parameters and it is the main factor used for predictions (i.e. advance rate, cutter consumption and the costs) of hard rock TBM tunnelling projects.

Advance rate determines the total boring advance achieved over a period (e.g. days, weeks, months…). Advance rate is given from the net penetration rate (m/h) and considering the machine utilization. The machine utilization is net boring time of the total available time expressed in percentage. Much of the available time is used for other activities than boring (e.g. re-gripping, cutter change and inspection, repair and service of the TBM and back-up, rock support, transport system installation and delays, tunnel service installation and delays, surveying and others). The final goal of performance prediction for hard rock TBMs is the estimation of time and cost.

Estimations should in addition consider assembly and disassembly of the TBM and the back-up, permanent rock support and lining, excavation of niches or branching, boring through and stabilizing zones of poor rock quality, probe drilling and pre-injection works, major machine breakdowns, dismantling of installations, additional time for unexpected rock mass conditions.

Several prediction models for estimates of performance and cutter wear in hard rock tunnel boring have been developed in recent decades. Models used to estimate penetration rates include those of CSM model (Rostami and Ozdemir, 1993; Rostami, 1997, Yagiz, 2014), the Gehring model (Gehring, 1995; Wilfing, 2016), the NTNU model (Bruland, 2000; Macias, 2016), the QTBM (Barton, 2000), RME (Bieniawski et al., 2006), Gong and Zhao (2009), Hassanpour et al. (2011) and Farrokh et al. (2012).

These models adopt very different approaches and their input parameters, especially in terms of rock mass properties, exhibit substantial variation. This makes balanced comparisons problematic. However, under ordinary conditions, the results of the models may exhibit satisfactory agreement. A further issue for consideration is the scope of applicability of the different models.

3 EXPERIENCES WHEN HARD-TO-VERY-HARD ROCK

3.1 *Introduction*

Tunnelling technologies continue to improve, and the TBM sector is no exception. Continuous updating and a better understanding of the tunnel boring process should be applied to the development and revision of prediction models.

Research and consulting collaborations on several hard rock TBM projects during the revise and extend the NTNU prediction model for TBM performance and cutter life (Macias,

2016) result in new experiences and outcomes giving a better understanding of the tunnel boring process. Latest and current consulting collaborations carry out by the undersigned are being used for validation and further development.

3.2 *Rock boreability and TBM predictions*

There is no single parameter that can fully represent the properties of jointed rock masses. Different parameters have different emphases and can only provide a satisfactory description of a rock mass in an integrated form (Singh and Goel, 2011).

To evaluate the influence of rock mass when hard-to-very hard rock can be decisive on the tunnel boring and it is not always easy or straightforward. A comprehensive understanding of the rock mass boreability requires different approaches to its evaluation (e.g. use of both, chip analysis and tunnel face inspection, to support engineering geological back-mapping).

Excavation costs predictions for hard rock TBM projects incorporate a geological risk, which becomes of major importance, from a cost point of view, when hard-to-very hard rock and degrees of fracturing are low.

The establishment of dimensional-related definitions for the wide variety of intact rock and rock mass discontinuities has proved to be problematic. Figure 1 presents a proposed length-based classification of the main types of discontinuities from an engineering geological perspective according to the NTNU back-mapping methodology.

The influence of geology on the prediction performance of the NTNU model increases as the degree of fracturing in the rock mass decreases. Based on mapping analysis and experience, the influence of the average spacing has been extended (up to 480 cm) within the latest version to date of the NTNU model (Macias, 2016) including a fracture class (s_f) "Class 1", which is intermediate between the formers fissure classes 0 and 0-I. Table 1 shows the fracture class terminology as defined by the average spacing between fractures (Macias, 2016).

Low values of degree of fracturing (e.g. St 0, 0-I and St I-) have a dramatic influence on excavation cost estimates. However, if the rock mass is highly fractured, then variations in degree of fracturing do not significantly influence excavation costs.

Figure 2 illustrates relative excavation costs as determined by the degree of fracturing for a 7 m diameter TBM with standard machine specifications and rock properties (medium drillability and abrasivity) by using the NTNU model. The reference excavation cost value applied is for fracture class St I.

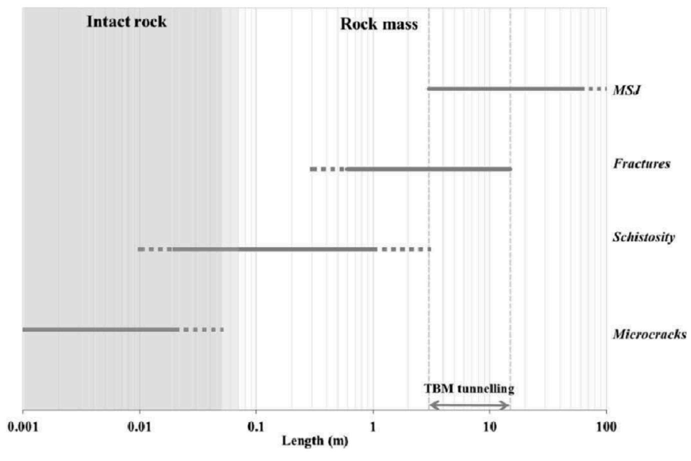

Figure 1. The main types of intact rock and rock mass discontinuities encountered during back-mapping in hard rock TBM tunnelling. Types are categorised according to length based on the NTNU methodology. The shaded area indicates where data have been derived from laboratory tests carried out on intact rock (Macias, 2016).

Table 1. Fracture class terminology as defined by the average spacing between fractures (Macias, 2016).

Fissure class (St) (Bruland, 2000)	Fracture Class (Sf) (Macias, 2016)	Average spacing between fractures a_f (cm)	Range class (cm)	Degree of fracturing
0	0	∞	480 – ∞	Non-fractured
0	1	320	240 – 480	Extremely low
0 - I	2	160	120 – 240	Very low
I -	3	80	60 – 120	Low
I	4	40	30 – 60	Medium
II	5	20	15 – 30	High
III	6	10	7.5 – 15	Very high
IV	7	5	4 – 7.5	Extremely high

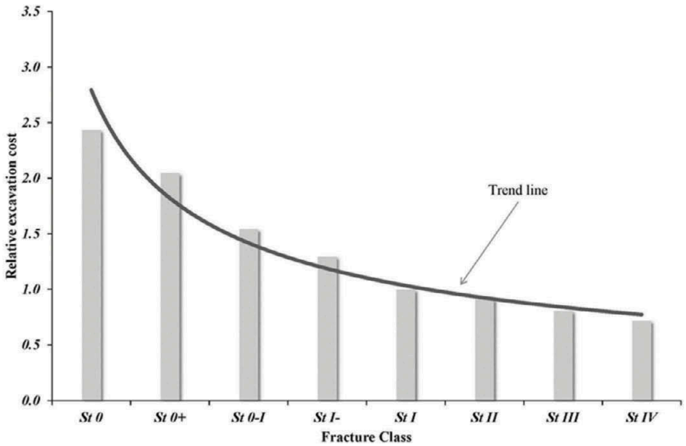

Figure 2. The relationship between relative excavation costs and degree of rock fracturing.

At lower degrees of fracturing, results indicate increments in predicted excavation costs of 20 to 70 per cent between individual classes, amounting to an increase in approx. 150 per cent relative to the reference standard, class St I. However, variation within highly fractured rock masses results in a reduction of the predicted excavation cost of 10 to 30 per cent between individual classes (amounting to a reduction of approx. 40 per cent relative to the reference). Important to bear in mind that additional time and cost associated with ground stability in highly fractured and faulted zones is not included.

Special care should thus be taken when predicting TBM performance and excavation costs in rock masses exhibiting low levels of fracturing.

3.3 *Cutter life*

The NTNU cutter life model has been reviewed based on detailed information about geology, rock mass, drillability testing and instantaneous cutter life based on selected tunnel sections at several projects (Macias, 2016).

Basic cutter ring life was back-calculated from the instantaneous cutter life parameter for every tunnel section, taking correction factors for TBM diameter, cutterhead rpm, number of cutters, abrasive minerals content and cutter thrust into consideration.

A variation factor of 15% of the cumulative distribution of CLI and quartz content is applied. In order to account for uncertainties arising from ring steel quality, set bearing capacity and other properties, a variation factor of 10% is used.

The updated version has been modified in the light of minimum cutter ring life values and data obtained from previous versions of the model (Figure 3).

The increment of the predicted basic cutter ring life in the updated version compared with the previous (Bruland, 2000) has been up to around 20%. This might be due to the effects of changes of cutter tip design and/or improvements in cutter technology over the last two decades.

Figure 4 shows plots of basic cutter ring life (h) for 432 and 483 mm cutter diameters obtained from the updated (2016) version of the NTNU model.

Calculations for 508 mm (20 inch) cutter diameters have not been included due to insufficient data, although it can be noted that results indicate a longer basic cutter ring life, as expected, for highly abrasive rocks (exhibiting extremely and very low CLI values).

3.4 *Other geological factors influencing cutter wear*

In fractured rock masses, or in situations where extremely good rock chipping occurs, the cutters will be exposed to large instantaneous loads. Entacher et al. (2013) measured momentary

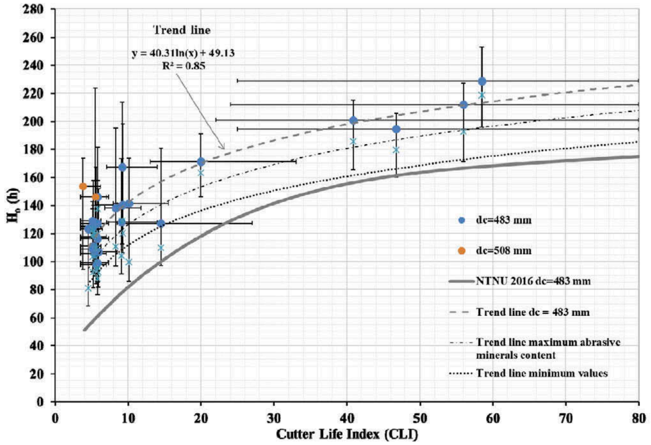

Figure 3. A plot showing basic cutter ring life obtained using the 2016 version of the NTNU model for 483 mm and 508 mm diameter cutters. Results from the uncertainty analysis are also plotted.

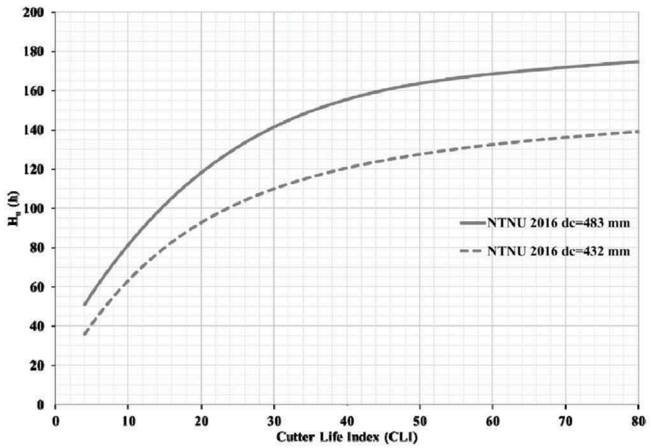

Figure 4. Plots showing basic cutter ring life (h) for 432 and 483 mm cutter diameters obtained from the updated (2016) version of the NTNU model.

loads in individual cutter discs up to 3.5 times higher than a nominal cutter load and up to 10 times higher than the average load in fractured rock.

Under such conditions, a cutter ring exhibits a tendency to chip along its edge. Extensive ring chipping and high cutter thrust may result in bevel edge wear, loosened rings and blocked bearings.

Additional loads will result in higher abrasion on protruding cutters when the difference in diameter between adjacent cutters is too large as a result of deficient wear height control. Heavy vibration of the cutterhead results in high lateral forces on the cutters, which in turn causes additional abrasion.

Fractured rock masses promote greater penetration rates and thus effectively prolong cutter life (in m/c and sm^3/c). However, due to the aforementioned effect of fractures, higher levels of cutter consumption, measured in hours, will be expected. This effect will be more dominant in rocks exhibiting low drillability and high abrasivity.

Figure 5 shows cutter life data (sm^3/c) and wear patterns taken from several tunnel sections exhibiting a variety of rock mass conditions. The contact skarn in Figure 5 is a tunnel section transitioning to a fractured rock type, which produces large instantaneous loads on the cutters resulting in a high rate of cutter replacement due to bearing set problems such as blockage.

Higher amount of chipping is related to fractured rock while blocked cutters occur in rock types transition and high cutter thrust.

3.5 *Influence of Cutterhead velocity influence on penetration*

The operational parameters (i.e. applied cutter thrust and cutterhead velocity), in combination with the rock boreability, have a great influence during tunnel boring in hard rock.

Efficient boring should be considered to improve the advance rate along the tunnel by applying an optimal net penetration rate considering cutter consumption, potential damage of cutters, probability of bearing failure and cutterhead damages, as well as energy consumption.

A reduction in cutterhead velocity (rpm) values may improve boring efficiency and reduce excavation costs. Lower cutterhead rpm will promote lower cutter rolling distances and velocities for a given section of tunnel, resulting in significantly higher cutter ring life and a reduction in potential damage to cutters. Moreover, for a given thrust level and fewer revolutions of the main bearing reduce the probability of bearing failure and cutterhead damages, as well as energy consumption.

An 'RPM test' measures cutterhead penetration over a given period at a variety of cutterhead velocities under constant cutterhead thrust. The aim of the test is to evaluate the

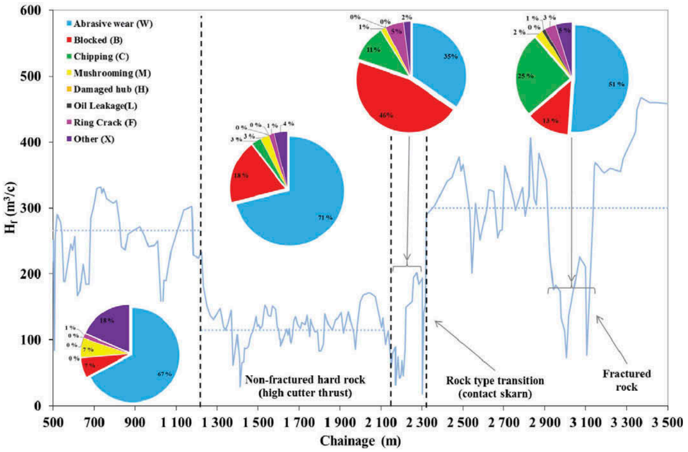

Figure 5. Cutter life data and wear patterns from several tunnel sections.

influence of cutterhead velocity (rpm) on penetration rate (mm/rev) for maximum net penetration rates (m/h) for a given machine, geology and thrust level (Macias, 2016).

The 'RPM' tests revealed that in general, a lower cutterhead velocity would result in an increase in penetration rate up to a given value beyond which it decreases. The values concerned are dependent on cutterhead design, rock mass properties and level of thrust.

The resulting values obtained from the 'RPM tests' include values of penetration rate (PR, in mm/rev) and net penetration rate (NPR, in m/h) for each cutterhead rpm at constant level of thrust. The 'RPM tests' usually result in a cutterhead velocity value and a maximum NBPR for a given machine, geology and level of thrust. For higher and lower cutterhead rpm values, the NPR is reduced. Lower cutterhead rpm result in an increase in PR up to a given value beyond which it decreases dramatically. This also causes the NPR to be reduced.

An increase in penetration rate (PR), without compromising the net penetration rate (NPR), results in improved tunnelling efficiency. The 'optimal' cutterhead velocity is thus defined as the cutterhead rpm value, which achieves maximum penetration rate while maintaining the 'optimal' level of net penetration rate for the geological conditions and level of thrust in question. Net penetration rate is assumed 'optimal' for a 5% from the maximum value. Figure 6 shows an example of an 'RPM' test in which the main parameters are exemplified.

The variation between the initial and optimal cutterhead rpm and PR values provides an indication of improvements in boring efficiency achieved during the tests for a given machine, geology and level of thrust. The results indicate that the tendency for all normalised 'RPM tests' is similar.

The influence of the operational parameters, cutter thrust and cutterhead velocity (rpm), in hard rock tunnel boring efficiency can be analysed on the basis of field trials or 'on-site' testing (Penetration tests and 'RPM tests'). 'On site' testing, involving penetration and RPM tests, can be used to evaluate the influence of the operational parameters and determine the 'optimal' values on a given geology (rock boreability) and for a given machine.

3.6 *Cutter thrust level influence on cutter consumption*

The influence of applied cutter thrust on cutter life has been analysed by Macias (2016) for tunnel sections within three different projects exhibiting hard rock conditions (high levels of strength, high abrasivity and slightly fractured rock mass properties).

The results of the analysis reveal the influence of gross cutter thrust levels in highly abrasive rock types where 4.5 < CLI < 5.9. The use of basic cutter ring life (hours) allows the

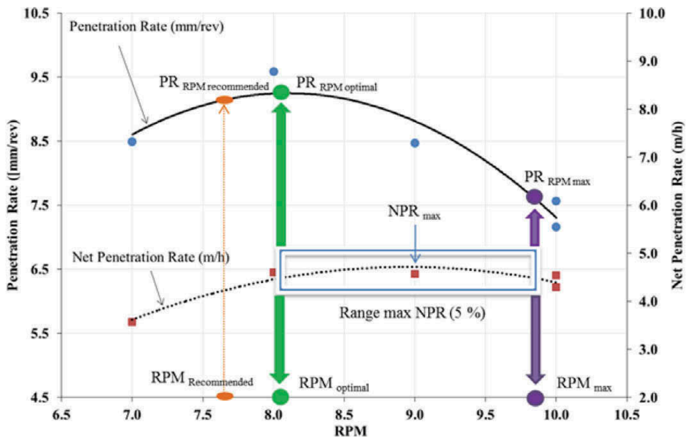

Figure 6. An example of 'RPM test' results. Vertical lines (from right to left) denote the start of the test, the cutterhead rpm reference and the cutterhead rpm optimal (from Macias, 2016).

comparison between the data from different TBM cutterhead diameters, cutterhead rpm levels or amount of abrasive minerals.

Figure 7 indicates that the increment of the applied cutter thrust will reduce considerably the basic cutter ring life while a more limited increment will result from a reduction of the applied cutter thrust. It is important to consider that, a variation of the thrust will result in variations on the net penetration and therefore in cutter life (expressed in m/c or m^3/c).

3.7 *Length Factor*

The length of the tunnel has great influence on the performances due to problems with the tunnelling system (transport system, supply delays, ventilation and/or water). In addition, longer tunnels have greater likelihood to have end rock mass qualities and, normally, a more deficient geology investigation.

It has been emphasized by Barton (2000) that the utilization is time-dependent with, in reality, a deceleration gradient. The machine utilization, and thus advance rate, is not a constant in tunnel length and therefore time.

Tunnel length exerts an important influence on the time taken to carry out tunnelling activities (Barton. 2000). During the initial "learning curve" period of a tunnelling project, certain operations take a relatively long time as the crew builds up its skills levels, and the tunnelling quality assurance system evolves. For long headings (>8 km), miscellaneous factors put increasing demands on available tunnelling time (Bruland, 2000).

The longer the tunnel, the higher the probability of problems arising linked to factors such as muck transport and ventilation, electricity and water supply systems, as well as other supply delays. Waiting times for transport will increase substantially if the capacity of the transport system is inadequate.

Problems linked to ventilation, electricity and water supplies will continue to increase with increasing tunnel length. Moreover, the transport system will be dependent on penetration rate and the amount of material that requires transportation. The higher the penetration rate, the greater the likelihood of downtime and other problems linked to supply delays and other issues with the transport system.

The NTNU model database is based on tunnels up to 10 kilometres in length. Time consumption data used in previous versions of the model were averaged over total tunnel length. The latest version of the NTNU model (Macias, 2016), includes additional time consumption (h/km) related to tunnel length with influence in machine utilization and therefore advance

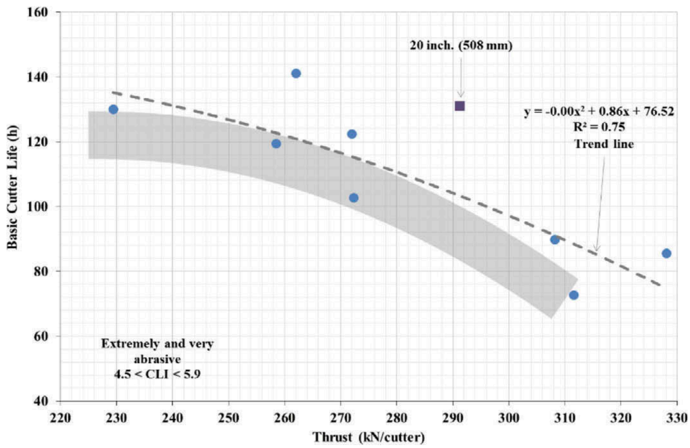

Figure 7. The influence of cutter thrust levels on cutter life (19-in. cutters) for highly abrasive rocks (4.5<CLI<5.9). The 20-in. cutter diameter value is deliberately excluded from the data used to construct the trend line (from Macias, 2016).

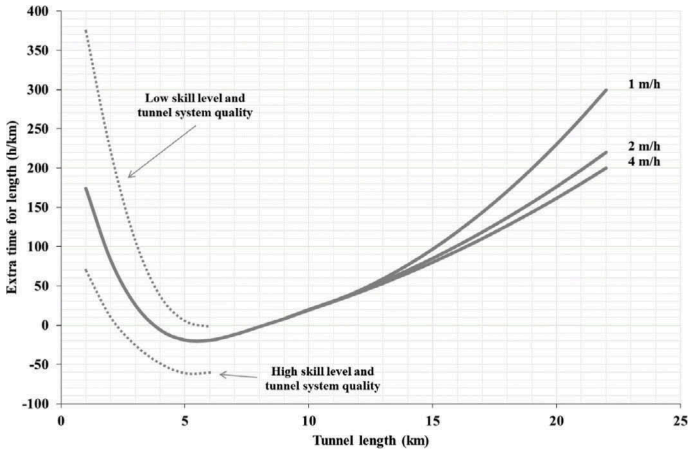

Figure 8. Additional time (h/km) plotted against tunnel length (Macias, 2016).

rate factor (Figure 8). Boundary limits have been included for low and high skills levels and tunnel system quality. The values for every kilometre correspond to the extra time during the last km.

The term ‘skills levels’ refers not only to crew members, but also to equipment manufacturers and others.

4 CONCLUSIONS

Tunnelling technologies continue to improve, and the TBM sector is no exception. Currently, the TBM method, due to the technology development is applicable in an increasingly wider range of rock mass conditions, given certain economic constraints.

A process of great complexity is involved when tunnel boring due to the interaction between the rock mass and the machine. The prediction of performances (e.g. Penetration rate) and cutter life are not straightforward issues and involve major risk assessments. When hard-to-very hard rock (i.e. low-to-extremely low boreability) the complexity is accentuated becoming, in many cases, critical for the achievement of the final schedule and reasonable tunnelling cost.

Continuous updating, likely resulting in a better understanding of the tunnel boring process, should be applied to the development and revision of prediction models.

The paper has concisely compiled experiences and outcomes from research and consulting collaborations on several hard rock TBM projects and during the revise and extend of the NTNU prediction model for TBM performance and cutter life (Macias, 2016): Rock boreability when low degree of fracturing, update cutter life assessments, other geological factors influencing cutter life, influence of applied cutter thrust on cutter life and tunnel length influence on advance rate, excavation time and cost.

Latest and current consulting collaborations carry out by the undersigned are being used for validation and further development.

REFERENCES

Barton, N. 2000. TBM tunnelling in jointed and faulted rock. *A.A. Balkema*, Rotterdam (2000). ISBN 90 5809 341 7.

Bieniawski, Z.T., Celada, B., Galera, J.M. & Alvarez, M. 2006. Rock mass excavability indicator: new way to selecting the optimum tunnel construction method. *Tunnelling and Underground Space Technology* Vol. 21, no.3–4 (2006), pp 237.

Bruland, A. 2000. Hard Rock Tunnel Boring: Vol 1–7, Background and Discussion. PhD thesis. *Norwegian University of Science and Technology (NTNU)*, Trondheim, Norway, 2000.
Entacher, M., Winter, G. & Galler, R. 2013. Cutter force measurement on tunnel boring machines – Implementation at Koralm tunnel. *Tunnelling and Underground Space Technology* Vol. 38 (2013), pp 487–496.
Farrokh, E., Rostami, J. & Laughton, C. 2012. Study of various models for estimation of penetration rate of hard rock TBMs. *Tunnelling and Underground Space Technology* Vol. 30 (2012), pp 110–123.
Gehring, K. 1995. Leistungs- und Verschleißprognosen im maschinellen Tunnelbau. *Felsbau*, Vol. 13, no. 6 (1995), pp 439–448 (in German).
Gong, Q.M. & Zhao, J. 2009. Development of a rock mass characteristics model for TBM penetration rate prediction. *International Journal of Rock Mechanics & Mining Sciences* Vol. 46 (2009), pp 8–18.
Hassanpour, J., Rostami, J. and Zhao, J. 2011. A new hard rock TBM performance prediction model for project planning. *Tunnelling and Underground Space Technology* Vol. 26 (2011), pp. 595–603.
ISRM International Society for Rock Mechanics. 1978. Suggested methods for the quantitative description of discontinuities in rock masses. – Commission on Standardization of Laboratory and Field Tests, Document No. 4, *International Journal of Rock Mechanics & Mining Science*, Vol. 15 (1978), pp 319–368.
Macias, F.J. 2016. Hard Rock Tunnel Boring: Performance predictions and cutter life assessments. PhD thesis, *Norwegian University of Science and Technology (NTNU)*, Trondheim, Norway (2016).
Macias, F.J., Andersson, T. & Eide, L.N.R. 2017. Project control by using the NTNU model methodology: The new Ulriken Tunnel. *Proceedings of the World Tunnel Congress 2017-Surface Challenges-Underground solutions*. Bergen, Norway.
Rostami, J. & Ozdemir, L. 1993. A new model for performance prediction of hard rock TBMs. *Proceedings, rapid Excavation and Tunnelling Conference (RETC 1993)*, Boston, Massachusetts, USA (1993), pp 793–809.
Rostami, J. 1997. Development of a force estimation model for rock fragmentation with disc cutters through theoretical modelling and physical measurement of crushed zone pressure, PhD Thesis. *Colorado School of Mines*, Golden, Colorado, USA (1997).
Singh, B. & Goel, R.K. 2011. Engineering Rock Mass Classification. *Elsevier Inc* (2011). ISBN 978-0-12-385878-8.
Wilfing, L. 2016. The Influence of Geotechnical Parameters on penetration Prediction in TBM Tunneling in Hard Rock. PhD Thesis, *Technical University of Munich*, Munich, Germany (2016).
Yagiz, S. 2014. Modified CSM model for predicting TBM performance in rock mass. *LAP (Lambert Academic Publishing)*, 2014.

Tunnels and Underground Cities: Engineering and Innovation meet Archaeology, Architecture and Art, Volume 6: Innovation in underground engineering, materials and equipment - Part 2 – Peila, Viggiani & Celestino (Eds)

A study of the analysis method of the cause of tunnel lining deformation using "TCI"

K. Maeda & Y. Shigeta
Pacific Consultants Co., Ltd., Tokyo, Japan.

S. Kaise, K. Maegawa, Y. Maeda & T. Ito
NEXCO Research Institute Japan, Tokyo, Japan.

H. Yagi
Central Nippon Expressway Co., Ltd., Nagoya, Japan.

ABSTRACT: Deformation causes of tunnel lining include external causes in which forces are applied from outside the tunnel (hereinafter referred to as "external force") and internal causes due to the material, construction etc. However, there are many unclear aspects in the characteristics of cracks classified according to their causes. Thus in this research, we set thresholds related to the possibility of deformation caused by external force from the cracks development plans of the linings in the road tunnels managed by Nippon Expressway Company (hereinafter referred to as "NEXCO") of Western, Central and Eastern Japan using Tunnel-Lining Crack Index (hereinafter referred to as "TCI"). Moreover, we analyzed the relationship between the set thresholds and the tunnels where external force deformations were observed.

1 INTRODUCTION

The causes of cracks in tunnel lining can be roughly divided into external causes such as the effect of external forces and internal causes due to the material, construction, etc. Generally speaking, cracks are generated by the complex interplay of deformation causes both external and internal. Therefore, the forms of tunnel lining cracks are extremely diverse. However, research/analysis of the characteristics of cracks and estimation of the deformation causes are important for assessing the stability and safety of a tunnel.

This paper conducts analysis of cracks information obtained from the inspections of road tunnels managed by NEXCO using Tunnel-Lining Crack Index (TCI), understands the characteristics of both cracks caused by internal causes and cracks caused by external causes, and examines an objective estimation method of deformation causes.

2 OUTLINE OF TCI

This section outlines the TCI that was used to quantitatively evaluate the features of cracks by investigating the crack deployment diagrams.

Rock mass properties (such as deformation modules and coefficient of permeability) are largely influenced by density, orientation, and width of cracks (joints) in the rock mass, then an index called "crack tensor" that can comprehensively quantify this influence has been studied in the field of Rock Mechanics. The index, TCI has been proposed in the preceding studies for evaluating cracks on lining concrete and the concept of this "crack tensor" has been introduced in the TCI. Width, length, and orientation of cracks on the lining surface are parameters of TCI, which makes possible to decide the “maximum width of crack”, “maximum length of crack”, “distribution of cracks”, and “general orientation of cracks”. Fundamental equation and conceptual image are shown respectively in Equation (1) and Figure 1.

$$F_{ij} = \frac{1}{A}\sum_{k=1}^{n}\left(t^{(k)}\right)^{\alpha}\left(l^{(k)}\right)^{\beta}\cos\theta_i{}^{(k)}\cos\theta_j{}^{(k)} \tag{1}$$

A: Area of lining concrete (A=Ls × La)
Ls: Longitudinal length of lining concrete (i.e., span length in general)
La: Transversal length of lining concrete
N: Number of cracks
l(k): Length of crack (k)
t(k): Width of crack (k)
i(k): Angle between the normal vector of crack (k) and x_i axis
j(k): Angle between the normal vector of crack (k) and x_j axis
α: Weighting factor on width of crack
β: Weighting factor on length of crack
F_0: Magnitude of TCI
F_{11}: Longitudinal component of TCI
F_{22}: Transversal component of TCI
F_{12} = F_{21}: Shear component of TCI

F_{11} and F_{22} given by Equation (1) are the longitudinal and transversal components of TCI, respectively. Deterioration index (F_0) of lining concrete is expressed by summation of these two components (F_0=F_{11}+F_{22}), which is the invariant of tensor. This deterioration index, F_0 is used as an evaluation value of the TCI, representing the progress of deformation. Furthermore, the features of cracks can be characterized and understood by each component (i.e., F_{11}, F_{22}, F_{12}, and F_{21}).

In this study, the weighting factor (α) for width and that (β) for length were set to be identical and to be 1.0 based on the preceding studies.

Since TCI is a tensor, the major orientation of average crack over the lining span shown in Figure 2 can be given by Equation (2).

$$\theta = \alpha = \tan^{-1}\left(\frac{F_{12}}{r + (F_{11} - (F_0/2))}\right) \tag{2}$$

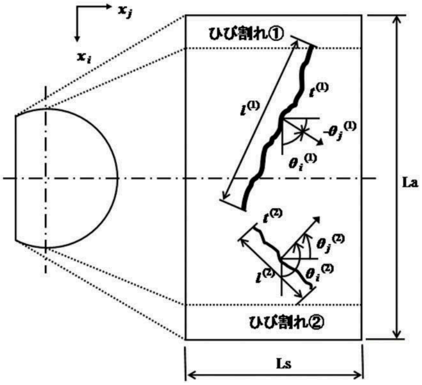

Figure 1. conceptual diagram of TCI.

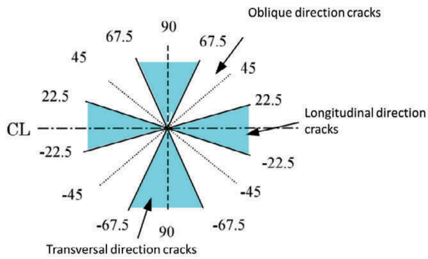

Figure 2. Definition of the major orientation of crack.

θ = Major orientation of cracks
α = Angle between x axis and a line connecting two points (F_{11} and F_{12}), on which TCI circle crosses x axis
r = Absolute value of (F_{11} - F_{22})

3 OVERVIEW OF EXAMINATION

3.1 *Examination method*

This analysis was conducted with the longitudinal direction component F_{11} and transverse direction component F_{22} of TCI. Figure 3 shows an example of the analysis. Horizontal axis of the graph was set as F_{11}, and vertical axis was set as F_{22}. The intersections of F_{11} and F_{22} calculated at each span of one lining were plotted on the graph. When the plots are distributed below the dotted line on the graph (F_{11}=F_{22} line), it is the longitudinal direction cracks predominant type, and when they are distributed above the dotted line it is the transverse direction cracks predominant type. When the plots are distributed on, or near the dotted line, it is the diagonal cracks predominant type. From this graph, it is inferred, that the following deformation causes can be estimated.

$F_{11}>F_{22}$: Longitudinal direction cracks on the crown due to loosening pressure, longitudinal direction cracks on the side wall due to water pressure or plastic pressure, etc.

$F_{11}=F_{22}$: Diagonal direction cracks due to landslide or side pressure topography, etc.

$F_{11}<F_{22}$: Transverse direction cracks due to sinking or rising of roadbed, etc.

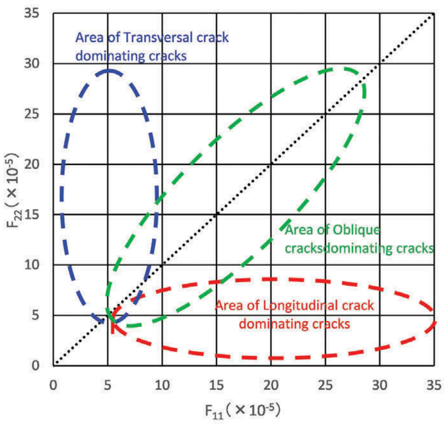

Figure 3. Analysis of deformation causes.

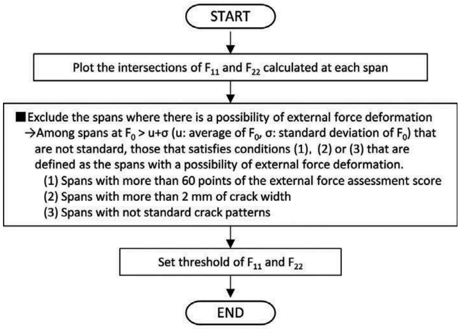

Figure 4. Conceptual diagram of TCI.

Table 1 . Averages and Standard Deviations of Subject Tunnels and Each Lining Method.

Lining Method		Lagging support Method	NATM
Span		3,339	6,020
F_{11}	Average u	6.31	3.15
	Standard Deviation σ	4.89	4.26
F_{22}	Average u	4.26	1.92
	Standard Deviation σ	3.83	3.47

In this examination, a distribution diagram of F_{11} and F_{22} in the subject tunnels excluding the spans where there is a possibility of external force deformation, and a threshold that includes this is set. The fact that what are included within the average u ± standard deviation σ among TCI components are deformation from internal causes (standard forms of cracks) shown in the existing study is utilized for this analysis. Thus, among spans at $F_0 > u + \sigma$ (u: average of F_0, σ: standard deviation of F_0) that are not standard, in other words spans with extensive damages by cracks, those that satisfies conditions (1), (2) or (3) that are shown in Figure 4 are defined as the spans with a possibility of external force deformation.

Here, the external force assessment score is the indicator that translates the deformation situation of lining into points, and spans with more than 60 points are considered to be inspection priority spans. Moreover, standard crack patterns are what defined in an existing study as cracks originating from construction, and having tendency for generating two lines of longitudinal direction cracks with the lagging support method, and having tendency for generating on line of longitudinal direction crack with NATM.

Thus, if an appropriate threshold can be set, it is inferred to be possible to set a threshold that enables estimation of deformation cause not to be external force deformation, in other words to be material degradation, installation-origin, etc. only by using TCI.

3.2 *Averages and standard deviations of subject tunnels and each lining method*

Table 1 shows the analysis subject tunnels. 50 tunnels lined with the lagging support method and lined with NATM where proximity visual inspection is conducted were selected respectively from the tunnels managed by NEXCO. The table shows their respective F_{11} and F_{22} average and standard deviation of subject span according to the method used.

4 ANALYSIS RESULT

4.1 *Threshold of Lagging Support Method*

Figure 5 shows the distribution of F_{11} and F_{22} of spans of the lagging support method that exclude the aforementioned conditions (1), (2) and (3) that have the possibility of being external force type. At this time, when a u+2σ line is drawn for both F_{11} and F_{22} as their thresholds, it becomes clear that the distribution is mostly below the thresholds.

Figure 6 shows the spans distribution in the area below these thresholds. 3,083 spans are below the threshold at this time, which is 92.3% of the entire 3,339 subjects. External force deformation is generally considered to be about 5% of entire tunnels. Thus these thresholds are considered to be broadly appropriate, and it is inferred that the deformation causes of the spans below the thresholds could be estimated to be material degradation, installation-origin, etc.

4.2 *Threshold of NATM*

The same analysis conducted for the lagging support method was also conducted for NATM. As a result, the number of spans that are distributed below the threshold was 5,460 when both F_{11} and F_{22} thresholds were set at u + 2σ as shown in Figure 7, which is 90.7% of the entire 6,020 subject spans. While these thresholds are slightly on the safety side, they are inferred to be broadly appropriate as was the case for the lagging support method.

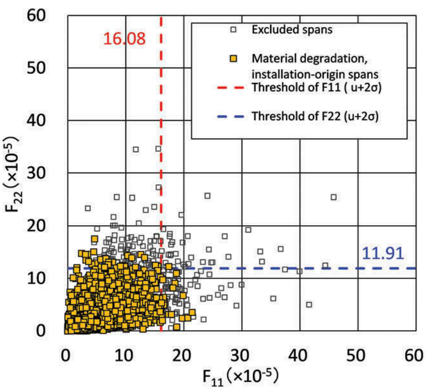

Figure 5. On setting of threshold.

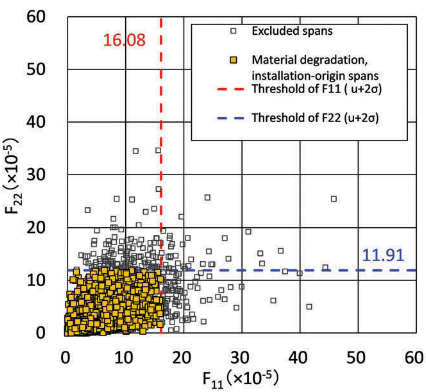

Figure 6. Thresholds of lagging support method.

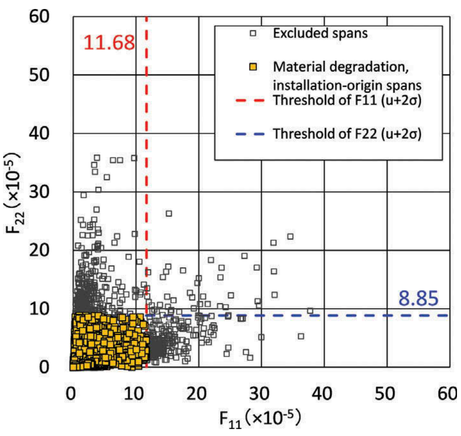

Figure 7. Thresholds of NATM.

Table 2. Tunnels with external force deformation (lagging support method).

No.	Tunnel Name	Deformation Cause	Deformation Situation
1	Tunnel A	Loosening Pressure	Longitudinal and Transverse Cracks
2	Tunnel B	Loosening Pressure	Longitudinal and Transverse Cracks
3	Tunnel C	Rising of Roadbed	Transverse and Diagonal Cracks
4	Tunnel D	Rising of Roadbed	Transverse Cracks
5	Tunnel E	Plastic Pressure	Longitudinal Cracks on the Shoulder
6	Tunnel F	Plastic Pressure	Longitudinal Cracks on the Shoulder
7	Tunnel G	Landslide Side Pressure	Longitudinal Cracks on the Shoulder
8	Tunnel H	Landslide Side Pressure	Longitudinal Cracks on the Shoulder
9	Tunnel I	Rising of Roadbed	Transverse Cracks
10	Tunnel J	Rock Mass Slippage	Transverse and Diagonal Cracks

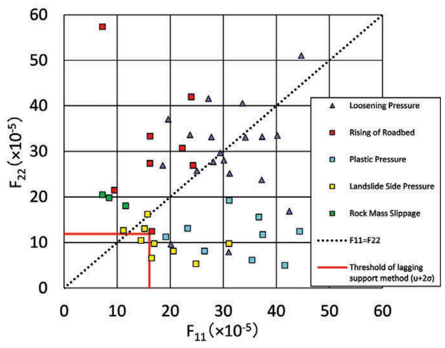

Figure 8. Relationship between external force deformation and threshold.

4.3 *Comparison of external force deformation and threshold (Lagging Support Method)*

Figure 8 shows the distribution of F_{11} and F_{22} of the lagging support method tunnels where external force deformation occurred in the past listed in Table 2 according to the deformation causes. When the aforementioned F_{11} and F_{22} thresholds u + 2σ of lagging support method are shown in this graph, it results in only one span among the spans where external force deformation occurred is included within the thresholds. Thus, it becomes clear that most of external force deformations are distributed outside the area of the thresholds.

Therefore, it is inferred that it is appropriate for the threshold that allows the deformation causes to be material degradation, installation-origin, etc. to be below u + 2σ for both F_{11} and F_{22}.

5 CONCLUSION

This examination revealed that there is a possibility for setting thresholds that enable estimation of deformation causes to be material degradation, installation-origin, etc. by using F_{11} and F_{22}. In future, it is inferred that there is a necessity for understanding the relationship between the external force deformation and progression and set a standard for appropriate health level determination. Moreover, we hope to improve the accuracy by increasing the number of analyzed tunnels and establish a deformation cause estimation method.

NEXCO must manage deteriorating road tunnels and devise repair plans. Meanwhile, the decrease in the number of technicians due to population decrease, birthrate decline and aging is also the cause for concern. In future, we believe that by establishing a deformation cause estimation method for further optimization of tunnel inspection that reduces discrepancy caused by the difference in the skill of technicians, we will be able to contribute to the selection of spans that require careful proximity visual inspection and tapping inspection and to the devising of the repair plan for large-scale restoration works.

Tunnels and Underground Cities: Engineering and Innovation meet Archaeology, Architecture and Art, Volume 6: Innovation in underground engineering, materials and equipment - Part 2 – Peila, Viggiani & Celestino (Eds)
© 2020 Taylor & Francis Group, London, ISBN 978-0-367-46871-2

The present situation of countermeasure of heaving in the expressway of Japan

K. Maegawa, T. Ito & S. Kaise
NEXCO Research Institute Japan, Machida-city, Japan

H. Yagi
Central Nippon Express Company Limited, Nagoya-city, Japan

S. Kunimura & Y. Okui
OYO Corporation, Saitama-city, Japan

ABSTRACT: On the Expressway of Japan, many structures are aging and renewal construction for a longer life is being promoted. The Main contents of the tunnel are to repair and reinforcement of the lining and countermeasure for heaving. The project scale is planned to be 130 km in 15 years from 2015 to 2030. In most cases construction will be carried out while opening one lane of two. As a result, the countermeasures works in a narrow space and the speed of progress is slow. Many problems remain with respect to the countermeasure construction of heaving. Therefore, innovations such as further efficient construction in a narrow space, rapid construction technique, new technology countermeasure of heaving not dependent on additional invert-concrete, construction machinery and materials, etc. are required.

1 INTRODUCTION

Since the opening of the Meishin Expressway in 1963, about 9,000 km of expressways have opened in Japan, out of which the tunnels (about 1,850 in number) have the total length of about 1,760 km.

Approximately 30% of the tunnels have been in use for over 30 years, showing the signs of aging.

NEXCO 3, the company which maintains Japan's expressways with the business license of the Ministry of Land, Infrastructure, Transport and Tourism, has been carrying out renewal constructions to extend the life of the structures.

The renewal constructions for the tunnel structures consists mainly of recovering lining strength reduced by cracks and other reasons, repair of the lining against external forces that occurred after the opening the tunnel, unexpected at the time of construction, countermeasures for heaving on parts that are hinder are expected to hinder passing vehicles due to road surface uplift or reinforcement work.

The tunnel renewal construction project is to cover 130 km in the 15 years of 2015 to 2030.

This report discusses the tunnel renewal constructions, focusing on the current state of countermeasures for heaving.

2 IMPLEMENTATION OF THE COUNTERMEASURES FOR HEAVING IN JAPAN

2.1 *Causes of deformation in cases using invert-concrete*

Figure 1 shows the tunnels with evident heaving, based on the survey of the relationship between heaving and the geological features. The survey was limited to expressway tunnels.

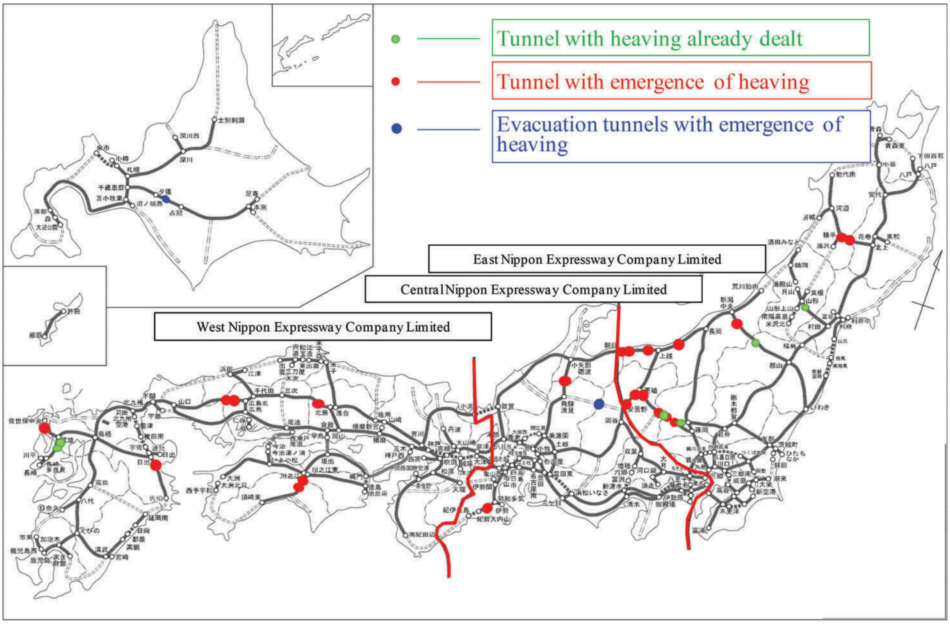

Figure 1. The tunnels under the jurisdiction of NEXCO, with evident heaving (as of September 1, 2016).

Table 1. Types of rocks and geological features likely to cause heaving.

1 Rock types clearly identified in design guidelines and others	Tuff, mudstone, shale, clay slate, serpentinite, weathered crystalline schist, solfataric clay, etc.
2 Rock types which need invert-concrete for sediment, portal, etc., based on current standards	Silt, disintegrated granite soil, talus, debris flow deposits, loam, embankment, weathered soil, top soil, etc.
3 Rock types without clear mentions of lithology but invert-concrete is considered necessary with topography including fault fracture zone	Fault, fault (estimated fault), fault fracture zone, a landslide deposits, landslide colluvium, fracture zone, etc.

Table 1 shows the result of the analysis of the geological features where heaving occurs and the types of rocks which are likely to cause heaving.

Although there are cases in which heaving occurred and progressed rapidly, destroying the invert-concrete of the tunnels, most heaving cases in Japan showed swelling, with expansile clay minerals such as smectite absorbing water and expanding, causing the road surface bulging.

Based on this fact, after 1998, construction of tunnels in the bedrock with rock types which show strength deterioration or expansion in the long term are carried out with invert-concrete installed even for medium hard rocks.

Figure 2 shows the analysis result of the rock types of the tunnels where road surface uplifts are recognized, by geological profile.

As shown in Figure 2, the sections where the road surface uplift occur have rock types which show strength deterioration and expansion in the long term. Many of these sections did not require installation of invert-concrete according to the previous standards 1)

But when the current construction standards are applied, the total length of the sections with the rock types which require invert-concrete accounts for about 90% or more of those sections.

2.2 *Choosing invert-concrete for countermeasures*

Table 2 shows the cases in which heaving such as uplift of pavement slabs occurred on expressways after they opened, and reinforcement work with invert-concrete were carried out.

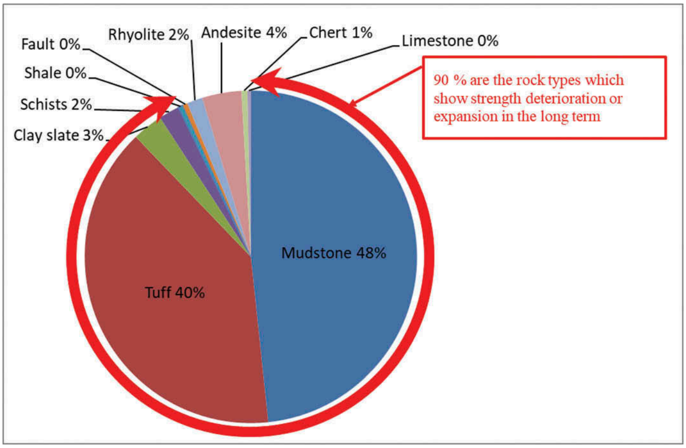

Figure 2. Ratio of rock types where uplift occurred.

Table 2. Cases of countermeasures for expressways using invert-concrete.

No.	Names of the tunnels	Total length	Total length of coutermeasures with invert-concrete	Support method	Other countermeasures
1	A Tunnel	1990 L=683m	1997 L=379.5m	NATM	rock bolt (preliminary reinforcement) reinforcement of the sections beneath the roadbed with rock bolt and micropiles before the invert-concrete was installed
2	B Tunnel	1990 L=2,609.5m	1997 L=505.5m	NATM	rock bolt (preliminary reinforcement) reinforcement of the sections beneath the roadbed with rock bolt and micropiles before the invert-concrete was installed
3	C Tunnel	1992.2 L=684m	1998.11 L=70m	NATM	rock bolt (preliminary reinforcement)
4	D Tunnel	1991 L=1,234m	2002 L=133.65m	NATM	
5	E Tunnel	1993 L=3,998m	2003 L=2,674.7m	NATM	
6	F Tunnel	1991 L=1,234m	2008 L=148m	NATM	
7	G Tunnel	2002 L=2,051m	2013 L=41.5m	NATM	
8	H Tunnel	1991 L=3,191m	2013 L=40.5m	NATM	
9	I Tunnel	1996 L=2,600m	2015 L=126m	NATM	

"A Tunnel" and "B Tunnel" were the first expressway tunnels to be implemented with the countermeasures, where the sections beneath the roadbed were reinforced with micropiles. Although the slowing of the displacement speed was recognized, it took installment of additional invert-concrete to stop the progress (Figure 3). For this reason, additional installation of invert-concrete has become the basic countermeasure for heaving on Japanese expressways.

3 SURVEY AND MEASUREMENT OF DEFORMATION

Survey of heaving by NEXCO clarifies the purposes of survey for each stage of heaving, by grading the conditions into three stages.

In the "latent risk stage," heaving has not yet occurred but the tunnels have geological features or potential. In the "progressive risk stage," heaving has been recognized for the first time or heaving is not serious but follow-up observations are carried out. In the "countermeasures stage," heaving has progressed or deformation is serious, requiring immediate response and countermeasures. Table 3 shows the purposes for survey on each stage and others.

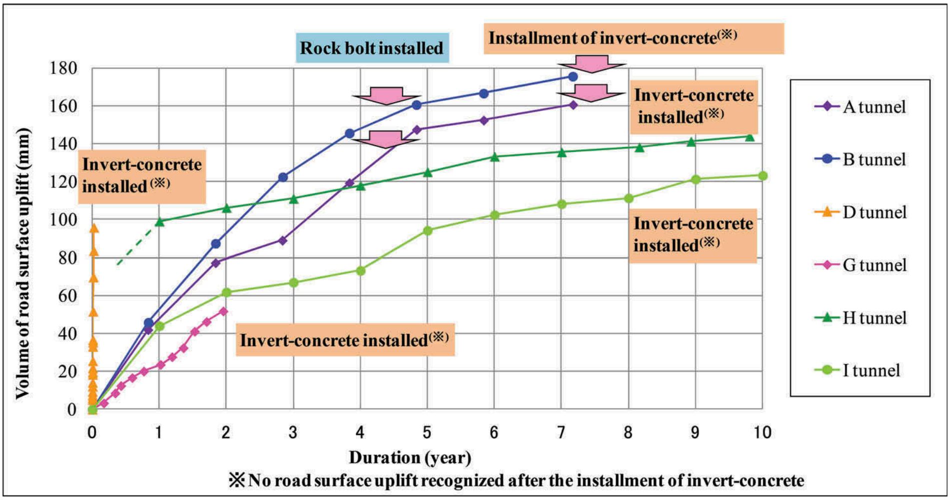

Figure 3. Relationship between the volume of road surface uplift before countermeasures and the years since measurement started.

Table 3. The state of deformation and purposes of survey.

Stages of deformation	State of deformation	Purposes of survey and overview
Latent risk stage	Heaving have not yet occured in tunnels but they have geological features or potential for heaving	To measure the normal level (initial level) before heaving occurs. Survey and measurement of the current road surface elevation and other conditions in sections with geological features with the potential for heaving
Progressive risk stage	Heaving has been recognized for the first time or heaving is not serious but follow-up observations are carried out	To continue observation of the degree of deformation and to grasp its progress. Survey and measurement of displacement of road surface elevation, inner space, etc. and presumption of deformation causes inside sections with heaving found by users and through patrols and tunnel inspections
Counter-measures stage	Heaving is obvious and progress of deformation is serious, requiring immediate response and countermeasures	Survey and measurement of sections with existing deformation to presume the deformation causes, predict future deformation and design countermeasures

In "latent risk stage," the objective of the survey is to measure the initial value before heaving occurs, and survey mainly consists of the leveling of the whole tunnels and collection of data at the time of construction.

In "progressive risk stage" which comes before "countermeasures stage," the survey is aimed at measuring the progressiveness of heaving since its occurrence and setting the schedule for countermeasures. Unlike "latent risk stage," the risk is observed on a continuous basis, with leveling or convergence measurement carried out four times a year, for example.

In "countermeasures stage," the purpose of the survey is to collect data for planning countermeasures with various surveys and bedrock sample tests.

4 PLANNING FOR COUNTERMEASURES

4.1 *The structure of countermeasures*

Cross section of the additional invert-concrete as countermeasures is decided based on numerical analysis using survey results. An example of the cross section is shown in Figure 4.

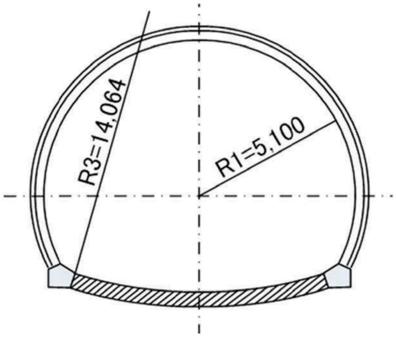

Figure 4. Cross section example of the additional invert-concrete.

Figure 5. Countermeasure using invert struts.

As shown in Figure 4, the bottom tip of lining is cut slantingly and invert is applied to it so that stress transmission to the lining will be smooth.

Figure 5. Countermeasure using invert struts. In many other cases, invert struts (Figure 5) are installed. In most of these cases, the countermeasures are adopted not necessarily from the design aspect. They are applied, for example, for deformation control when unexpected external force is applied due to excavation around the invert.

4.2 *Circumstances around expressways*

In Japan, expressways are an indispensable part of neighboring residents' life. Due to social needs and limited traffic capacity of detour roads, it is difficult to close the entire expressways for renovation. Therefore, when carrying out the countermeasures for heaving, it is common to leave open one lane on the two-lane roads.

As a result, the countermeasure works are usually conducted in narrow spaces, slowing the construction speed.

4.3 *Designing countermeasures*

The numerical analysis for designing countermeasures for heaving is carried out using finite element method (FEM) or finite difference method (FDM). These methods are used to presume the mechanism of deformation by analyzing the current deformation state of batholith and lining, stress condition of lining and more and to reproduce the current state of deformation as well as confirming the effectiveness of the invert reinforcement work against the progress of deformation in future.

Generally, two-dimensional numerical analysis is used to examine tunnel structures and three-dimensional numerical analysis is used to study the effects of countermeasures.

Figure 6 shows the general procedures of numerical analysis.

(1) As the analysis of survey results, deformation mechanism is presumed by grasping the state of heaving and deformation of lining, based on examinations of existing deformation, geological survey, etc.

    The state of geological feature distribution around the tunnels is grasped for modeling, based on bowling survey results and face observation results.

(2) For reproduction analysis, the situation at the time of the tunnel building (displacement measurement result) is reproduced. The bedrock's modulus of deformation and state of initial stress are grasped roughly with inverse analysis using measured values.

(3) For the reproduction analysis of deformation, the bedrock properties are set for reproduction of current deformation conditions. Displacement volume (the uplift volume,

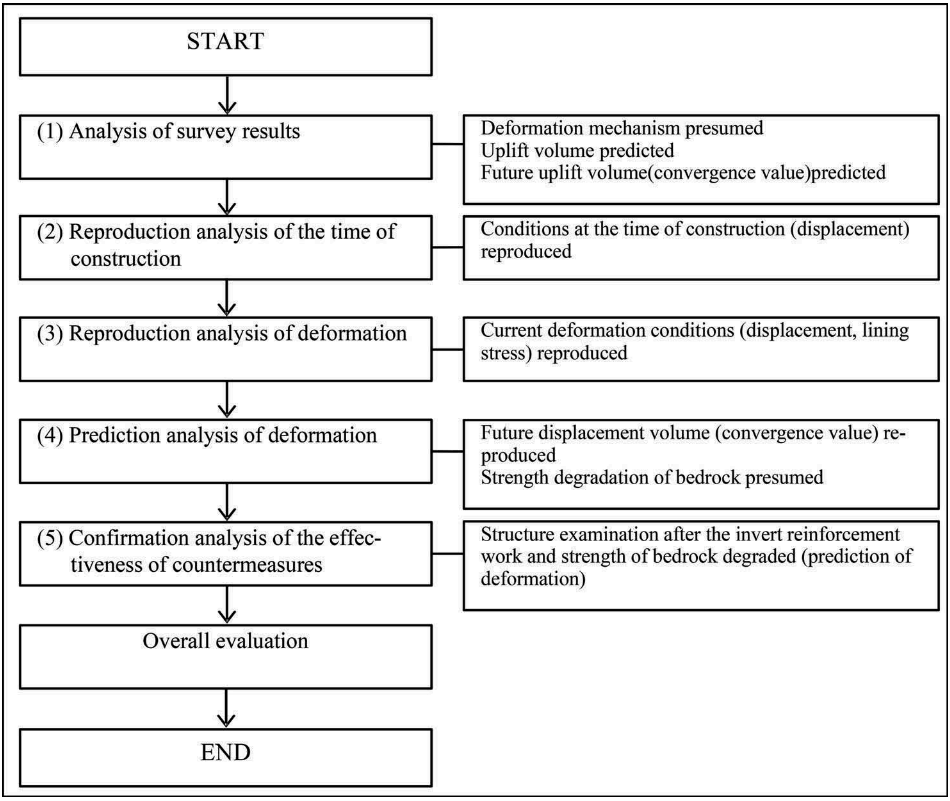

Figure 6. Process of analysis using structure examination with two-dimensional analysis.

displacement volume of inside section and underground), stress value (lining stress) and range of looseness based on deformation survey are reproduced.
The ranges of looseness is calculated on the whole area surrounding the tunnel, the area lower than SL and area lower than pavement slab in order to presume and establish the ranges of looseness which can reproduce the measuring results of deformation survey and tendencies of deformation.

(4) For prediction analysis of deformation, displacement volume is presumed from changes in measured values due to aging, and the material properties value is identified so that it may match the estimated value.
(5) As confirmation analysis of the effectiveness of countermeasures, invert reinforcement work is modeled and the tunnel structure with invert and concrete lining is examined with the calculation using the material properties value of the prediction analysis of deformation.

For two-dimensional analysis for tunnels, over-the-counter software or original software developed by user companies are used. For three-dimensional analysis, the FLAC 3D (ITASCA), analysis software of FDM, is often used. This is presumably because the shear strength reduction method (SSRM), to be mentioned later, can be used for reinforcement design.

4.3.1 *Modeling for bedrock*

4.3.1.1 ELEMENT

Dynamics model for bedrock consists of elastoplastic body, viscoelastic body and viscoelastic plastic body.

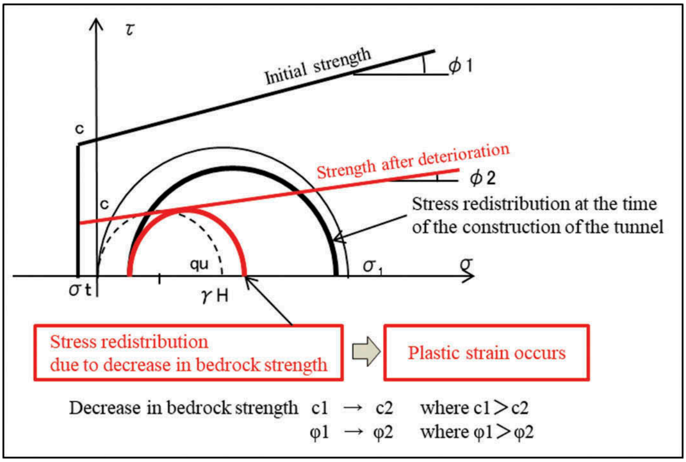

Figure 7. Conceptual diagram of SSRM for bedrock.

4.3.1.2 INPUT MATERIAL PROPERTIES VALUE

Input material properties value of bedrock are generally based on various survey results and bedrock sample examinations.

The material properties which can reproduce measured values and predicted values of road surface in different stages (at the time of construction, reproduction of present state and future prediction) are set by inverse analysis with modulus of deformation, Poisson's ratio, cohesion and an angle of internal friction as parameters.

For modeling of weakening of bedrock, SSRM is used, as shown in Figure 7.

4.3.1.3 MODELING DOMAIN OF BEDROCK

Generally for modeling, 5D (D : tunnel representative diameter) to the sides is taken for lateral domain, about 4D for lower domain and 4D for upper domain with big earth covering, and to the ground level when the earth covering is small.

4.3.2 *Modeling for existing lining and additional invert-concrete*

4.3.2.1 ELEMENT

For shotcrete, existing lining and additional invert-concrete, modeling is done with elastic body and elastoplastic body (strain softening) etc.

For rock bolt, modeling is generally not done except in cases applied as supplementary construction method of countermeasure works.

There is no set modeling for methods of linking existing lining with additional invert-concrete, due to lack of sufficient knowledge. However, when the axial tension is excellent, rigid connection is applied.

4.3.2.2 INPUT MATERIAL PROPERTIES VALUE

The input material properties value is the shape (thickness of lining, cross-sectional area, geometrical moment of inertia and weight per unit volume) and strength (the elastic modulus, the compressive strength and the tensile strength).

For these, actual measurement are available at times, but they are usually set based on the cross-sectional form and thickness of component and design value of component (concrete strength and the elastic modulus) at the time of tunnel construction.

5 COUNTERMEASURES

5.1 *Construction process*

As mentioned above, countermeasure works are generally carried out with lane restrictions.

Figure 8 shows the cross section of the general construction with lane restrictions and Figure 9 shows the construction process.

For preparatory operations necessary for constructions with lane restrictions, soldier piles are built and protection fences are installed. These operations are not necessary for constructions with entire road closure.

Excavation work and installment of soldier piles are especially time-consuming because they are conducted in narrow spaces with lane restrictions, allowing the use of only few kinds of building machines and requiring extreme caution with passing vehicles nearby and countermeasure works on heaving of bedrock with soft rock or harder.

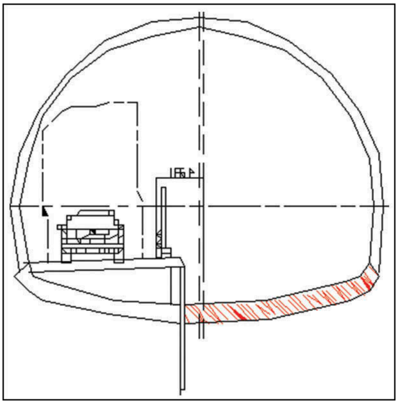

Figure 8. Cross section of the construction with lane restriction.

Preparation : Temporary construction of water pipes, communications cables, etc.

↓

Installment of invert : Soldier piles and temporary protection fences installed
Inspection gallery removed
Invert-concrete installed
Inspection gallery restored
Central drainage restored
Water pipes, communication cables restored

↓

Switching lanes for construction

↓

Installment of invert : Inspection gallery removed
Invert-concrete installed
Inspection gallery restored
Central drainage restored
Water pipes, communication cables restored
Temporary protection fences removed

Figure 9. Construction process with lane restrictions.

5.2 *Technical development of construction technique*

5.2.1 *Cases of actual operation*

Countermeasure works with additional invert-concrete have been carried out at "J Tunnel", with the total length of 1,960 meters, from 2016 to 2018,

Efficiency of countermeasures with lane restrictions has improved by changing 0.45m^3 tip of the excavator, without changing the entire machinery. Figure 10.

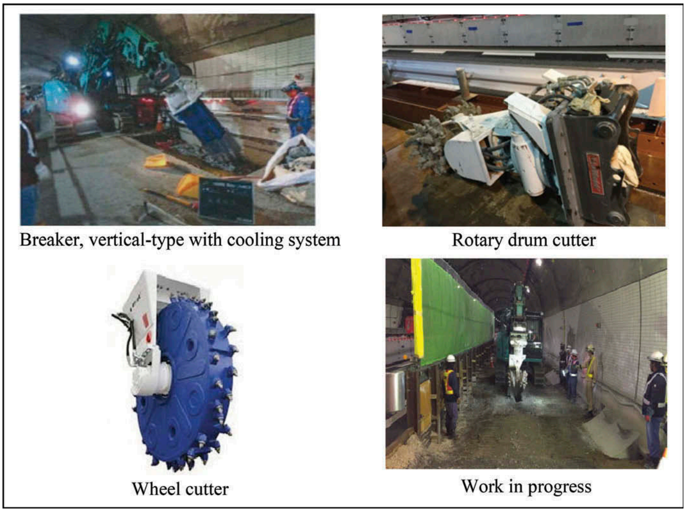

Figure 10. 0.45m^3 Excavator attachment(commercially available machine).

5.2.2 *Method of invert of hybrid structure using steel pipes and concrete (IHUPC)*

For places where it is physically difficult to improve the vehicles' safety and driving environment and to secure sufficient passage width during construction period, a new method of invert of hybrid structure using steel pipes and concrete (IHUPC) was developed. Central part of roads are not excavated to avoid any troubles of traffic control but instead, steel pipes are inserted, and for the side walls, cast-in-place concrete is installed after the excavation of batholith.

Figure 11 shows the image of IHUPC method.

With leaving the central part non-excavated, this method reduces the volume of excavation and the speedup of construction process is expected. The adoption in actual operations is expected in the future.

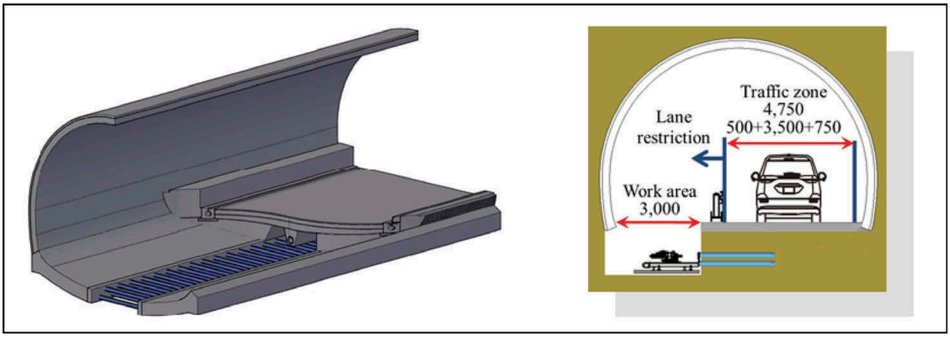

Figure 11. The image of method of IHUPC (patent method in Japan).

6 ISSUES TO BE TACKLED

6.1 *Accelerating the process*

In the 15 years from 2015 to 2030, 130 km of tunnel renewal construction must be carried out.

Given the labor shortage due to the disaster reconstruction of Great East Japan earthquake in 2011 and the preparation for 2020 Tokyo Olympics, the speed for the tunnel renewals needs to be about 50 meters per month in order to accomplish 130 km in 15 years.

Current construction methods with lane restrictions only allows for the progress speed of 10 to 20 meters per month can, so substantial speedup is needed.

For the speedup, followings are being considered. In the places where heaving has actually occurred, adoption of IHUPC method and the capacity improvement of the construction machinery are considered on the premise of implementing countermeasures with additional invert-concrete. For preventive countermeasures, new methods to take place of additional invert-concrete need to be established, including reinforcement of parts under the roadbed.

A committee of experts has been discussing these issues.

6.2 *Removal of lane restrictions during holidays*

Some expressways have substantially more traffic during holidays than on weekdays. Lane restrictions during holidays on these expressways cause traffic jams and its social impact is serious.

This is also true for the countermeasures for heaving in tunnels. The lane restriction of one lane out of two that begins on Monday needs to be re-moved by the end of Friday.

When a pilot construction project was executed in the above-mentioned “J Tunnel”, the work for the 10-meter lane including demolition and excavation of the pavement, installment of additional invert-concrete, back-filling and temporary paving were all done on weekdays partly due to the good conditions of roadbed with no spring water from underneath.

The implementation process is being studied for further speedup.

7 CONCLUSIONS

Expressways of Japan are currently renewed to extend the structures’ life.

The renewal of tunnel structures mainly consists of repair and reinforcement of the lining and countermeasures for heaving on the parts which hinder or are expected to hinder passing vehicles due to road surface uplift.

The tunnel renewal construction is scheduled to last 15 years, covering 130 km.

For the survey and design of the countermeasures, the conditions of heaving are graded into three stages. The purposes of the survey for each stage are clarified before scheduling for countermeasures and deciding on the survey items needed as data for design.

Numerical analysis are carried out using FEM or FDM for designing the measures. Although some issues still need to be tackled, the procedures and methods of numerical analysis for the design techniques are mostly established.

The circumstances of Japanese expressways usually do not allow for the entire road closure and the constructions are usually done while leaving one lane out of two opened.

Therefore, countermeasure works are implemented in narrow areas and the speed is slow.

To renew 130 km of tunnels in 15 years, construction speed needs to be 50 meters per month. Using the present construction techniques and with lane restrictions, the speed of only 10 to 20 meters per month can be achieved, so substantial speedup is necessary.

For the speedup of countermeasure works, various means are adopted such as the use of efficient building machines fit for work in narrow spaces and dividing roads into three sections to leave the middle section unexcavated which results in reduction of the excavation volume.

However, in order to achieve the desirable speedup, further efforts are needed, including improvement of building machine capability, establishment of new methods to replace the installment of additional invert-concrete and more.

Tunnels and Underground Cities: Engineering and Innovation meet Archaeology, Architecture and Art, Volume 6: Innovation in underground engineering, materials and equipment - Part 2 – Peila, Viggiani & Celestino (Eds)
© 2020 Taylor & Francis Group, London, ISBN 978-0-367-46871-2

Back analysis of ground settlements induced by TBM excavation for the north extension of Paris metro, line 12

S. Mahdi, O. Gastebled & S. Khodr
TRACTEBEL ENGIE, Paris, France

ABSTRACT: The north extension of Paris metro line 12 consists in 3.8 km of double track tunnel and 3 stations, constructed in two main stages. The first stage, between 2010 and 2011, included the tunnel boring with an EPB TBM. The monitoring of settlements was particularly dense and provided a wealth of topographic data. A back analysis based on non-local least square method showed that a very good agreement could be found between a calibrated Peck formula and the empirical data. An inverse analysis allowed to deduce the characteristic trough width parameter of each formation. Eventually, a detailed back-analysis based on finite element modelling allowed to derive a law relating confinement to volume loss. This allowed establishing a predictive model based on Peck formulation complemented by two empirically calibrated laws which is shown to match closely the full data set and could be used on projects currently under study.

1 PRESENTATION OF NORTH EXTENSION OF PARIS METRO LINE 12

The extension works of Paris metro line 12 started in 2008 with the construction of the first of three stations, Front-Populaire, which was completed in 2012. Between 2010 and 2011, 3.8 km of 9.15 m diameter tunnels were bored by an EPB shield named Elodie in two drives. This first construction stage allowed early commissioning of an initial one stop extension by the end of 2012. Since 2013, the two other stations, Aimé-Cesaire and Mairie-d'Aubervilliers are under work. The commissioning of the complete extension is planned by the end of 2019.

In the first construction stage, the owner, RATP, appointed XELIS as design engineer and site supervisor, while TRACTEBEL was appointed as geotechnical reviewer. The works were contracted to a consortium of companies: EIFFAGE and VINCI. Contrary to the first drive, the track alignment of the second drive that extends between the TBM launching shaft located adjacent to the Aimé-Césaire station and a receiving shaft located 900 m beyond the Mairie-d'Aubervilliers station, remained under three main streets in Aubervilliers (Av. Victor Hugo, Bvd Anatole France and Bvd Pasteur), which allowed dense and continuous monitoring of the settlements.

2 BACK-ANALYSIS: OBJECTIVE AND APPROACH

The continuous growth and densification of the urban periphery of Paris requires the development and modernisation of its underground metro network. Existing lines 4, 11, 12 and 14 are currently subject to extension works. Furthermore, four new automatic metro lines, part of the Grand Paris Express project (GPE), are either under construction (south of circle line 15 and suburban line 16) or under design/tendering (east and west of circle line 15, airport line 17 and Saclay line 18).

The planned tunnels of line 16, line 15 east and line 17 are to be bored in the same geological context as the north extension of line 12, i.e. the Plaine de France basin. This makes the latter a valuable feedback case, on which to improve design choices and risk assessment while boring new tunnels in similar conditions. This paper presents an approach which not only aims at retro-fitting the monitoring settlement data of line 12, but also offers a calibrated predictive tool for the study of the impact on the urban environment of the coming tunnelling works in the vicinity.

3 GEOLOGICAL AND GEOTECHNICAL CONTEXT

The geology encountered by the line 12 extension, Figure 1, consists from grade down, in quaternary deposits (fills and alluvions) and the succession of Eocene strata:

- Priabonian marls (Marnes infragypseuses)
- Bartonian marls and silty sands (Calcaire de Saint-Ouen and Sables de Beauchamp)
- Lutetian calcareous marlstones and limestones (Marnes et Caillasses and Calcaire grossier)

The main geotechnical characteristics derived from the contractual geological baseline report (GBR) are summarized in Table 1:

- Quaternary deposits are relatively weak
- The Ducy formation at the base of Calcaire de Saint-Ouen stratum appears to be altered by gypsum dissolution phenomena
- The silty sand stratum, Sables de Beauchamp, is particularly compact and stiff, with a slightly softer clayey intercalation in the middle of the layer.

In terms of hydrogeology, le TBM bores under the water table, with a water height at the axis varying from 10 m at the launch shaft to 20 m at the exit shaft.

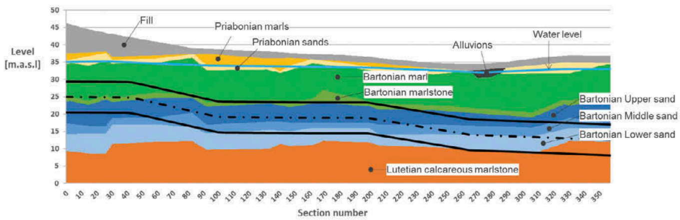

Figure 1. Geotechnical profile from GBR.

Table 1. Geotechnical characteristics from GBR.

Formation	Pressure meter			Effective		Short term	
	E_m [MPa]	Pl^* [MPa]	α [-]	c' [kPa]	φ' [°]	E_{Young} [MPa]	K_0 [-]
Fills	8.5	0.6	0.50	0	25	10	0.58
Alluvions	4	0.4	0.50	0	10	5	0.83
Priabonian marls/Marnes Infragypseuses	18	1.8	0.50	20	25	25	0.58
Priabonian sands/Sables de Monceau	18	1.8	0.50	20	25	25	0.58
Bartonian marls/Calcaire de Saint-Ouen	12	1.5	0.50	30	25	80	0.58
Bartonian marlstone/Calcaire de Ducy	6.5	0.7	0.50	30	25	20	0.58
Bartonian Upper Sables de Beauchamp	38	4.0	0.33	20	30	190	0.50
Bartonian Middle Sables de Beauchamp	28	3.1	0.50	60	15	140	0.74
Bartonian Lower Sables de Beauchamp	35	4.1	0.33	20	30	160	0.50
Lutetian calcareous marlstone/ Marnes et Caillasses	48	4.5	0.50	50	30	240	0.50

4 BACK-ANALYSIS METHODOLOGY

4.1 *Back-analysis fundamentals*

The settlement trough induced by a TBM can generally be described by a Gaussian curve, Peck (1969) and Schmidt (1969). O'Reilly and New (1982) characterised the shape of the trough using only two parameters, i.e. the distance of the inflexion point from the axis (i) and the maximum settlement at the axis (s_{max}). The transversal distribution of the settlements is then defined by Equation (1). The first step of the back-analysis consists in determining the empirical parameters s_{max} and i by curve fitting on site monitoring data. The following complementary parameters are also derived:

– the trough width parameter, k_{eq}, = i/z_0, whith z_0 is the depth of tunnel axis, Equation (2),
– the volume loss parameter, defined as the ratio between le volume of the settlement trough and the excavated section, see Equation (3)

$$s = s_{max}.exp\left(-\frac{y^2}{2.i^2}\right) \tag{1}$$

$$i = k_{eq}.z_0 \tag{2}$$

$$V_{Loss} = \frac{s_{max}\,.\;i\,.\sqrt{2\pi}}{V_t} \tag{3}$$

with V_t is the excavated section of the tunnel, i.e. 65.76 m^2 for a bored diameter of 9.15 m.

According to Chiriotti (2000), the equivalent trough width parameter k_{eq} can be expressed as a weighted average of the width parameters of each ground layer making the overburden from the tunnel axis up. The second step of the back-analysis consists in taking the geological profile into account to derive a characteristic value of width parameter for each ground layer.

The settlement trough may also be assessed using finite element analysis, 2D or 3D, which gives also access to the deformations of the ground mass. The results should however be treated with caution as those methods tend to overestimate the trough width and to underestimate the maximum settlement and maximum inclination, ITA/AITES (2006). Nonetheless, compared to Peck empirical approach, numerical analysis has the advantage of deriving the relationship between volume loss and confinement pressure applied by the TBM.

The practice in France is to derive the moduli used in the constitutive models of the finite element analysis from pressure meter data, based on empirical correlations which depend on the nature of the ground and on the type of works (tunnelling, retaining walls, foundations…). Similarly, to Peck's parameters, the parameters of these moduli correlations can be fitted on site monitoring data. The third step of the back-analysis will therefore consist in retro-fitting the correlations of the equivalent moduli for finite element analysis and derive simple laws relating volume loss to confinement pressure.

4.2 *Step 1 – Fitting of Peck's curves on site monitoring data*

Available site monitoring data originate from 300 survey points located on the facades of buildings and 163 survey points located on the road, with an average density of 0.25 points per meter along the tunnel axis. Curve fitting has been carried out through an advancing process in 5m steps, thus allowing to consider the variation in tunnel depth and in encountered geology: a total of 360 fitting sections has been processed. Each section uses a 50 m long and 40 m wide data screening. Fitting of Peck's parameters is achieved using a non-local non-linear least square method, see § 4.2.2.

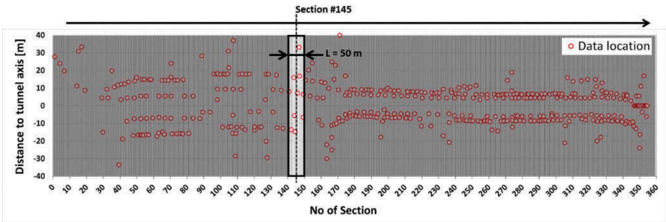

Figure 2. Advancing fitting process.

4.2.1 *Solving for least square by nonlinear regression*
Peck's curve (equation 1) is fitted on the monitoring data by the least square method using nonlinear regression. The minimum is found through an iterative procedure starting from the initial conditions s_{max_0} = 5 mm and $i_{\_0}$ = 10 m. Iteration is considered converged when the parameter increments are less than 0.1%.

4.2.2 *Non-local fitting by data weighting*
Considering that the settlement trough in a cross-section results from the cumulated effects of tunnel advance on a certain influence length and that the survey points are irregularly located, it was chosen to carry out fitting at a given section using data in the vicinity of the section, weighted according to their axial distance to the considered section. Data weighting is achieved using a normal distribution (Gaussian curve) with a standard deviation of 10 m, which means that survey points further than 25m away from the section become negligible.

Taking into account that the resolution of the monitoring data is in the order of 1mm, it was also chosen to filter out the "noise" away from the tunnel axis using a transversal weighting of the data, equally based on a normal distribution with a standard deviation of 5m. Only the sections with at least 3 measures per meter within 10m of the tunnel axis are considered meaningful and are processed.

This non-local advancing process results in a smooth and continuous distribution of Peck's parameters along the tunnel axis, with an overlap in a range of 8m.

4.3 *Step 2 – Assessment of trough width parameter of each layer*

The 1.8km long geotechnical and tunnel profiles are discretised in 5m steps, similarly to the advancing fitting process. The equivalent trough width parameter can be expressed as a weighted average of the characteristic width parameter of each of the *p*=*m*+*n* overburden layers, Chiriotti (2000):

$$k_{eq} = \frac{(1-\lambda).\sum_{i=1}^{m} z_i.k_i + \lambda.\sum_{j=m+1}^{n} z_j.k_j}{(1-\lambda).\sum_{i=1}^{m} z_i + \lambda.\sum_{j=m+1}^{n} z_j} \tag{4}$$

with λ a weight depending on the distance of the layer from the tunnel axis. Layers closer than one diameter from the tunnel are weighted with 1-λ, while layers further away are weighted with λ. In accordance with Chiriotti (2000), we use λ = 65 %.

The inverse problem searching for characteristic width parameters (one per geotechnical unit) matching best the 360 fitting sections is solved using a probabilistic method presented in Mahdi (2016). To simplify the problem, strata have been grouped in 4 significant geological units.

4.4 *Step 3 – Constitutive models, volume loss and confinement pressure*

2D finite element analysis is used to calibrate the deformation parameters of the Hardening Soil Model (HSM) against the volume loss measured for a known confinement pressure applied at the face. Once calibrated, the finite element model can provide, for a given geotechnical configuration, the evolution law of volume loss against variation of the confinement pressure.

The following deformation parameters of the HSM are used, with α the Menard's rheological factor and μ a correlation factor depending on the type of loading (stand-up time and stress path):

$$E_{50} = \mu \frac{E_m}{\alpha} \tag{5}$$

$$E_{oed} = 1,2.E_{50} \tag{6}$$

$$E_{ur} = 3.E_{50} \tag{7}$$

The fixed ratios chosen for the determination of E_{oed} and E_{ur} are common values for sands and marlstones encountered in the Plaine de France. The stress dependency of soil stiffness has not been considered.

5 BACK-ANALYSIS RESULTS

5.1 *Data relevance*

Before any data treatment, the relevance of data points is verified by checking if settlement appearance coincides with the arrival of the TBM. Figure 3 shows that the great majority of data points are consistent with expected TBM advance rate. Only 9 survey points displaying heave instead of settlement have been discarded for further back-analysis.

5.2 *Considered sections for fitting*

Figure 4 shows in blue the sections used for fitting and in red the sections deemed too poor in data to allow meaningful fitting. The data are particularly poor in the first 150m (27 discarded sections), just enough for fitting between 150m and 800m (between section 27 and section 170) and particularly dense between 800m and 1800m. In total 329 sections, i.e. 92 %, are processed.

5.3 *Peck's parameters*

Solving for least square converged in 315 sections out of 329, i.e. 96%. In sections with a wealth of data, curve fitting is particularly successful as can be seen in Figure 5.

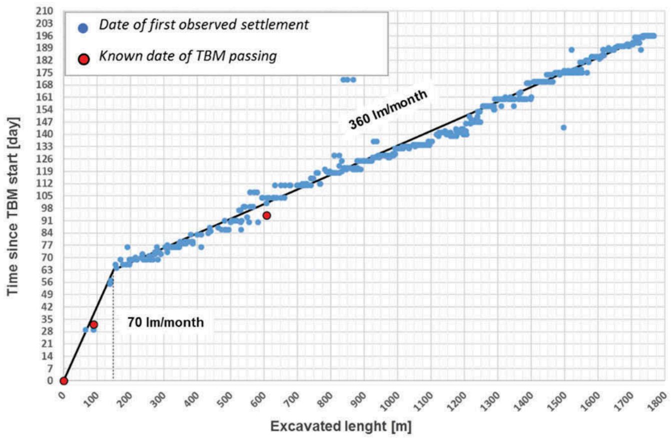

Figure 3. TBM advance rate derived from first settlement detection.

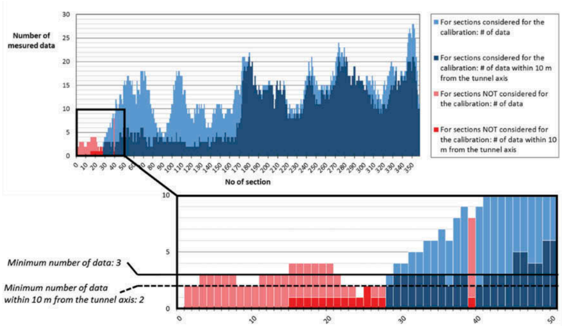

Figure 4. Number of survey points for each fitting section.

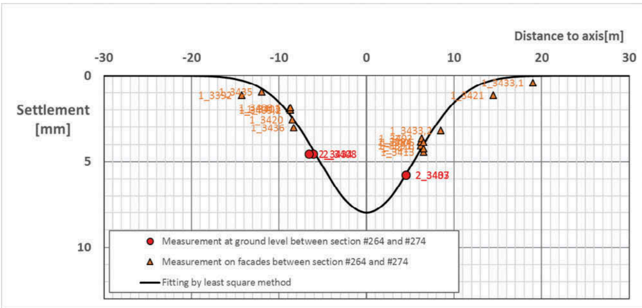

Figure 5. Example of Peck's curve fitting on data around section #269.

5.3.1 *Equivalent trough width*

The equivalent trough width parameters (k_{eq}) resulting from the fitting process are shown in Figure 6. Over the first half of the drive, the TBM bores with an overburden made of calcaire de Saint Ouen and fills. Fitted k_{eq} values are then quite high (0.6 on the average) and display some local anomalies (values around 1). The results over the first half must be considered with caution as data density is not high enough to achieve good reliability of the fitting. Over the second half of the drive, the TBM bores full face in the Sables de Beauchamp with an overburden composed mainly of Calcaire de Saint Ouen. The k_{eq} values fitted in this denser zone are more stable and within the range [0.3, 0.5], in accordance with reported empirical values for this type of ground.

5.3.2 *Characteristic trough width parameters of individual layers*

Solving for the inverse problem formulated by Equation (4) gives probabilistic values of trough width parameters of individual layers, as presented in Table 2. Solved values fall within the empirical range. Reassessing the apparent k_{eq}, Figure 6, from this data set falls within +/- 0.1 of the fitted k_{eq} value in 76% of the considered sections.

5.3.3 *Volume loss and maximum settlement*

The volume loss and maximum settlement resulting from the fitting process are shown in Figure 7. These values correspond to a well-controlled TBM drive, with volume loss always remaining well below 0.3% and maximum settlement below 10mm, expect on the first 300m (from section 1 to section 60) from the launching shaft and within 50m of the reception shaft.

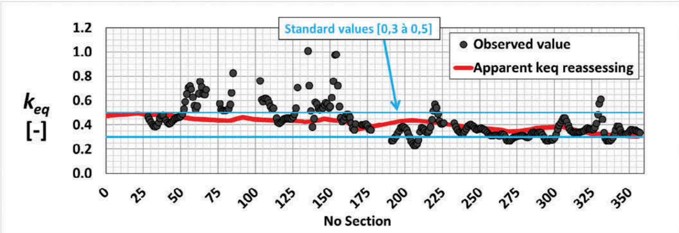

Figure 6. Comparison between observed k_{eq} values fitted along the entire TBM drive and reassessed based of characteristic trough width parameters given in Table 2.

Table 2. Characteristic trough width parameters of ground layers in Plaine de France.

Formation	Solved values
Fills	0.30
Alluvions	0.30
Marnes Infragypseuses	0.50
Calcaire de Saint-Ouen	0.55
Sables de Beauchamp	0.20

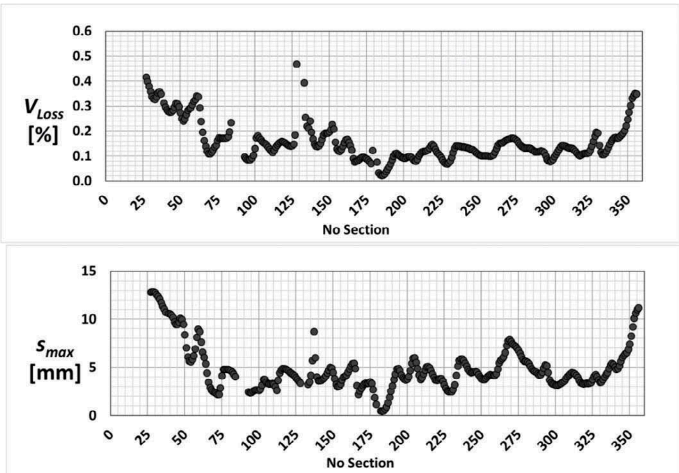

Figure 7. V_{Loss} and s_{max} values as fitted along the entire TBM drive.

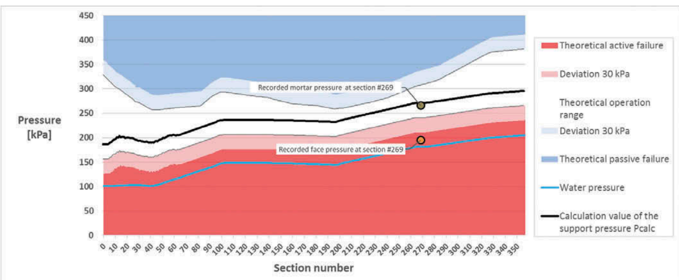

Figure 8. Operation range of the confinement pressure along the TBM drive.

5.4 *Back-analysis based on 2D finite element modelling*

5.4.1 *Confinement pressure upper and lower bounds*

Before carrying out finite element analysis, face stability conditions are considered to define theoretical upper and lower bounds to the confinement pressures. The approach developed by Anagnostou & Kovari (1994) and completed by de Broere (2001) is adopted to define the active and passive failure bounds with safety factors of 1.05 on pore pressure and of 1.5 on earth pressure, see Figure 8. A deviation of +/-30 kPa on the control of the confinement pressure in a EPB is further introduced, DAUB (2016).

The full confinement profile applied on site is not available. However, the measured confinement pressure and the grouting pressure at section #269 are reported to be 1.95 bar and 2.66 bar respectively. While the applied confinement pressure is relatively low, just above pore pressure, the applied grouting pressure reaches values high enough to minimise settlements. This is in accordance with observations made by Aristaghes (2001):

- Face support pressure ensures tunnel face stability but has only a negligible effect on settlement control
- When implemented, support pressure along the shield tail plays a sensitive role for settlement control
- Annular gap grouting pressure keeps on the action of the shield tail support pressure when the latter is implemented, or can even heaves the previously unconfined soil along shield tail

5.4.2 *Correlation between pressure meter moduli and HSM moduli*

Knowing the confinement pressure for section 269, the correlation factor μ is calibrated by finite element analysis against fitted volume loss. The agreement is obtained for μ = 4 both in Calcaire de Saint Ouen and in Sables de Beauchamp formations.

The correlation factor μ is also calibrated in 5 other sections, #6, #32, #60, #150 and #340 which cover the various geotechnical contexts encountered by the TBM. It has been done assuming that the apparent confinement pressure is given by the black line in Figure 8. Again, overall agreement is obtained for μ = 4 both in Calcaire de Saint Ouen and in Sables de Beauchamp formations.

5.4.3 *Curve fitting for volume loss as a function of confinement pressure*

On the 6 modelled sections, the response of volume loss to confinement ratio has been studied and it was concluded that power laws $Vloss = A.(P_c / \sigma_v)^B$ can relate these parameters, see Figure 9.

Two slightly different families of curves can be distinguished: the a-curve corresponds to boring with the upper half in Calcaire de Saint Ouen, A= 0.1 and B=2.2, while the b-curve corresponds to boring full face in Sable de Beauchamp, A= 0.04 and B=3.1.

Once these laws are calibrated, it becomes possible to determine the volume loss associated to the confinement ratio derived from by the confinement pressure given by the black line in Figure 8, and to confront the calculated settlement value with the observed values.

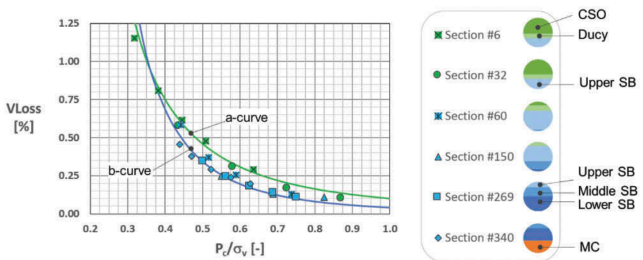

Figure 9. Evolution of V_{Loss} with confinement ratio.

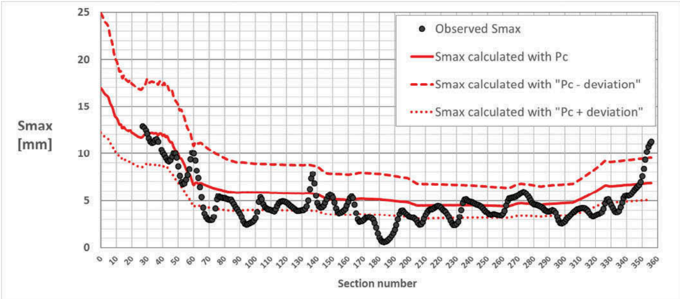

Figure 10. Comparison between observed S_{max} and calculated S_{max}.

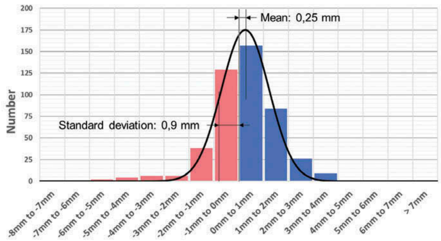

Figure 11. Difference between observed settlement at survey points location and calculated settlement based on proposed model parameters.

Using V_{Loss} laws and k values previously presented, Figure 10 shows a very good agreement between the observed settlement values and calculated ones. The observed maximum settlements along the entire tunnel alignment are well framed by the calculated values obtained considering the theoretical confinement deviation of +/-30kPa.

It is noteworthy that 100m around section #182 where an 8 levels building is located, settlements are very low, which seems to indicate that confinement pressure has been purposely increased to pass this sensitive building.

These calculation process and parameters allow to achieve an estimate very close to the field data. Indeed, the difference between recorded settlement values at the 463 survey points on site and calculated values can be characterized with a normal distribution, nearly centered and with a narrow standard deviation, below 1 millimeter, see Figure 11.

6 MAIN CONCLUSIONS

The extension works of Paris metro line 12 includes a 3.8 km 9.15 m diameter tunnel that was bored by an EPB shield between 2010 and 2011. The back-analysis of settlement monitoring and the resulting proposed predictive model presented in this paper aim to improve design choices and risk assessment while boring new tunnels in similar geological context, i.e. the Plaine de France basin.

The proposed model is particularly suited to carry out vulnerability analysis of planned tunnels of line 16, line 15 east and line 17 of the future Grand Paris metro, that are to be bored in the same geological context.

The back-analysis of monitored settlements has been performed by the least square method using nonlinear regression and non-local fitting by data weighting using 463 survey points data. It shows settlement troughs in near greenfield condition are well described by Peck 's formula.

The volume loss depends on the confinement ratio, see Figure 9, and commonly obtained values are around 0.1% to 0.2%. Observed settlement trough wide parameter values are between 0.3 and 0.4, see Figure 7, and k values presented in Table 2 combined with Equation (4), Chiriotti (2000), give a good estimate of the apparent trough width parameter at surface k_{eq}.

Once observed Peck's parameters has been defined, 2D FEM analysis has been carried out to define modelling parameters that allow the best fitting over these data.

While FEM gives an erroneous estimate of the settlement trough width, it gives however a good estimate of the volume loss, from 2D FEM and HSM soil model, considering a correlation factor for the pressure meter μ =4 both in Calcaire de Saint Ouen and in Sables de Beauchamp formations, see §4.4.

The confinement pressure used in the FEM model is set to the grouting pressure, which can be chosen between 0.5 and 1 bar above the face stability pressure. While this calibration is carried out on a single fully instrumental section, the generalization of the deduced empirical law for volume loss yields an excellent match of maximum settlement deduced from monitoring data over the full length of the drive, within the usual deviation on EPB face pressure.

REFERENCES

Anagnostou G. & Kovari K. 1994. The Face Stability of Slurry-shield-driven Tunnels. *Tunnelling and Underground Space Technology*, Vol. 9.

AristaghesP & Autuori P. 2001. Calcul des tunnels au tunnelier. *Revue Française de Géotechnique*. No 97

BroereW. 2001. Tunnel face stability and new CPT Applications. PhD Thesis, Technical University of Delft.

Chiriotti E. Marchionni V. Grasso P. 2000. Porto Light Metro System, Lines C, S and J. Interpretation of the Results of the Building Condition Survey and Preliminary Assessment of Risk. Methodology for Assessing the Tunnelling Induced Risks on Buildings along the Tunnel Alignment. *Normetro – Transmetro, Internal technical report*.

DAUB. 2016. Recommendations for Face Support Pressure Calculations for Shield Tunnelling in Soft Ground.

ITA/AITES Report. 2006. Settlements induced by tunneling in Soft Ground. *Tunnelling and Underground Space Technology*. No 22.

Mahdi S. Houmymid F.Z. Chiriotti E. 2016. Use of numerical modelling and GIS to analyse and share the risks related to urban tunnelling - Greater Paris - Red Line – South section, ITA-AITES WTC 2016.

O'Reilly M.P. and New B.M. (1982). Settlements above tunnels in the United Kingdom - Their magnitudes and predictions, *Tunnelling* 1982.

Peck R.B. 1969. Deep excavations and tunnelling in soft ground, 7th International Conference on Soil Mechanics and foundation Engineering, Mexico City, State-of-the-art Volume.

Schmidt B. 1969. Settlements and Ground Movements associated with Tunnelling in soils, PhD Thesis University of Illinois, Urbana.

Tunnels and Underground Cities: Engineering and Innovation meet Archaeology, Architecture and Art, Volume 6: Innovation in underground engineering, materials and equipment - Part 2 – Peila, Viggiani & Celestino (Eds)
© 2020 Taylor & Francis Group, London, ISBN 978-0-367-46871-2

Addressing the radial joints behaviour of Steel Fibre Reinforced Concrete (SFRC) segments under concentrated loads

M. Mangione, M. Ceccarelli & A. Pillai
Arup, London, United Kingdom

C. Agostini
S.G.S. Studio Geotecnico Strutturale, Rome, Italy

ABSTRACT: Precast concrete tunnel segments are subjected to high concentrated compressive stresses generated by the transfer of hoop loads across the radial joints. This effect is emphasized by the joint opening associated with diametrical deformations resulting by tolerances during lining installation and deformations imparted by external actions. These concentrated stresses produce tensile bursting forces at radial joints that may lead to critical joint damage, especially in SFRC segments. The bursting stress intensity and distribution depends strictly on the contact area at the joint location. While the bursting stresses can be evaluated by means of analytical formulas, the estimation of the joint rotation and contact area is more complex due to the non-linear behaviour of the concrete material. This paper provides an analytical method for the evaluation of radial joint behaviour and it is tested against advanced numerical modelling using geometrical properties of the segmental lining of the Airport Link Project, one of the largest designed and built SFRC segments.

1 INTRODUCTION

Mechanized tunnelling is widely adopted in different ground conditions due to its efficiency and enhanced safety. In TBM driven tunnels, the lining consists of a ring composed by precast concrete segments assembled within the TBM shield.

The tunneling industry in several countries is moving towards a preference in use of SFRC segments, where conventional reinforcement is eliminated in favour of steel fibres added to the concrete mix (fib 2017). The use of SFRC improves manufacturing efficiency and optimises production cost. From a structural perspective, steel fibres enhance the post-crack properties of concrete, leading to a more ductile material behaviour. Such ductility is due to the ability of the fibres to transfer tensile stresses across a cracked section, providing improved toughness of the material, which leads to less damage due to impact, improved quality of the finished segments, structural capacity in tension and limitation to crack development.

Tunnel segments are subjected to many loading conditions from the precast plant (e.g. demoulding, stacking and handling) to the tunnel installation (e.g. TBM thrust, tail injection). In long term conditions, precast segments are loaded by compressive hoop forces, arising from surrounding soil and groundwater, which generate high concentrated compressive stresses in correspondence of radial joints. The stress concentration is emphasized by the joint opening and the consequent reduction of contact area between two adjoining segments (Figure 1a). The opening of radial joints is associated with diametrical deformations resulting by assembly tolerances of the ring within the TBM and deformations imparted by external actions.

The concentrated compressive hoop force at radial joints redistributes over the thickness of the segment generating orthogonal tensile bursting stresses (Figure 1b) in accordance with the theory firstly developed by Leonhardt (1964). Bursting stresses may lead to concrete cracks

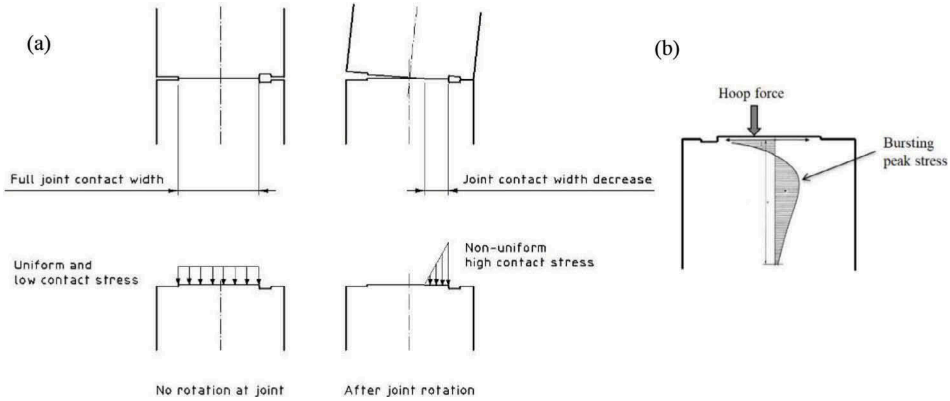

Figure 1. Effect of contact area on compressive stress distribution (a) Bursting stress distribution at the radial joint (b).

which may affect serviceability and ultimate limit state requirements. In traditionally reinforced segments, reinforcement at the joints is included to meet the demand for bursting stresses. However, deeper understanding of the behaviour of the radial joints is a most significant benefit for the structural design of SFRC segments, to ensure that the tensile forces arising by the concentrated joint stresses are duly assessed and the need for localised reinforcement is eliminated or reduced.

Bursting stresses are assessed by means of analytical approaches, e.g. the Leonhardt's theory or equations proposed by standard codes, such as Eurocode 2 or ACI-318. Whereas the intensity and distribution of the bursting stress can be deducted from these references, they do depend on the definition of the zone of contact between segments at the radial joints. There is no clear guidance in international codes and manuals on how to estimate the contact area accounting for tolerance and future deformation on the rings and this may lead to practical limits on evaluating the ultimate capacity of the SFRC segments at the radial joints.

The estimation of the contact area is function of the ovalization and the joint behaviour, which is influenced by the non-linearity in the concrete material. At the ultimate limit state, for example, the crushing of concrete enhances the joint closure, so the compressive hoop force is distributed over a larger surface of the joint. The assessment of the joint contact area is also dependent on the joint type (convex or flat joint). This paper will focus on flat-flat joints.

This paper aims to provide an alternative approach to represent the radial joint behaviour, compare it to the current methodology available to the tunnelling community, and present results from numerical modelling with an advanced material constitutive law to justify the presented approach. In particular, Chapter 2 briefly gives an overview of the analytical methods from literature commonly used for the evaluation of the contact area and highlights some simplifications of these approaches relative to the evaluation of the contact area. Chapter 3 describes the alternative method, developed and proposed by the Authors to overcome such limitations. Finally, the results in terms of joint rotation-contact area derived by both literature approaches, Authors approach and numerical modelling on a case study are presented and discussed in Chapter 4.

2 RADIAL JOINT BEHAVIOUR: EXISTING DESIGN APPROACHES

For the design of the ring, the radial joint local behaviour for an ovalised geometry must be properly addressed especially in case of SFRC only lining.

The ovalization of the ring can be caused by poor build, tolerances during installation within the TBM shield and ground loading. This initial deformation is typically expressed as diametrical distortion, defined in project specifications or guidelines such as the BTS Specification for Tunnelling (BTS 2010). Additional distortions may be imposed by Clients as a long-term performance requirement.

Establishing the contact area at radial joints is complex due to the effect of the diametrical deformation of the ring and the associated rigid body rotation of segments which results in an opening of the joints. As the hoop load is transferred, the concentrated contact stress produces strains over the segment length which lead to localised segment shortening which results in an increase in contact area (closing effect) until a state of equilibrium is achieved. The extent of joint closure is a function of lining geometry, concrete stiffness and magnitude of applied hoop load.

Analytical approaches have been proposed by different Authors, e.g. Janssen (1983), Blom (2002), Tvede-Jensen et al. (2017) to describe the behaviour of flat-flat joints.

The radial joint behaviour can be idealized in three stages, which are function of the magnitude of the hoop force applied. Along with the increase of joint rotation, the radial joint at first exhibits a linear-elastic behaviour (Stage 1 - linear) with a constant rotational stiffness: at this stage, the radial joint is fully closed. Then a non-linear elastic behaviour (Stage 2 – geometrical non-linearity) occurs when the joint starts opening. A third stage is reached when the concrete elastic strain is overcome (Stage 3 – concrete non-linearity).

The three analytical approaches, mentioned above, have been derived considering that the joint deformed zone presents a constant strain and it extends for a length equal to the joint thickness. Janssen (1983)'s method is based on the elastic theory and it does not account for the non-linear behaviour of the concrete, i.e. Stage 3.

This method has been further expanded by Blom (2002), who adds to Janssen's approach the third stage considering a bi-linear stress-strain relationship for the concrete (i.e. elastic perfectly plastic behaviour). The rotational stiffness is non-linear and the maximum stress is equal to characteristic compressive strength of the concrete, until the ultimate strain is reached.

Recently, Tvede-Jensen et al. (2017) refined Blom's method, modifying the third stage. They considered the parabola-rectangle stress-strain relationship and, more importantly, they accounted for the increased of compressive strength and strain limit due to partial loaded area and confined concrete effects, respectively. To include those effects, Eurocode 2 equations have been adopted.

Details about the mathematical formulations of the three approaches can be founded in Tvede-Jensen et al. (2017).

The aforementioned methods are widespread in the current design practice; however, they present some limitations. In particular, the spreading of compressive stress from the joint face to the full thickness of the segment is not accounted, assuming that the strains caused by the hoop load are only localised in close vicinity of the joint loaded area. The shortening of the segment, due to the compressive force is therefore not considered, providing a conservative estimate of joint closure and associated bursting stresses. The approach proposed by the Authors and described in the following chapter aims to address this aspect.

3 PROPOSED APPROACH: THE JOINT CONTACT METHOD

The proposed method, hereinafter the "Joint Contact Method", has been developed by the Authors and it has been applied successfully on several projects worldwide. The Joint Contact Method was developed to assess the contact area and stress distribution at radial joints to perform an optimised design of joints, in term of bearing and bursting requirements.

The contact area is the result of the rotation at segment joints and deformation of the concrete. As mentioned above, already after the ring installation, joint opening and rotation are expected because of assembly tolerances of the ring within the TBM and deformations imparted by external actions.

The initial joint opening ("birdsmouthing") of the unloaded ring can be calculated assuming an elliptical deformation of the ring and infinitely stiff segments so that all deformation occurs by rotation of the joints as shown in Figure 2. This initial opening of the joints is counteracted, to some extent, by the closing effect associated with the transfer across the joint of hoop forces arising from the external loads. A distribution of compressive stresses from the hoop loads shall be defined so that the resulting strains imparting a shortening/deformation of the concrete within the contact area can be calculated.

As per the methods presented before, the Joint Contact Method considers three possible scenarios for the radial joint behaviour for an applied hoop load. When joint closure occurs, it is assumed that any component of the hoop load above the value that leads to closure will have a constant stress distribution along the joint thickness (Case 1 in Figure 3). However, the closure of the joint may not occur if the concrete segments are significantly stiff, the imposed initial deformations are high, or the maximum hoop force is relatively low in magnitude. In this instance, the joint will close partially, and the contact area will be lower than the available joint thickness (Case 2 and 3 in Figure 3). If compressive stresses exceed the design bearing capacity of the concrete section, the contact stress is expected to distribute over a larger area (Case 3 in Figure 3). The bearing strength is calculated with the partial loaded areas rule following Eurocode 2.

The eccentric hoop force at the radial joint produces strains and deformation, leading to shortening and section rotation, which can be derived using the theory of elasticity. A critical consideration for the approach is that the stress distribution within the segment is not constant over the length of the segment. To calculate segment deformation, the segment is ideally divided in two different regions, D and B (Figure 4) according to Leonhardt's strut and tie theory.

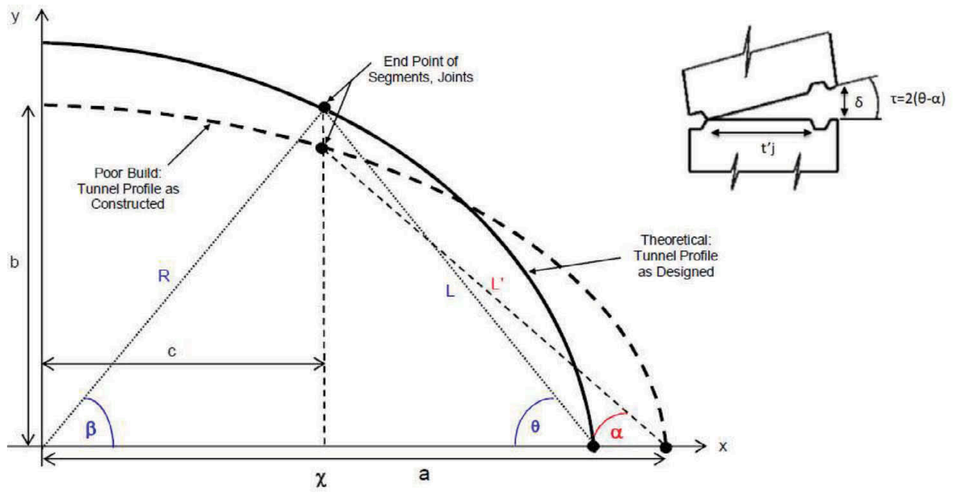

Figure 2. Schematic radial joint opening due to assumed elliptical deformation.

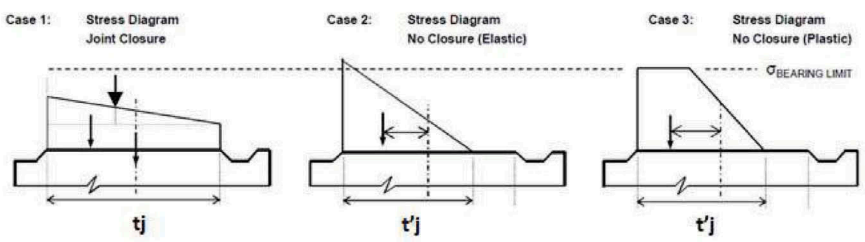

Figure 3. Possible configurations of contact area depending on joint closure.

In the case of segmental lining, the so-called D-region (where D stands for discontinuity or disturbance) refers to the first part of the segment, where the beam theory is not valid due to the high compressive force transferred at the radial joint. The D-region is assumed to extend over a length equal to the segment thickness and the method assumes that the variation of hoop force and bending moment imparted by external load is negligible within this region. Therefore, the stress at the boundary necessary for the equilibrium of the D-region can be easily calculated (Figure 4) and the stresses distribution within this region can be derived through Leonhardt's strut and tie approach. In the D-region, stress and strain distribution are non-linear, however the mean circumferential strains can be conservatively computed as:

$$\varepsilon_{A,mean} = 0.5\,(\varepsilon_A + \varepsilon_{A'}) \tag{1}$$

$$\varepsilon_{B,mean} = 0.5\,(\varepsilon_B + \varepsilon_{B'}) \tag{2}$$

i.e. a linear variation between the edges AB and A'B' (Figure 4) is assumed. This approach is considered conservative as it produces a lower joint closure and therefore a higher concentration in stresses.

In the B-region (where B stands for Bernoulli or beam), the Bernoulli hypothesis of planar section is considered valid and the internal state of stress can be derived from the sectional forces. The present method assumes that in the B region the eccentricity of the load is reduced progressively up to the distance L from the joint, where an inflection point (i.e. zero bending moment) occurs, resulting in a constant stress distribution. Such length can be reduced to allow for a more robust design.

The mean values of strain can be derived in both D and B-regions from stresses at the boundaries and consequently the movement of points A and B (Figure 4) can be computed.

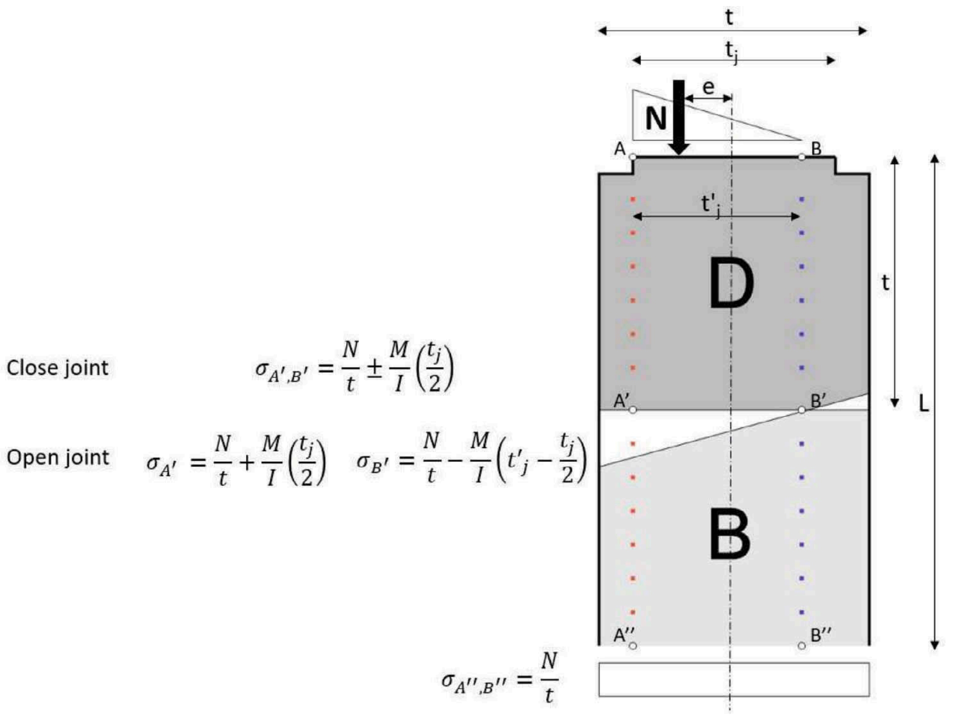

Figure 4. Assumption of circumferential stress distribution over the segment length.

The rotation of the joint imparted by external loads is then given by the differential movement between the two points over the contact length. The so obtained rotation is used to recalculate the joint closure and the contact area.

As a result, the Joint Contact Method aims to provide a rational approach, accounting for the mechanical response of the whole segment and not only a small portion near to the joint as per Janssen (1983), Blom (2002) or Tvede-Jensen et al. (2017). Moreover, plastic concrete behaviour at high stresses is adopted along with the bearing strength gain due do the partially loaded area. These key features allow for a more realistic assessment of radial joint behaviour, extremely beneficial in case of SFRC-only lining.

However, the structural behaviour of the ring is complex and geometrical as well as material non linearity is difficult to incorporate in an analytical design approach, and only advance numerical modelling can give insight on the complex radial joint response. The Joint Contact Method has been verified with both 2D and 3D finite element during detailed design of segmental lining. In this paper, the Joint Contact Method and its assumptions were tested against advanced numerical modelling using the geometrical properties of the lining of the Airport Link Project.

4 CASE STUDIES

In order to better understand the development of the contact area with the increase of tunnel ovalisation and to validate the method proposed above, a parametric study for different load conditions has been carried out with DYNA-LS.

The non-linearity has been accounted by using advanced non-linear numerical analysis where all segments were modelled as solid elements. The software DYNA-LS has been used to run such model while an elastic perfectly plastic constitutive law for the Steel Fibre Reinforced Concrete was adopted, including the failure surface developed by Ottosen (1977), which offers a more realistic approximation to the different triaxial stress states that lead to failure in concrete.

The advanced numerical tool has been used in a full soil structure interaction model (Figure 5) to recreate the Airport Link Project ring. The ring is loaded with ground stresses and is deformed diametrically to match the design ovalisation of the ring.

This approach using DYNA-LS can give a better and more realistic estimation of the joint contact area as the whole ring is modelled accounting for the real thickness of the segments and the ground stiffness. The loading conditions are applied as external loads and the constitutive model can provide a more realistic contact area including softening effects of the concrete at high compressive stress regime (localised crushing) as well as softening due to the non-linear stress-strain relationship of the concrete in tension.

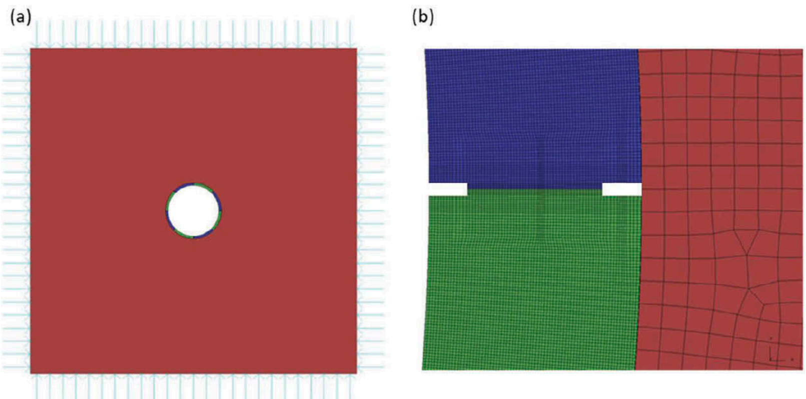

Figure 5. Ground and ring model in DYNA-LS (a). Radial joint detail (b).

4.1 *FE models features*

The Airport Link geometry has been considered with an internal diameter of 11.35m and thickness of segmental lining equal to 400mm. A recess of 80mm at both sides of the segment has been considered for gasket positioning and caulking groove.

The SFRC has been modelled using an elasto-plastic constitutive model where the following properties have been applied:

- Characteristic compressive strength f_{ck} = 50.0 MPa;
- Characteristic residual tensile strength $f_{R3,k}$ = 2.235 MPa.

Two different overburden levels have been analysed, considering two lateral pressure coefficients:

Table 1. Loading conditions considered for the DYNA-LS analysis.

	Vertical Stress	Horizontal stress (k_m = 0.8)	Horizontal stress (k_m = 1.5)
Mid-level (34m of depth)	681 kPa	545 kPa	1022 kPa
Deep-level (68m of depth)	1360 kPa	1088 kPa	2040 kPa

The ground load is applied as boundary condition: the loads are applied at the time step 0 and are kept constant during the analysis. At the same time, the proper initial value of the internal stress in the whole domain is imposed.

As the method proposed in the paper is focused on the structural response on the lining, for sake of simplicity the surrounding ground has been assumed as linear elastic material with an elastic modulus of 100MPa, and a Poisson's ratio of 0.2. The interface between lining and soil is set as a full slip condition, whereas the joint-joint interface is characterized by a frictional coefficient equal to 0.6.

It is important to highlight that, due to model computing limitations, at the time step 0 the tunnel is undeformed, and it gets deformed with the gradual application of the external loads. Therefore, construction tolerances and joint opening related to poor building are forced in the loaded ring, which is an accepted approximation for the purpose of defining the contact area.

4.2 *Results*

The results obtained with the advanced numerical analyses are satisfactory. As expected, the higher is the deviatoric stress the higher is the ovalisation of the tunnel. In fact, in the cases of lateral pressure coefficient of 1.5, larger ovalisation and higher reduction of contact area are observed. Table 2 presents a range of results varying magnitude of load and diametrical distortion.

As mentioned above, the concrete behaviour plays a significant role in the overall joint response. In fact, in the case of lateral pressure coefficient equal to 1.5, the deeper tunnel exhibits a wider area of plastic stress in correspondence of the radial joint, whereas, the lower hoop stress in the mid tunnel stay in the linear elastic branch. This justifies the difference of contact areas between the two models: i.e., the concrete plastic behaviour enhances the joint closure and consequently the contact area increase (Table 2).

A first check on the assumptions adopted in the Joint Contact Method has been made. As shown in Figure 6, the disturbed area of circumferential stresses due to the hoop load transferred at the joint presents a limited extent. As expected, the so-called D-region extends for a length within the segment thickness. Moreover, an important assumption of the Joint Contact Method was the location of the inflection point, where the bending moment is zero, occurs in correspondence of the radial joint at 45deg above the tunnel springline, so L (the length of the chord) is approximately equal to 4.6m, which is in line with what assumed in the Joint Contact Method.

Table 2. Hoop force, ovalisation and contact length reached in the last analysis step.

	Deep level $k_m = 1.5$	Deep level $k_m = 0.8$	Mid level $k_m = 1.5$	Mid level $k_m = 0.8$
Hoop force (MN/m)	10.39	7.69	5.36	4.00
Diametrical displacement (mm)	104.4	48.8	47.7	23.8
ovalisation (%)	(0.92%)	(0.43%)	(0.42%)	(0.21%)
Contact length (mm)	169	200	140	212

The Joint Contact Method has been tested with the numerical modelling evidence and the methods from literature, presented in Chapter 2. The joint rotation arising in DYNA-LS are plotted against the contact area (Figure 7) and are compared to the analytical solutions by Janssen (1983) Tvede-Jensen et al. (2017) and the method proposed by the Authors. The plot shows a similar behaviour of the three approaches. In particular, the Joint Contact Method aligns better with the numerical data at low angles, confirming that the current approaches are conservative for joint closure. In joint opening, the response of the concrete within the ring is stiffer than what the Joint Contact Method produces. Further analysis will be required to check the Joint Contact Method with different tunnels size, loading conditions and concrete properties.

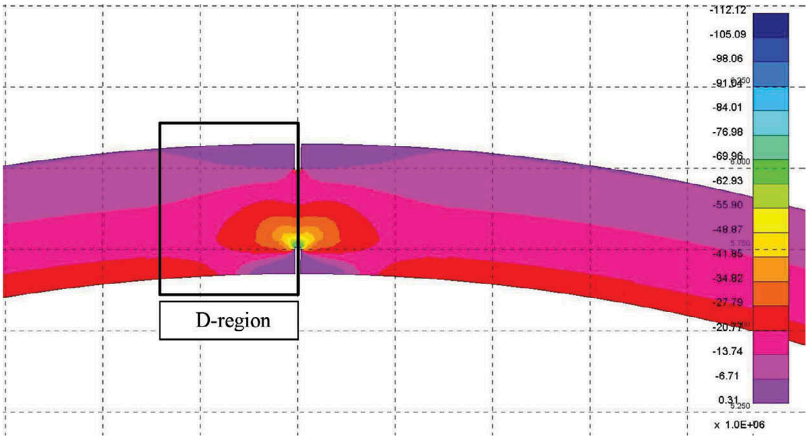

Figure 6. Circumferential stress in correspondence of the joint at the crown.

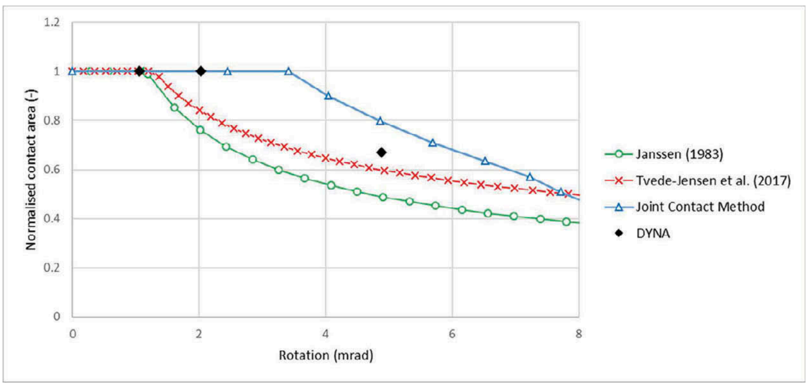

Figure 7. Comparison of DYNA-LS results with analytical formula for hoop force of 5200 kNm/m.

5 CONCLUSION

The behavior of radial joints is the key point of structural design of segmental lining, especially with steel fibre reinforced concrete (SFRC). A reliable assessment of the behaviour of the radial joints can ensure that the tensile bursting forces arising by the concentrated stresses are properly assessed, leading to a partial or complete removal of traditional reinforcement.

Assessing the contact area at radial joints is complex, there is limited guideline and its value is a critical parameter for the design. The Authors have developed a close form approach, tested in a number of projects over the last decade. However, the Joint Contact Method here presented has been tested with numerical analysis. In fact, numerical modelling can address properly the joint behaviour, in term of contact area and bursting stress for different loading conditions. These preliminary results are quite satisfactory: the analytical Joint Contact Method seems to represent well the radial joint non-elastic behaviour by providing a good match with the results obtained by the numerical analysis. A good estimation of the joint contact area which takes into account the non-elastic behaviour of the concrete allows to perform a reliable design avoiding over-conservatism in the estimation of the bursting stresses and consequently in the reinforcement design. This aspect is of even more important in case of SFRC-only ring design, where the tensile resistance is only provided by the post-crack properties of the fibres.

To justify full applicability of the method, the Authors plan to run further analyses with different tunnel geometries and load case scenarios to cover a wider spectrum of design situations, validated by non-linear numerical analyses.

ACKNOWLEDGEMENT

The Authors would like to acknowledge the Arup tunnelling team for the support and valuable input and the Arup Advance Technology and Research team for the contribution to the numerical modelling.

REFERENCES

ACI 318M-14. Building Code Requirements for Structural Concrete. American Concrete Institute.

BTS 2010. Specification for Tunnelling, Third Edition. Thomas Telford.

Blom, C.B.M., 2002a. Design philosophy of concrete linings for tunnels in soft soils. PhD thesis Technische Universiteit Delft.

EN 1992- 1-1 2004. Eurocode 2: Design of concrete structures – Part 1-1: General rules and rules for buildings.

Fib CEB-FIP 2010. Model Code for Concrete Structures 2010.

Fib CEB-FIP 2017. Bulletin 83 Precast tunnel segment in fibre-reinforced concrete.

Janssen, P., 1983. Tragverhalten von Tunnelausbauten mit Gelenktübbings. PhD thesis Technische Universität Braunschweig.

Leonhardt, F. 1964. Prestressed concrete, design and construction. Wilhelm Ernst & Sohn, Inc., Berlin and Munich.

Ottosen, N.S., (1977) "A Failure Criterion for Concrete," Journal of the Engineering Mechanics. Division, Volume 103, Number 4, July/ August, pages 527–535.

Tvede-Jensen, B., Faurschou, M. and Kasper, T., 2017. A modelling approach for joint rotations of segmental concrete tunnel linings. Tunnelling and Underground Space Technology, 67, pp.61–67.

Tunnels and Underground Cities: Engineering and Innovation meet Archaeology, Architecture and Art, Volume 6: Innovation in underground engineering, materials and equipment - Part 2 – Peila, Viggiani & Celestino (Eds)
© 2020 Taylor & Francis Group, London, ISBN 978-0-367-46871-2

Fiber glass and "green" special composite materials as structural reinforcement and systems; use and applications from Milan Metro, Brenner Tunnel up to high speed train Milan – Genoa

G. Manuele, M. Bringiotti & G. Laganà
Maplad Srl – Catania, Italy

D. Nicastro
GeoTunnel Srl – Genoa, Italy

ABSTRACT: Glass Fibre-Reinforced Polymer (GFRP) is nowadays a common practice in tunnelling; they are used in several applications as provisional structures, in a safe and cost effective way. Classical example is the so called "soft eye" where a TBM has to pass. GFRP bars have a much higher tensile strength than steel rebars, they are easily machined and can be broken down into small pieces by the cutter head and can then be transported by the conveyor system together with the spoil. We'll describe other different applications of this kind of material as structural elements in the conventional tunnelling, manual constructed reinforcement cages in big launching shafts, ending in special products in the railway industry, where the anti-galvanic corrosion properties are unique. Maplad is working also on special basalt fiber polymer elements, which show increased mechanical and physical properties, most probably the product of the next future.

1 GLASS FIBER REINFORCED POLYMER PROFILES

1.1 *The material*

Fiber reinforced plastic (FRP), also known as fiber reinforced polymer, is a composite material made up of a polymer matrix blended with certain reinforcing materials, such as fibers. The fibers are generally basalt, carbon, glass or aramid; in certain cases, asbestos, wood or paper may be used as the fibers. Composite material is greater than the sum of its parts. The matrix, which is the core material devoid of fiber reinforcement, is hard but comparatively weaker, and must be toughened through the addition of powerful reinforcing fibers or filaments. It is the fiber which is critical in differentiating the parent polymer from the FRP.

The matrix is composed of unsaturated resin as the polymer (normally used are polyester or vinylester and sometime, for particular applications, different resins are used, but hardly for profiles intended for the construction market).

Catalysts and additives are added in the batch with the resin.

1.2 *Pultrusion process*

In the traditional pultrusion process the fibres are pulled from a creel through a resin bath and then on through a heated die. The die completes the impregnation of the fiber, controls the resin content and cures the material into its final shape as it passes through the die. This cured profile is then automatically cut to length. Fabrics may also be introduced into the die to provide fiber direction other than at 0°.

To make the rebars, it is used a different process: the fibers are pulled from creel through a resin bath, cross a ring used to define the diameter of the rebar and they are wound by a

Table 1. Comparison between GFRP and other traditional materials.

Property	GFRP	Steel	Aluminum	PVC	Unit
Density	1.8	7.8	2.8	1.4	g/cc
Tensile strength	300–600	370–500	200–400	40–60	MPa
Flexural resistance	400–450	330–500	200–400	70–100	MPa
Elastic modulus	25–30	210	70	2.8–3.3	GPa
Bending modulus	15–20	210	70	2.8–*3.3	GPa
Tensile elongation	1.5–2.0	13–35	5–35	10–80	%
Impact resistance	200	400	200	85–95	MPa/m^2
Thermal conductivity	0,25–0,35	100–230	100–230	0,15–0,25	W/m°C
Dielectric capacity	5–15	-	-	40–50	KV/mm
Volumetric resistance	10^{10}–10^{14}	0,2–0,8	0,028	$>10^{16}$	ωcm

transversal thread that reduces the section so as to create the improved adhesion of the profile. Catalysis does not take place inside the molds but through ovens.

Pultrusion is a continuous process, generating a profile of constant cross-section.

1.3 *Comparison with other materials used in construction and advantages of GFRP*

The following table, Table 1., shows the average values of the main mechanical and physical characteristics of the profiles in GFRP in comparison with other materials mostly used in constructions.

We can deduced that the GFR profiles are light materials with elevated mechanical features able to replace the steel profiles, but at the same time electrically insulating, with low thermal conductivity resistant to chemical agent; similar characteristics to plastic materials.

The GFRP profiles are also characterized by UV resistance, discoloration resistance and, being a light material, easy to install and assemble.

2 GFRP IN THE TUNNELING'S INDUSTRY

2.1 *Slope and face stabilization – Adeco Technique*

The ADECO-RS (Analysis of Controlled Deformations in Rocks and Soils) is a design philosophy that places at the center of the design of an underground work the deformations that occur in the middle in which the excavation proceeds, analyzing them in depth and identifying their more effective systems to control them.

It was born about 30 years ago from a theoretical/experimental research during which modern constructive technologies were developed - including the reinforcement of the core-face with fiberglass reinforcement - and they were severely tested in the field.

The method focuses attention on the study of the Deformative Response considering:

– the medium through which construction takes place,
– the action taken in order to accomplish the excavation and
– the reaction (or Deformation Response) produced following the above-mentioned action.

The medium is the terrain which, in depth, is subject to triaxial stress states.

The action is produced by the advancement of the excavation front at a determined speed V and causes a stress perturbation in the surrounding soil both in the transverse and longitudinal direction altering the pre-existing tension states.

The speed rate V depends as well to the excavation system used (mechanized or conventional): high speed rates reduce the propagation of the perturbation, influencing the Deformation Response which conditioned by the choice of the excavation system.

The ADECO-RS works on the base of three different components of the Deformative Response:

Figure 1. TOTO S.p.A., job site La Spezia. SIG at visit, drilling and manual long bar junction procedure.

- the extrusion, its primary component, which largely gets within the core and manifests itself, in correspondence with the surface delimited by the excavation face, in a longitudinal direction to the axis of the tunnel;
- preconvergence, identified as a secondary component of the Deformative Response;
- convergence, identified as the third component of the Deformative Response.

According to the ADECO-RS the convergence, therefore, is only the last stage of a very complex deformation phenomenon that originates upstream of the excavation face in the form of extrusion and preconvergence of the advance core and then evolve downstream of the same in the form of convergence of the cavity.

The novelty of the ADECO-RS is to always advance to full section and stabilize the excavation by first intervening on the ground upstream of the front using the core as a "control tool" upstream and the immediate closure of the pre-covering with the inverted arch as a downstream control instrument.

The ADECO-RS, having understood the true genesis and evolution of the Deformative Response, concentrates all efforts on the control of the extrusion which, being the "initial stage" and the source of the deformation process, if properly maintained in the elastic field, evolves towards preconvergence and convergence phenomena also in the elastic field, thus allowing to minimize the thrusts on short and long-term coatings.

The same method identifies three categories of fundamental tensile-deformational behavior:

- category A or stable core-face behavior;
- category B or short-term stable core-front behavior;
- category C or unstable core-face behavior.

It is therefore evident that in order to stabilize a tunnel during excavation in the short and long term (Figure 1), type B and type C behaviors must be reported to category A, intervening on the stiffness of the advance core by means of conservative pre-assembly of the cable and, subsequently, regulating, downstream of the excavation face, the extruding manner of the core-face, by closing and stiffening the first phase covering, close to the front, with the inverted arch.

The analysis and the control of the Deformative Response play a fundamental role as indispensable steps to design and correctly realize a work in the underground:

- the analysis must be performed using suitable analytical or numerical calculation tools based on the forecasts made and the designer must also make the necessary operational choices, in terms of systems, phases, digging cadences, consolidation and stabilization tools;
- control takes place at the "construction moment", when, by proceeding with the excavation, the design choices are made and verified by the measurement of the Deformative Response of the means to the actions implemented.

  It follows that to correctly design and build a work in the underground is essential:
- in the planning phase:
  - preliminary study of the tenso-deformative behavior (Deformative Response) of the ground, in the absence of stabilization works;

- define the type of pre-containment or containment actions necessary to regulate and control the Deformative Response of the excavation vehicle;
- choose the type of stabilization work;
- to compose, according to the expected behavior of the ground, the typical sections defining, in addition to stabilization interventions more appropriate to the context in which it is expected to operate, phases, cadences and times of implementation of the same;
- sizing and checking, the selected interventions to achieve the desired behavior of the excavation and the necessary safety coefficient of the work, also providing the tensile-deformative behavior of the same thus stabilized;

- under construction:
  - verify, during construction, that the tunnel's behavior during the excavation is the same as that foreseen by analytical way during the design phase. Then proceed with the development of the project by balancing the weight of the interventions between the core-front and the perimeter.

2.2 *Diaphragms walls and piles – Soft-eye Technique*

For several decades, TBM's have been used for the construction of tunnels. Depending on the local situation, the TBM may be placed at the start or at the end of its drive; for example maybe in a precut in the open terrain or maybe by lowering it into an excavation shaft down to the tunnel level. This latter technique is used mostly in congested city areas. A few years ago, starting and receiving a TBM in an excavation shaft required extensive measures such as breaking through the walls of the shaft, which are secured out of steel reinforced concrete. This preparation work needed time and has been expensive. In recent years however the use of Soft-Eyes in these areas are becoming more and more popular. A Soft-Eye may for example be a diaphragm wall or bore piles reinforced with Glass Fiber Reinforced Polymer bars (GFRP) instead of reinforcement out of steel. Also an anchored tunnel face with GFRP anchors will not obstruct the TBM head driving through. The use of GFRP products in tunnelling is getting more and more common in Southeast Asia and is widely applied in Europe and Japan nowadays.

Soft-Eyes consist usually of bore piles or diaphragm walls, which are locally reinforced with GFRP bars. The sections below and above the tunnel are reinforced conventionally. Depending on the designer and contractors preferences, full rectangular sections are built out of GFRP bars and the fiber reinforcement follows more closely the tunnel section resulting in a circular arrangement of the GFRP links or may be a circular sections.

Both possibilities have their advantages. While a rectangular arrangement saves time during the design and assembly of the cages, following more closely the tunnel section thus reducing the material costs for the GFRP bars. Often applied as a compromise, where the vertical bars cover a rectangular section, while the shear links follow the circular layout. Experience shows that this approach decreases the material costs for the GFRP material by less than 5% still maintaining the detailed design and managing the assembly of the cage to be efficient. Building the corresponding reinforcement cages out of GFRP bars on site requires the same working procedures as for an equal steel cage.

The necessary bars are tailor made and delivered to site where the assembly takes place. The bars are fixed together with binding wire, cable binders or similar products. U-bolts are used for clamping bars together when high loads have to be transferred over a connection.

This is a connection between the vertical GFRP bars and the corresponding steel bars, which have to carry the dead load of the reinforcement cage during the lifting process and lowering of the cage into the trench. Welding as is commonly done with steel reinforcement but not possible with GFRP bars.

2.3 *Railways and subways*

The polymeric nature of the materials used for the production of glass fiber reinforcement polymer profiles as well as the insulating characteristics, the chemical resistance, atmospheric agents and the mass pigmentability allow installation and use with practically zero maintenance, thus producing high technical/economic advantages compared to the traditional use of aluminum, steel, wood or PVC.

The elements lend themselves easily to normal assembly and coating operations by means of connections by bolts, screws and rivets or simply by gluing and painting.

The traditional solutions in steel or wood type materials, although apparently cheaper, require assembly operations with heavy vehicles due to their high weight as well as to painting and/or surface treatments that make them partially resistant to the aggressions of the typical environments in which they are used.

3 APPLICATIONS

3.1 *Isarco, Rebars*

The Brenner Base Tunnel is the central element of the new railway line that connects Munich to Verona and will represent the longest underground railway link in the world with its 64 km. The construction lot called “Sottoattraversamento Isarco” is the extreme southern part of the Base Tunnel before access to the Fortezza station (BZ).

The construction of the works is technically very complex: the tunnels of the main tubes and interconnections will pass below the Isarco River, the A22 motorway, the SS12 state road and the Verona - Brennero historic railway line.

Before starting the tunnel construction work, a series of preliminary surface activities must be carried out, including the displacement of the SS12 national road, the construction of two bridges, over the Isarco river and the Rio Bianco, and the construction of the loading area/unload on the A22 which will be necessary for the transport and supply of construction materials. As part of the implementation phases of the intervention, the definitive deviation of the historic Verona-Brennero railway line for a stretch of about 1 km is also required. The construction of 4 deep wells of about 30 ml includes the temporary reinforcement in GRFP, the assembly of which is made with straight bars and curvilinear elements (Figure 2).

3.2 *M4, Reinforcement for soft-eye*

MM Line 4: Usage of GFRP Rebar Cages for Tunnel Boring Machine “Soft-eye” openings Metro Line 4 will be serving the densely populated areas in city centre of Milan. In order to minimize disruption caused by construction activities, it has been designed to be compatible with other modes of transport and maintain sufficient groundwater level. Metro Line 4 will have twin tunnels with single tracks in each direction. Extensive use of tunnel boring machines (TBM) will be required. Metro Line 4 will have a total of 21 stations, including interchange stations on Lines 1, 2 and 3. The 21 stations, including the terminal, are San Cristoforo FS, Segneri, Gelsomini, Frattini, Tolstoi, Washington-Bolivar, Foppa, Parco Solari, S. Ambrogio, De Amicis, Vetra, S. Sofia, Sforza-Policlinico, San Babila, Tricolore, Dateo, Susa, Argonne, Forlanini FS, Q.re Forlanini and Linate Airport.

The stations are built in open construction pits: An open central shaft and blind-hole side tunnel technique will be implemented to facilitate passage of the TBM and minimize excavation.

Figure 2. Isarco shaft consolidated with GRFP i-BARS in the bypass tunnel area.

TBMs can not cut through steel-reinforced concrete drilled shaft walls as the steel bars get caught in the shovels of their shield. In addition, the steel bars can not be cut into pieces small enough to allow their transport by the TBM's conveyor belt system. As a result, the conventional construction method with steel-reinforced drilled shaft walls needs the manual removal of the steel reinforcement in the path of the TBM. Not only is this time-consuming and expensive in itself, it also required the stoppage and retraction of the TBM in front of each shaft wall. Finally, to ensure that neither the soil nor potential groundwater outside the shaft wall would collapse into the opened hole, complex and expensive soil stabilization measures are required outside the wall. All these time-consuming and costly measures are not required when the areas of the launch shaft head walls to be penetrated by the TBM are reinforced with glass fibre-reinforced polymer (GFRP). Even though these bars have a much higher tensile strength than steel rebars, they are easily machined and can be broken down into small bar segments by the cutter head of the TBM. These segments can then be transported by the machine's conveyor system together with the excavated soil. The TBM does not have to be stopped, and soil stabilization measures are not required, as the soil is always stabilized by the TBM. The resulting savings in the overall construction time and cost are substantial.

Construction of the first two shafts for the project, at Argonne and Frattini Stations, was opened for bids in January 2015. In both cases, GFRP reinforcement was specified in the bid documents. In early July 2015, MAPLAD was awarded the contract to deliver the soft-eyes GFRP rebar cages (Figure 3).

3.3 *Cociv, i-PIPE profile for face stabilization*

The new high-speed railway line called Terzo Valico develops for a total of 53 km, 36 km of which in the tunnel, and covers 14 municipalities in the provinces of Genoa and Alessandria and the regions of Liguria and Piemonte.

In detail, the line, starting from the railway junction of Genoa (Bivio Fegino), develops almost entirely in tunnels (Galleria di Valico and Galleria Serravalle) up to the Piana di Novi, with the exception of a short section in the open air at Libarna. The Valico Tunnel, about 27 km long, has four intermediate adit tunnels, both for construction and safety reasons.

By the most advanced safety standards, the sections in the tunnel will be largely made of two single track tunnels side by side and joined together by transversal connections so that each can serve as a safety tunnel for the other. From the exit of the Serravalle tunnel the line develops mainly outdoors until you enter the Pozzolo Gallery, at the exit of which the line develops outdoors until it joins the existing line Pozzolo Formigaro - Tortona (to Milan); in the uncovered section between Novi Ligure and Pozzolo Formigaro, the construction of the artificial tunnel link from and to Turin on the current Genoa-Turin line is planned.

Figure 3. Metro Milano breakthrough in "GFRP mode".

Figure 4. Left: Consorzio Tunnel Giovi (Pizzarotti S.p.A. & Collini S.p.A.), GFRP at the front face. Right: Oberosler S.p.A.. radial and face long bars for front excavation and subsequent cavern enlargement.

For the sections to be made in traditional excavation, the consolidation of the fronts is done by stabilizing the core-face with fiberglass reinforcement and the design and construction phases are managed through the ADECO-RS method.

MAPLAD is presently working in practically all the contracts (Figure 4).

4 RESEARCH APPLIED ON NEW MATERIALS – IBAR® BS BY MPLD

4.1 *Basalt fibers*

Basalt fiber is a material made from extremely fine fibers of basalt, which is composed of the minerals plagioclase, pyroxene and olivine.

It is similar to carbon fiber and fiberglass, having better physic mechanical properties than fiberglass, but being significantly cheaper than carbon fiber.

Basalt fibers are 100% natural and inert. Tested and proven to be non-carcinogenic and non-toxic and easy to handle. In contrary, fiberglass is made from a mixture of many materials, some of which are not environmentally friendly.

Since basalt is the product of volcanic activity, the fiberization process is more environmentally safe than that of glass fiber. Basalt continuous filament is a green product. Abundant in nature so can never deplete the supply of basalt rock.

The "greenhouse" gases that might otherwise be released during fibre processing were vented millions of years ago during the magma eruption so won't affect the current pollution scenario.

Further, basalt is 100 percent inert, that is, it has no toxic reaction with air or water and is non-combustible and explosion proof.

4.1.1 *Advantages*

Superior Thermal Protection: Maplad's Basalt has a thermal range of -260 ˚C to +982 ˚C (1800 ˚F) and melting point of 1450 ˚C. Fibers are ideal for fire protection and insulative applications.

Durable: Tough and long-lasting, fibers deliver acid, alkali, moisture and solvent resistance surpassing most mineral and synthetic fibers. They are immune to nuclear radiation, UV light, biologic and fungal contamination.

They're stronger and more stable than alternative mineral and glass fibers, with tenacity that exceeds steel fibers many times over.

Additionally, basalt fibers are naturally resistant to ultraviolet (UV) and high-energy electromagnetic radiation, maintain their properties in cold temperatures, and provides better acid resistance.

In Table 2 and 3 some technical data are reported.

4.1.2 *Mechanical and physical characteristics of basalt fiber reinforced polymer rebar*

Basalt rebar has a lower Young's modulus compared with steel, but is 15–30% higher than fiberglass rebar. It is strong in tension and has very little stretch.

Table 2. Comparison between basalt fiber and glass or carbon fiber.

Capability	Basalt fiber	E-Glass fiber	S-Glass fiber	Carbon fiber	Unit
Tensile strength	3000–4840	3100–3800	4020–4650	3500–6000	MPa
Elastic modulus	79.3–93.1	72.5–75.5	83–86	230–600	GPa
Elongation at break	3.1	4.7	5.3	1.5–2.0	%
Diameter of filament	6–21	6–21	6–21	5–15	μm
Tex	60–4200	40–4200	40–4200	60–2400	
Temperature of Application °C	(-260)-(+500)	(-50)-(+380)	(-50)-(+300)	(-50)-(+700)	

Table 3. Breaking strength of basalt fiber for different diameter.

Capability						Unit
Filament diameter	5	6	8	9	11	μm
Breaking strength to weight ratio of elementary fibers	215	210	208	214	212	kg/mm^2

Table 4. Comparison between basalt rebar and fiber glass rebar.

Properties	Glass Rebar	Basalt Rebar	Unit
Elastic modulus	>30000	>50000	N/mm^2
Elongation at break	>2	>2.5	%
Fiber content	>60	>70	%
Shear strength	>16	>20	Ksi

If rebar is subjected to beyond the spec limits then it will break rather than stretch. The rebar placement design needs to allow for this.

The structural engineering needs to consider "tensile modulus". In a properly structurally engineered design, the rebar will not be subjected to anything like the force needed to break it.

The thermal expansion coefficient is very close to that of concrete (whereas steel is very different). This helps a lot to avoid concrete cracking.

Table 4 is a short properties comparison sum up.

4.2 *Green pultrusion*

A strongly growing demand for reinforced concrete reinforcements in GFRP has been recondited on the market in the last decade,

Especially for underground works realized by mechanized excavation, the traditional reinforcement is a limitation because it cannot be easily demolished.

In this specific field of application, experimentation on the applicable materials aims above all at the development of innovative and sustainable pultrusion processes.

Hence the "Green Pultrusion" project fielded by the Universities of Catania and Palermo and by some Italian companies headed by Maplad, a leading company in the sector of pultruded elements production.

The phases of the project include the design and construction of a prototype pultrusion plant dedicated to the production of environmentally friendly products, using raw materials of natural origin, totally reusable with a recycling process with low environmental impact.

The steps of the project include the study of the characteristics of natural fibers in relation to their use in the developed pultrusion process, the optimization of a recyclable and